UNIVERSIDADE ESTADUAL DE CAMPINAS
Faculdade de Engenharia Elétrica e de Computação

Moisés Martins do Nascimento

Data-Driven Secondary Voltage Control Design using PMU Measurements

Controle Secundário de Tensão Baseado em Dados Usando Medições de PMU

Campinas
2021

UNIVERSIDADE ESTADUAL DE CAMPINAS
Faculdade de Engenharia Elétrica e de Computação

Moisés Martins do Nascimento

Data-Driven Secondary Voltage Control Design using PMU Measurements

Controle Secundário de Tensão Baseado em Dados Usando Medições de PMU

Dissertation presented to the School of Electrical and Computer Engineering of the University of Campinas in partial fulfillment of the requirements for the degree of Master in Electric Engineering in the Department of Energy System.

Dissertação apresentada à Faculdade de Engenharia Elétrica e de Computação da Universidade Estadual de Campinas como parte dos requisitos exigidos para a obtenção do título de Mestre em Engenharia Elétrica, na área de Energia Elétrica

Supervisor: Prof. Dr. Daniel Dotta

Este trabalho corresponde à versão final da dissertação defendida pelo aluno Moisés Martins do Nascimento, orientado pelo Prof. Dr. Daniel Dotta

____

Campinas
2021

Ficha catalográfica
Universidade Estadual de Campinas
Biblioteca da Área de Engenharia e Arquitetura
Rose Meire da Silva - CRB 8/5974

N17d

Nascimento, Moisés Martins do, 1989-
Data-driven secondary voltage control design using pmu measurements / Moisés Martins do Nascimento. – Campinas, SP : [s.n.], 2021.

Orientador: Daniel Dotta.
Dissertação (mestrado) – Universidade Estadual de Campinas, Faculdade de Engenharia Elétrica e de Computação.

1. Sistema de energia elétrica. 2. Sistema de energia elétrica - Controle. I. Dotta, Daniel, 1978-. II. Universidade Estadual de Campinas. Faculdade de Engenharia Elétrica e de Computação. III. Título.

Informações para Biblioteca Digital

Título em outro idioma: Controle secundário de tensão baseado em dados usando medições de pmu
Palavras-chave em inglês:
Electrical energy system
Electrical energy system control
Área de concentração: Energia Elétrica
Titulação: Mestre em Engenharia Elétrica
Banca examinadora:
Daniel Dotta [Orientador]
Ricardo Coração de Leão Fontoura de Oliveira
Antonio Felipe da Cunha de Aquino
Data de defesa: 18-06-2021
Programa de Pós-Graduação: Engenharia Elétrica

Identificação e informações acadêmicas do(a) aluno(a)
- ORCID do autor: https://orcid.org/0000-0001-9851-672
- Currículo Lattes do autor: http://lattes.cnpq.br/1304885436015947

COMISSÃO JULGADORA - DISSERTAÇÃO DE MESTRADO

Candidato(a):Moisés Martins do Nascimento RA: 226848
Data de defesa: 18 de Junho de 2021
Título da Dissertação: "Data-Driven Secondary Voltage Control Design using PMU Measurements"
Título em Português: "Controle Secundário de Tensão Baseado em Dados Usando Medições de PMU"

Prof. Dr. Daniel Dotta (Presidente, FEEC/UNICAMP).
Prof. Dr. Ricardo Coração de Leão Fontoura de Oliveira (Membro Interno, FEEC/UNICAMP).
Prof. Dr. Antonio Felipe da Cunha de Aquino (Membro Externo, UFSC).

A Ata de Defesa, com as respectivas assinaturas dos membros da Comissão Julgadora, encontra-se no SIGA (Sistema de Fluxo de Dissertação/Tese) e na Secretaria de Pós-Graduação da Faculdade de Engenharia Elétrica e de Computação.

To my family for their support and love in this path.

Acknowledgements

First, I would like to thank God and Jesus Christ, for giving his life for us. I am very grateful to my mother Esmeralda Martins do Nascimento, my father Miguel Bindá do Nascimento Filho, my wife Kelly Aguiar, and my siblings Luis Miguel, Michael, and Michelany for their care, love and support.

I would like to express my deep and sincere gratitude to my advisor, Dr. Daniel Dotta, for giving me the opportunity to be his master student, and patience in discussions and debates with me.

To my friends Iury Bessa, Ronaldo Portela, Orlem Lima, and Raul Torres for your support, and patience in discussions and debates about several themes, including this work.

To Dr. Ricardo C. L. F. Oliveira and Dr. Antonio Felipe da Cunha de Aquino to their corrections and suggestion to make this work better.

To the university of UNICAMP, for the great public infrastructure capable of providing and encouraging the science in Brazil.

Abstract

With the growing consumer demand and the high penetration of renewable energy, power systems are increasingly operating in conditions of stress. Voltage disturbances can cause cascading failures and large-scale blackouts in interconnected transmission systems. For the safety, reliability and economical operation of the electric power system, control of bus voltages and reactive power flow is essential. The Secondary Voltage Control (SVC) is slower than Primary Voltage Control in which capacitor/reactor banks, load tap changes and sometimes Automatic Voltage Regulators (AVR) in an area perform the control actions. The SVC updates the PVC set point to improve the voltage of the buses in a controlled area. Traditional methods of SVC are based on the steady state linear and nonlinear model of the system. Accurate high-order linear or nonlinear models need to be constructed for these methods to calculate a multi-variable quadratic optimization control criterion. This calculation is complex and consumes a high processing time, and the good performance of these model-based methods cannot be guaranteed. With the advancement of communication technology and global positioning systems (GPS), it is possible for the Phasor Measurement Units (PMU) to measure voltage, current and power in each bus, in phasor mode, on a scale of time to allow to observe the dynamics of the system. Therefore, the Data-Driven Control (DDC) methods can deal with the model-based problems. In this work, two DDC methodologies for the SVC design are presented. A DDC SVC based on Virtual Reference Feedback Control (VRFT) approach is proposed as an offline method, and Model-Free Adaptive Control (MFAC) as an online method. Both methods are validated with the application in New England Model benchmark. Nonlinear time domain simulations are performed to evaluate the designed controllers performance.

Keywords: Primary Voltage Control. Secondary Voltage Control. Data-Driven Control. Phasor Measurement Unit. Virtual Reference Feedback Tuning. Model-Free Adaptive Control.

Resumo

Com a crescente demanda dos consumidores e a alta penetração de energia renovável, os sistemas de energia estão cada vez mais operando em condições de estresse. Perturbações na tensão podem causar falhas em cascata e blecautes em grande escala em sistemas de transmissão interconectados. Para a segurança, confiabilidade e operação econômica do sistema elétrico de potência, o controle das tensões dos barramentos e do fluxo de potência reativa é essencial. O controle secundário de tensão (SVC - Secondary Voltage Control) é um controle mais lento que primário de tensão (PVC - Primary Voltage Control) no qual bancos de capacitores/reatores, mudanças de *tap* do transformador e, às vezes, *Automatic Voltage Regulators* (AVRs) em uma área executam as ações de controle. O SVC atualiza o *set-point* do controle PVC para melhorar a tensão dos barramentos em uma área controlada. Os métodos tradicionais de SVC são baseados no modelo linear e não linear de estado estacionário do sistema. Modelos lineares ou não lineares de alta ordem precisos necessitam ser construídos para esses métodos para calcular um critério de controle de otimização quadrática multivariável. Esse cálculo é complexo e consome muito tempo de processamento, e o bom desempenho desses métodos baseados em modelo não pode ser garantido. Com o avanço da tecnologia de comunicação e sistemas de posicionamento global (GPS), é possível para as Unidades de Medição Fasorial (PMU) medirem a tensão, corrente e potência em cada barramento, no modo fasorial, em uma escala de tempo que permite observar a dinâmica do sistema. Portanto, os métodos de controle baseado em dados (DDC- Data-Driven Control) podem lidar com problemas dos métodos baseados em modelos. Neste trabalho, duas metodologias de DDC para o projeto SVC são apresentadas. Uma abordagem DDC SVC baseada no algoritmo VRFT (Virtual Reference Feedback Control) é proposta como um método offline, e MFAC (Model-Free Adaptive Control) como um método online. Ambos os métodos são validados com a aplicação no *benchmark New England Model*. Simulações não lineares no domínio do tempo são realizadas para avaliar o desempenho do controlador projetado.

Palavras-chave: Primary Voltage Control. Secondary Voltage Control. Data-Driven Control. Phasor Measurement Unit. Virtual Reference Feedback Tuning. Model-Free Adaptive Control.

List of Figures

List of Tables

List of abbreviations and acronyms

VRFT	Virtual Reference Feedback Tuning
MFAC	Model-Free Adaptive Control
PVC	Primary Voltage Control
SVC	Secondary Voltage Control
TVC	Tertiary Voltage Control
DDC	Data-Driven Control
IFC	Iterative Feedback Tuning
ADP	Approximate Dynamic Programming
SPSA	Simultaneous Pertubation Stochastic
CbT	Correlation-based Tuning
ILC	Iterative Learning Control
LL	Lazy Learning
EdF	Électricité de France
WAMS	Wide Area Measurement System
WAPSS	Wide Area Power System Stabiliser
PMU	Phasor Measurement Unit
AVR	Automatic Voltage Regulators
LTC	Load Tap Changer

Contents

1 Introduction

1.1 Motivation and Literature Review

In recent years, power systems around the world have been experiencing significant changes, resulting of the massive integration of renewable generation and the difficulty to build new transmission lines due to environmental constraints, these are two of the some reasons. In a recent review (SUN et al., 2019), the authors discussed the effect of these changes on voltage control. The authors clearly stated the necessity of new voltage control methods and schemes to cope with new challenges. Some of the key technologies to improve voltage control performance are the Wide Area Measurement Systems (WAMS) and the hierarchical control schemes.

The hierarchical voltage control scheme is divided into primary voltage control (PVC), secondary voltage control (SVC), and tertiary voltage control (TVC) (LEFEBVRE et al., 2000). In this work, the main goal is to improve the performance of the secondary level, which is responsible for maintaining the voltage profile at an acceptable level across the entire power grid. The SVC consists of a feedback control loop that regulates transmission-side voltage at some selected pilot buses. Practically, this is accomplished by adjusting individual generator Automatic Voltage Regulators (AVR) set-points, static or synchronous condensers voltage set-points, and transformer taps, etc. It should be noted that pilot bus voltage must represent the voltage in its neighborhood.

Traditionally, the SVC is designed off-line using high-order linear or nonlinear models (ILIC et al., 1995; MORADZADEH; BOEL; VANDEVELDE, 2013; ELMITWALLY; ELSAID; ELGAMAL, 2015). Obviously, the performance of the resulting SVC controller is directly dependent on the accuracy of the obtained model. Wind Turbine and Solar generators are sophisticated devices whose accurate modeling is a complex and challenging problem. Detailed representation of these devices with all associated controllers may take significant effort and require using models with a substantial number of states. Depending on the level of detail of the models and the size of the system, these models may not accurately represent all the system dynamics and their control interactions. Therefore, the performance of these model-based methods can be impaired in power systems with massive penetration of renewable generation. In this context, data-driven control (DDC) methods represent a potential solution to improve voltage control performance of emerging power systems. By choosing a data-driven approach, some problems that arise from model-based methods, such as unmodeled dynamics and the difficulty of obtaining accurate power systems models, are avoided.

In the literature, some data-driven methods, like Iterative Feedback Tuning (IFT), Virtual Reference Feedback Tuning (VRFT), Approximate Dynamic Programming (ADP), and Model Free Adaptive Control (MFAC), are available (HOU; WANG, 2013). The IFT algorithm was applied to two different turbine controllers in (SOLINGEN; MULDERS; WINGERDEN, 2017): drivetrain damping and collective pitch control. An application of the VRFT algorithm in UPS systems to obtain reference tracking for sinusoidal signals was proposed in (CORLETA et al., 2016). An adaptive optimal control for a class of continuous-time uncertain interconnected systems using output-feedback and the ADP algorithm is proposed in (GUO et al., 2016). In (ZHAO; LU, 2018), MFAC was proposed to design a decentralized SVC with PMU measurements. In the MFAC algorithm, a pseudo-partial derivative is estimated online by using I/O data according to some weighting factors (ZHAO; LU, 2018). These weighting factors are important adjustable parameters for system stability and performance. However, there are no guidelines for an appropriate selection of these parameters. On the other hand, the VRFT algorithm is a method which directly finds the controller's parameters without any weighting factors.

This work investigates and analyzes the application of VRFT and MFAC techniques in SVC problems.

1.2 Power System Stability

The stability of power systems can be defined as the capacity of the system, for a given initial point of operation, to converge to a new equilibrium point, in which most of its variables remain within acceptable operational limits keeping the system practically unchanged, after the occurrence of a certain physical disturbance (KUNDUR et al., 2004; HATZIARGYRIOU et al., 2020). It is essentially a single problem that is influenced by different factors, so to be properly studied and classified, consider the following aspects:

- The physical nature of the variable in which instability is observed. In this case, it is divided into angle stability (rotor), voltage and frequency;
- The intensity of the disturbance considered that determines the method of analysis to be used. In this case, the disturbances are classified as small (small load variations, performance of continuous and discrete controllers, etc.) and large disturbances (faults, disconnection of transmission lines, loss of generation, etc.);
- The equipment, the processes and the time interval necessary for the correct identification of the variables involved in the phenomenon of instability. In this respect it is separated into short and long term stability (Figure 1).

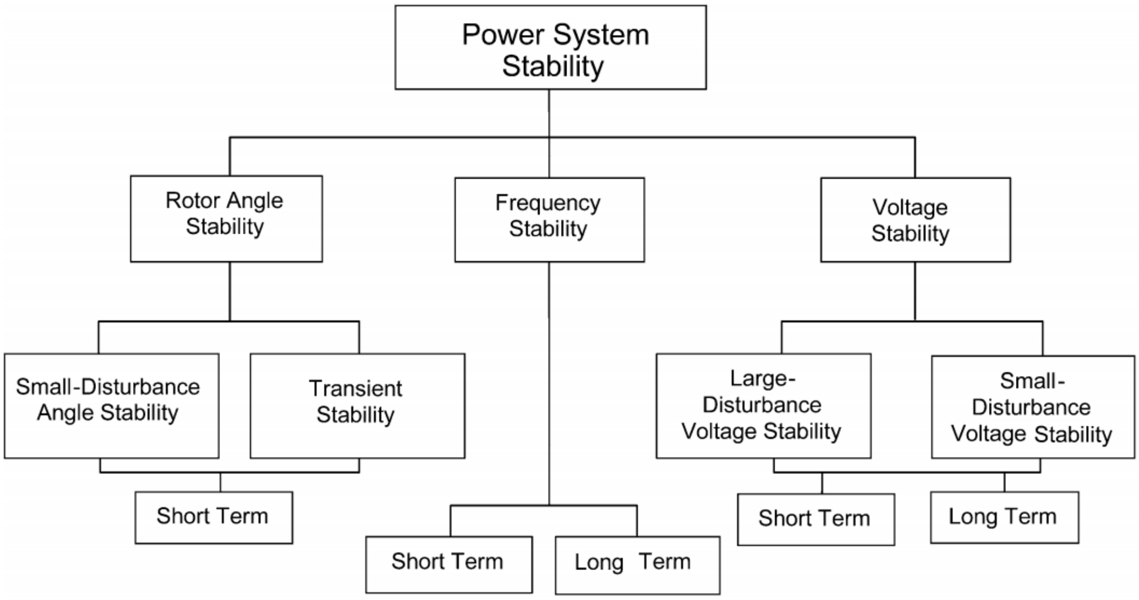

Figure 1 – Classification of power system stability (KUNDUR et al., 2004).

1.2.1 Angular Stability

Angular stability is associated with the ability of an interconnected electrical system to keep your machines in sync after a disturbance occurs. It is decomposed into angular stability of small signals and transient stability.

The angular stability of small signals is strongly influenced by the initial point of operation from which the disturbance occurred. Its study can be performed through of analysis of linear systems methods, for this it is necessary to linearize the system at the operating point under examination. The time interval of interest varies from 10 to 20 s, since the beginning of the disorder, that is, it is a short-term phenomenon.

In the transient angular stability, the effects of large disturbances, such as faults, loss of transmission lines and loss of generation, are analyzed. These events cause significant variations in the angles of the generator rotors, power flows, voltage value in the bars, etc. The phenomenon is strongly influenced by the non-linearities of electrical systems and also depends on the initial operating point of the electrical network. It is perceived in first seconds after the disturbance. The time interval of interest is 3 to 5 s, which can be extended to 10 to 20 s in large systems. For its study, it is necessary to carry out simulations in the time domain, solving the differential equations that model the dynamics of the system (KUNDUR et al., 2004).

1.2.2 Frequency Stability

The frequency stability is the ability of an electrical system to keep its frequency stable, after the occurrence of a major disturbance that caused a considerable imbalance between generation and load, with the least possible unintentional loss of load. This type of instability is usually preceded by significant variations in frequency, power flows, voltage values in the bars, etc. The phenomenon can be short-term, a few seconds, as in the case of the islanding of a part of the system that does not have the capacity to generate all the energy necessary to supply its load or long-term, such as, for example, the instability caused by problems in the over-speed control of steam turbines that can last from tens of seconds to a few minutes (KUNDUR et al., 2004).

1.2.3 Voltage Stability

Voltage stability can be defined as the ability of an electrical system to maintain its voltage profile within previously specified limits, after being subjected to a disturbance, for a defined initial operating condition (KUNDUR et al., 2004). It can also be treated as a problem of load stability, which for a given transmission bar can be the sub-transmission system, the distribution system or a large consumer (TAYLOR; BALU; MARATUKULAM, 1994). Voltage stability is considered a dynamic process directly associated with the response of loads in relation to voltage variations in the system buses.

After the occurrence of a disturbance such as load growth, output of the transmission line, loss of generation, etc., it is observed that the system is unable to meet the demand for reactive energy in some areas, causing the slow and progressive fall of the voltage profile of some load bars of the electrical network. In response to this, the voltage control devices attempt to restore the voltage levels on these buses. The rise in voltage restores the load power, aggravating the problem of decreasing the voltage in the high voltage bars, which is reflected in the low voltage bars, in a feedback process, until the controls reach their limits of action.

The sequence of events described leads the electrical system to a voltage collapse which is characterized by a progressive and uncontrollable reduction in the voltage of the bars in a given area of the system. This event is the result of the loss of the electrical network's capacity to maintain the voltage within the defined operational limits.

In addition to the instability characterized by the gradual decrease in voltage, the possibility of instability due to overvoltage also exists and is caused by the capacitive behavior of transmission lines, operating below their natural power, and by the actuation of under-excitation limiters, preventing synchronous machines from absorbing these excess reactive power. It is noted that in this case the instability is associated with the malfunction of the transmission system together with the generation system in low load conditions (KUNDUR et al., 2004).

Voltage instability can last from a few seconds to several minutes and basically depends on the ability to maintain or restore the balance between generation and load. It is mainly associated with the reactive support capacity and the loading conditions of the transmission system (TAYLOR; BALU; MARATUKULAM, 1994).

The phenomenon is classified in relation to the intensity of the disturbance that started the instability process, in voltage stability to major disturbances and small disturbances, and as for the time of triggering the phenomenon in short-term or transient and long-term voltage stability.

1.2.4 The Voltage Control Problem

The evolution of electrical power systems, with an increase in the number of consumers and energy production units, interconnections between previously isolated systems and commercial practices involving free agents bring the system close to its operational limits, causing regulatory authorities and the companies make efforts to increase the efficiency of the system's operation. In this context, it is highlighted, as one of the principal functions of a System Operation Center, the control of voltage and reactive power.

The voltage control problem in power systems comprises the ability to regulate the voltage profile of the system, contributing to its safety, operational efficiency and quality in the supply of energy to consumers (J.V. et al., 2000). Based on these aspects, some requirements for a voltage control system can be cited.

- **Quality**: The voltage at the terminals of all equipment in the system must be within their acceptable limits. Both system equipment and consumer equipment connected to the system are designed to operate within a given voltage range. The prolonged operation of this equipment outside this range can affect their performance and cause damage;
- **Safety**: The voltage control must respect the follow aspects:
  - Losing a transmission line or generation unit cannot take the entire system out of operation, sufficient reactive reserve should be made available for emergency conditions;
  - Voltage control efforts should be distributed in proportion to the capacity of the available control equipment, thus avoiding excessive efforts on isolated equipment;
  - Control actions must be coordinated, thus contributing to the stability of the system.
- **Economic**: The cost of producing reactive power, and the reactive power flow in the transmission system, should be minimized.

Meeting all the requirements mentioned above is not a simple task, mainly for the natural characteristics of power systems involving many continuous and discrete states, different time scales, besides non-linearities.

1.2.5 Equipment for Voltage and Reactive Power Control

1.2.5.1 Synchronous Generators

Synchronous generators are the main reactive power sources used to control voltage in power systems. The machine is able to inject or absorb reactive power smoothly to regulate its terminal voltage as desired. Lack of reactive power support from generators or disconnection of the machine is one of the main causes of voltage instability. Reactive power is controlled by means of adjusting the field current, which is carried out by the AVR. As operated in voltage control mode, the AVR senses the generator terminal voltage and compares this value with the reference voltage. If mismatch between the two quantities appears, the AVR will adjust the field current to eliminate the error. Although synchronous machines are a powerful tool to control voltage, they also have certain physical limits. Therefore, the machine is equipped with limiters, protective relays or other functions to maintain operating parameters within its constraints. These factors have a large impact on voltage instability (CORSI, 2015).

1.2.5.2 Synchronous Compensator

A synchronous compensator/condenser is a synchronous machine that runs without a mechanical load. Depending on the value of the excitation, it can absorb or generate reactive power in the same way a synchronous generator does (CORSI, 2015). These devices were connected, at the transmission and subtransmission level, to increase the voltage stability margin and keep the voltage levels within the desirable limits, under load variation conditions and in emergency situations. One of the significant advantages of the synchronous compensator is its flexibility of operation in all load conditions of the system. When used as a voltage regulator, the compensator can automatically operate overexcited during periods of heavy load and underexcited during periods of light load. The advantage of synchronous compensators comparing to other equipment intended for voltage control is the ability to supply reactive energy, both capacitive and inductive, giving greater flexibility to its operation.

1.2.5.3 Static Compensators

The static compensator is a device that acts quickly in the supply of reactive power, allowing a large margin of control within its performance range. The performance of this device is based on the variation of the shunt susceptibility connected to a transmission bus. A static compensator operates the electronic soft switching of its own shunt reactors and/or capacitors, achieving continuous reactive power variation. It is ideally suited to the control of varying reactive power demand of large fluctuating loads and overvoltage dynamics due to load rejection (CORSI, 2015). The term "static" is used to indicate that, unlike the synchronous compensator, it has no moving or rotating components.

1.2.5.4 The Renewable Energy Sources

Due to the high penetration of renewable energy sources, several countries have implemented hierarchical systems to coordinate the reactive power production in their plants using the available amount of reactive power (CHIANDONE et al., 2014). The integration of non-dispatchable renewable power plants into the voltage control architecture is a significant challenge. Some authors present solutions to integrate the photovoltaic (CHIANDONE et al., 2015b) and wind (CHIANDONE et al., 2015a) plants in the coordinate voltage control. In Brazil, a legal requirement obliges wind and photovoltaic generators to provide voltage control in their PVC, in order to maintain the voltage profile within the tolerated limits (ONS, 2020).

1.3 The Hierarchical Voltage Control

EdF (Électricité de France) implemented the first hierarchical voltage control structure in France in the mid-1970s (PAUL; LEOST; TESSERON, 1987). In this structure was added a new control loop, called secondary voltage control, superimposed on the control loop of the generator's AVR (primary voltage control) (CORSI et al., 1995). This new control loop aimed to regulate the voltage of some important system buses by adjusting the reactive power injection of generation units electrically close to these bars. A few years later, ENEL decided to implement in the Italian system a scheme similar to the French, with the inclusion of a new control loop overlapping the secondary control, in order to manage the reactive power flow between the different areas of the system. This new hierarchical level would be responsible for providing the reference voltages to the secondary level through optimization programs, which was called tertiary voltage control (CORSI et al., 1995). In 1989, EdF proposed an improvement in its hierarchical voltage control system, also adding the tertiary level, creating coordination between areas, or what is called Coordinated Voltage Control (PAUL; LEOST; TESSERON, 1987).

Hierarchical voltage control has been organized into three different hierarchical levels: primary, secondary, and tertiary control, all levels being spatially and temporally independent. The temporal independence minimizes the interactions between the three different levels, thus minimize of risks of oscillation and instability by control actions conflicting.

The PVC is always to control the AVR of generators or the Load Tap Changer

(LTC) of transformers that maintain its own bus at a certain voltage level. The PVC levels are controlled by the system operators or higher control levels, such as SVC. Compared to the other control levels, the response for this level is faster and within a few seconds.

As mentioned above, PVC control is one of reactive power resource with the function to provide and maintain the voltage in the power systems terminals. SVC will control multiple reactive power resources based on measurements of one or multiple buses. Voltages will be altered by SVC for AVRs, LTCs or synchronous capacitors. Secondary voltage control plays an important role both during normal operating conditions and in front of contingencies (CORSI et al., 1995):

- In normal grid operation, it ensure:
  - Maintenance of network voltages at a specified value and reduction in their variations;
  - Increase in dispatch control efficiency;
  - Coordination of real-time controls of reactive power resources;
  - Dynamic performance of first-order type to voltage transients, with a dominant time constant of about 50s.
- Under disturbed conditions, secondary voltage regulation:
  - Offers timely controls of generated/absorbed reactive powers in the perturbed area;
  - Speedily recovers the perturbed area voltage level;
  - Imposes a first-order dynamic response to voltage transients in accordance with PI control law, with a dominant time constant of about 50 s (an I-control law effect) as well as fast recovery of most of the peak variations (due to large perturbation) during the first seconds of heavy transients (a P-control law effect).

TVC will play a higher role than the SVC. Compared to the lower control level, TVC doesn't only provide an improved voltage profile but also an optimal voltage profile for the whole power system. It provides optimal voltage set points for the target buses controlled by SVC.

The philosophy of hierarchical voltage control is to divide the system into decoupled areas so that disturbances can be handled regionally by a set of control devices, varying their voltage references and their participation in reactive power generation. Each voltage control area is represented by a representative voltage bus, measured in real-time, providing the appropriate control signals. Figure 2 represents the hierarchical voltage control.

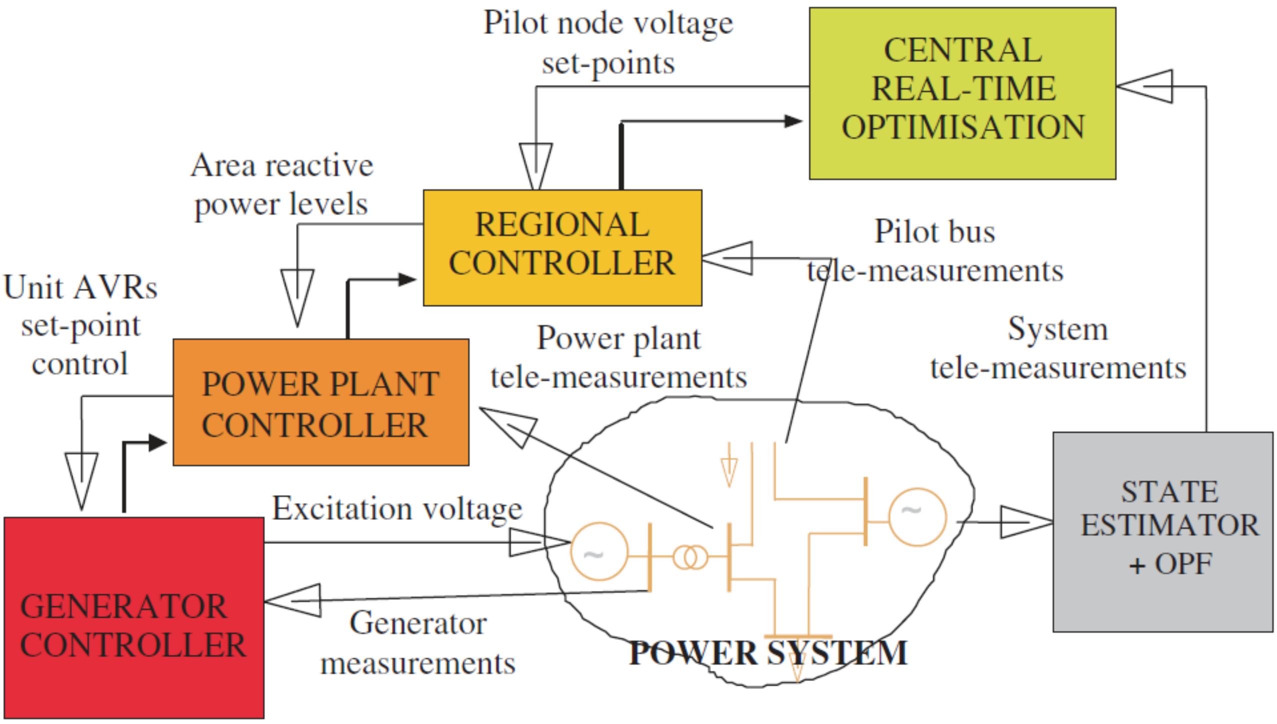

Figure 2 – A hierarchical voltage control structure (CORSI, 2015).

1.4 Objectives

The main contribution of the present work is to explore the potential of two DDC methods (VRFT and MFAC) to enhance the voltage control in power systems. To reach this goal, the following partial objectives are proposed:

- To explore the capabilities of the VRFT for SVC problems;
- To compare the VRFT with some known methods of literature;
- To explore the capabilities of the MFAC for SVC problems;
- To compare the MFAC with some known methods of literature;
- To understand how MFAC parameters are set in literature;
- To propose improvements in MFAC parameters settings.

1.5 Thesis Outline

The outline of this thesis is organized as follows:

In Chapter 2 a literature review of the remarkable studies in DDC, and its applications in power system are presented. Also, the mathematical formulation of the DDC methods used in this work is described.

In Chapter 3 the physical characteristics involved in a SVC scheme are presented.

In Chapter 4 the detailed steps to design a SVC based on DDC are presented.

In Chapter 5 the simulations are carried out, and the discussions about its results are presented.

Finally, conclusions and future works are presented in Chapter 6.

2 DDC Methods

2.1 Introduction

The aim of this chapter is to review the main concepts involved in DDC methods. Differents DDC methods and its applications in energy power system are presented. Two methods are chosen to be detailed and their mathematical formulation are presented.

2.2 Data-Driven Control (DDC)

In industrial schemes, the dynamics of plants are typically approximated by low-order models, since the controller synthesis is easier to implement for lower order processes. However, this approximation can impair the performance of a controller, since low-order models are subject to model uncertainty. In a data-driven methods, a controller is designed by directly using online or offline input/output data (instead of designing a controller based on first modeling of a given plant). Data-driven methods aim to design controllers through direct usage of the process data while eliminating the challenging and tedious issues associated with the modeling process. In this manner, stability and performance can still be guaranteed under certain reasonable assumptions. A survey on the differences associated with model-based control and data-driven control has been addressed in (HOU; JIN, 2013) and (BAZANELLA; CAMPESTRINI; ECKHARD, 2011). The authors assert that model-based control methods are inherently less robust due to the unmodeled dynamics of a process, and that these controllers may possibly be unsafe for practical applications. With the data-driven control scheme, the parametric uncertainties and the unmodeled dynamics (for linear time-invariant systems) are irrelevant and the only source of uncertainty comes from the measurement process. Given the available resources of a digital computer, access to huge amounts of measured process data can easily be collected due to the well-developed information technology (i.e., collected information from stored historical data or online data in real-time during process runs).

There are more than ten DDC methods available in literature like Iterative Feedback Tuning (IFT), Virtual Reference Feedback Tuning (VRFT), Approximate Dynamic Programming (ADP), Model-Free Adaptive Control (MFAC), Simultaneous Perturbation Stochastic Approximation (SPSA), Unfalsified Control (UC), PID, Correlation-based Tuning (CbT), Subspace Method, Non-iterative Data-Driven Model Reference Control, Iterative Learning Control (ILC), and Lazy Learning (LL) (HOU; WANG, 2013). These methods are sorted according to the type of data usage (on-line, off-line data or hybrid) or by controller structure design (pre-specified fixed controller or unknown controller structures). Indeed, contrary to offline techniques, online techniques also require to study the convergence of the proposed schemes. Moreover, the tools used to study closed-loop stability are rather different in both cases. When it comes to offline techniques, most stability criteria are based on the winding number or the small-gain theorem. These conditions are useless in online approaches where BIBO stability has to be studied.

In addition to avoiding the problem of unmodeled dynamics, the use of controllers with pre-defined structures is also important. In the classical robust control design method, the order of the resulting full-order controllers can be quite large; in fact, the order can be as large as the order of the augmented plant. However, the increased dependency on computers for control systems has fostered a need for control designs in a digital framework. Thus the notion of fixed-structure controller synthesis becomes an important subject in today's controller design scheme. In fact, the proportional-integral and proportional-integral-derivative (PI/PID) controllers are still the most widely used controller structures in today's industry due to their ease of implementation. It is known that more than 90% of all control loops are PID (ÅSTRöM; HäGGLUND, 2001).

2.2.1 Application in Power Systems

To the best of our efforts in the literature review, a few works with application em SVC were to find out. The most applications of DDC methods in power systems are in damping control field.

- **MFAC Method**

In (JIANHUA et al., 2011) the authors proposed a MFAC controller for a Buck Converter. Comparing and analyzing the simulated waveforms with the method of optimal control of buck converter by state feedback linearization, the authors affirmed that this method is simple and it avoids some complex steps such as building a precise mathematical model, and distinguishing continuous conduction and discontinuous conduction modes.

In large scale wind turbine design, the wind turbine loads can impact the performance of controller. Thus, (YAO et al., 2013) proposed a MFAC individual pitch control algorithms to mitigate the rotor unbalance structural load for variable speed wind turbine. The controller strategy can effectively stabilize wind turbine power output and reduce aerodynamic loads.

Wide-area power system stabiliser (WAPSS) is an effective device to damp the inter-area low-frequency oscillation, caused by interconnection of regional power grids. In (LU et al., 2015) MFAC algorithm is improved to meet the wide-area damping control requirements in consideration of system disturbances. With the consideration of the interactions among the controllers and system noises, a novel decoupled multiple-input–multiple-output power system description for WAPSS coordination design are given in (ZHAO et al., 2016).

In (ZHANG et al., 2017), it is investigated the coordinated power sharing issues of interlinked ac/dc micro-grids. An appropriate control strategy, based on MFAC algorithm, is developed to control the interlinking converter to realize proportional power sharing between ac and dc micro-grids.

In (ZHAO; LU, 2018), the authors proposed an improved SVC approach to enhance the power grid voltage stability with PMU measurements, based on MFAC. Besides, the initialization of the MFAC parameters was presented based on zeros and poles of pre-existing PID-SVC. The simulations performed in the New England 39-bus power system have shown that the proposed approach can maintain the system voltage profile at acceptable levels under different operating conditions.

In (LIANG et al., 2018) a MFAC methodology is used to design a voltage source converter controllers for power supply in urban networks. Based on the IEEE-13 node distribution network model, an AC/DC distribution network model is used to test the controller.

In (SHI et al., 2020a) a MFAC wide-area damping control of wind farms considering unknown control direction and zero steady-state controller output is proposed for enhancing the damping of power system oscillations and improving power system stability.

In (LI; WANG; LI, 2020) an improved MFAC by considering the differential of tracking error in cost function (MFAC with the differential of tracking error), to compensate for potential effect of the system dynamic characteristics under random disturbance is proposed for pitch control when it operates above rated wind speed.

In (SHI et al., 2020c) the problem of secondary frequency control for islanded microgrid is transformed into the target frequency tracking problem. Then, the MFAC algorithm and pseudo partial derivative estimation and reset algorithm are designed based on the dynamic linear data model of the control system.

In (MOSAAD; ALENANY; ABU-SIADA, 2020) four MFAC controllers are employed to control the series of shunt converters of the unified power flow to enhance the DFIG wind energy conversion systems dynamic performance during wind gust and fault conditions. To validate the superiority of the proposed controller, the performance of the system employing MFAC is compared with the system performance when conventional PI controllers are used.

In (SHI et al., 2020b) an improved MFAC, which employs the pseudo-partial derivative to linearize the nonlinear power system dynamically, considering wide area damping control requirements and system disturbances is proposed to damp out the inter-area oscillation for wind farm. In addition, to compensate for communication delays in a WAMS, an adaptive delay compensator is employed to reimburse both constant and variable delays.

- **ADP Method**

A neural-network-based ADP method, namely, the direct heuristic dynamic programming is applied in two power system stability control problems in (LU; SI; XIE, 2008). The first case involves static var compensator supplementary damping control, which is used to provide a comprehensive evaluation of the learning control performance. The second case aims at addressing a difficult complex system challenge by providing a new solution to a large interconnected power network oscillation damping control problem that frequently occurs in the China Southern Power Grid.

In (JIANG; JIANG, 2012) and (JIANG; JIANG, 2013) it is presents an approach to decentralized control design of complex systems with unknown parameters and dynamic uncertainties. The strategy uses the theory of robust ADP and the policy iteration technique. An iterative control algorithm is given to devise a decentralized optimal controller that globally asymptotically stabilizes the system. The effectiveness of the proposed computational control algorithm is demonstrated via the online learning control of multi-machine power systems with governor controllers.

In (TANG et al., 2014) the authors investigates the on-line learning and control approach based on ADP for wind farm control and integration with the grid. This controller can effectively damp the oscillation of the wind farm system after the ground fault of the grid.

A goal representation ADP based static compensator controller is proposed in (SU et al., 2014), to deal with the control of the voltage on the point of common coupling of wind farm.

The adaptive optimal control problem for a class of continuous-time uncertain interconnected power systems using output-feedback and ADP is presented in (GAO et al., 2016).

An online supplementary learning controller design method to compensate the traditional power system controllers for coping with the dynamic power grid is proposed in (GUO et al., 2016), due the presence of high penetration of wind generation. This is a supplementary controller based on ADP, which works alongside an existing power system controller.

An adaptive wide-area power oscillation damper based on goal representation heuristic dynamic programming algorithm for photovoltaic plant to enhance damping of the concerned inter-area mode is presented in (SHEN et al., 2017). A case study is carried out on a 16-machine 68-bus system with a large-scale photovoltaic plant.

In (YANG; HE; ZHONG, 2018) the authors proposed a robust regulation method for partially unknown continuous-time nonlinear systems subject to unmatched perturbations.

By selecting a proper value function for the auxiliary system, the algorithm converts the robust regulation problem into an optimal regulation problem. Then, the solution of the robust regulation problem is obtained by solving the optimal regulation problem. Under the framework of ADP, the authors developed a simultaneous policy iteration algorithm to derive the solution of the optimal regulation problem.

In (DUAN; XU; LIU, 2018) the authors proposed a wide-area damping control of wide-area power systems under both physical and cyber uncertainties. The cyber uncertainties addressed in this paper include both communication delay and package dropout.

In (SHEN et al., 2019), it is proposed a goal representation heuristic dynamic programming, which is one of the members of the ADP family, based on resilient wide-area damping controller for voltage source converter high voltage direct current employing redundant wide area signals as input signals to tolerate communication failure.

In (CHEN et al., 2020) a robust variable pitch controller based on ADP is proposed. Of which the purpose is to stabilize the output speed of the control system at the rated speed when the wind turbine in an environment with higher wind speed than the rated speed. On the basis of the simulation results, the authors concluded that the control performance of the proposed controller is better than others, and system speed can be maintained at the rated rotor speed basically, and it also controls the fluctuation in a small range.

In (DISSANAYAKE; EKNELIGODA, 2020) a decentralized, online optimal feedback control strategy to optimally stabilize active loads in islanded DC microgrids is proposed.

- **IFT Method**

In (SOLINGEN; MULDERS; WINGERDEN, 2017) the IFT algorithm is applied to two different turbine controllers: drivetrain damping and collective pitch control.The typical controller configurations used for wind turbine control require three closed-loop experiments to be carried out. With the data that are collected during these experiments, it has been shown that IFT can be successfully applied. The results indicate that starting the optimization from a baseline controller with decent performance can already improve the performance within a few iterations. It has also been shown that IFT can be applied to both disturbance rejection and reference tracking control for wind turbines.

- **SPSA Method**

In (DONG et al., 2018) the authors proposed a DDC strategy to solve the load frequency control problems of power systems, with complete convergence analysis. The approach is designed based on the SPSA. The data-based controller is constructed using a function approximator, which is fixed as a neural network. Being the control parameters, the connection weights of the neural network controller are updated at each iteration step. An one-area load frequency control problem with system parametric uncertainties has been introduced for simulation tests. The proposed control strategy can achieve much smaller overshoot and more stable performance than the sliding mode control method.

- **Subspace Method**

In (ZHANG et al., 2012) the authors presents an adaptive wide-area damping control scheme in which the robust stochastic subspace identification is adopted to first online identify inter-area oscillation modes and then construct the wide-area damping controllers on-demand with their parameters and input derived adaptively, and a simple but practical time delay compensator is designed to eliminate the effects of signal transmission time delay. Simulations on IEEE 16-generator 5-area test system have validated that the proposed adaptive wide-area damping control scheme is effective and robust.

- **VRFT Method**

In (CORLETA et al., 2016) the authors presents the application of VRFT approach to the control of uninterruptible power supply systems in order to obtain reference tracking for sinusoidal signals. Two controllers are designed: a resonant controller and a current feedback gain. In order to apply the VRFT to current feedback design, the VRFT method is adapted since the controller is in the feedback loop, an unusual topology to data-driven applications.

In (VALDERRAMA; HERNANDEZ, 2017) the authors presents the application of the VRFT method to control a single phase inverter. Inverters has a number of industrial applications, such as AC motor drives, renewable energies, transportation, uninterruptible power supplies. The main goal is the tracking of a sinusoidal signal able to deal with disturbances and non linear loads.

The VRFT method with flexible criterion is applied to estimate the controller gains for the output voltage regulation of dc-dc converters in (REMES et al., 2020), so the limitation due to the nonminimum phase zero, if it exists, is taken into account by the algorithm.

Based on the effectiveness and simplicity of application we chose to explore the VRFT and MFAC methods in this dissertation. Further details of these methods are presented as follows.

2.3 Virtual Reference Feedback Tuning - VRFT

2.3.1 The VRFT Idea

This method was first introduced in (GUARDABASSI; SAVARESI, 2000), and it was extended for dealing with noisy environments in (CAMPI; LECCHINI; SAVARESI, 2002). The VRFT is a direct data-driven method, which means that it is capable of directly estimating the controller parameters from a plant using only I/O data (referred as a controller identification problem (GUARDABASSI; SAVARESI, 2000)). This is an off-line design approach with low computational burden for the control synthesis (one-shot method).

To understand the basic idea of the method, consider a feedback control system illustrated in Figure 3. This physical system is composed of a process $G(z)$ and a controller $C(z;\theta)$. The transfer function $M(z)$ is defined as the reference model used by the designer to define closed-loop dynamic performance. With the control objectives specified in $M(z)$, the main goal is to estimate the value of θ (vector of parameters of the controller) for the physical plant.

To estimate the controller parameter (θ), the authors in (CAMPI; LECCHINI; SAVARESI, 2002) proposed using the concept of *virtual reference* ($\tilde{r}(k)$). This concept consists in imposing that the closed-loop system has the same transfer function as the reference model. As a result, the output of the two systems should be the same for a common $\tilde{r}(k)$. Figure 3 shows the two systems with the same *virtual reference* and output ($y(t)$). Assuming that the process model is unavailable, a set of N input-output samples $\{u(k), y(k)\}_{k=1:N}$ can be obtained from an open-loop experiment. With the reference model $M(z)$ and the output signal $y(k)$ available, the *virtual reference* signal $\tilde{r}(k)$ can be obtained using:

$$\tilde{r}(k) = M^{-1}(z)y(k) \tag{2.1}$$

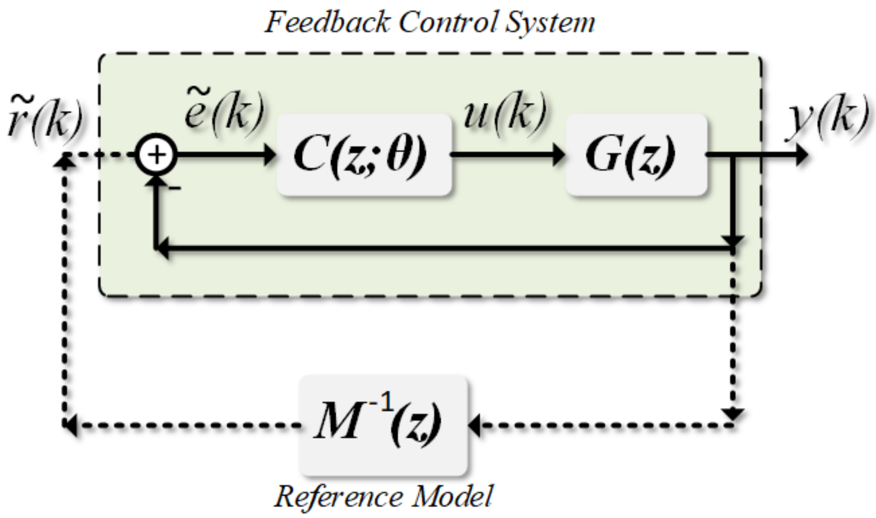

Figure 3 – Diagram of virtual reference signal.

where z is the shift operator ($z^{-1}x(k) = x(k-1)$). It should be noted that this *virtual reference* represents the signal that must be applied in reference model $M(z)$ to obtain the output $y(k)$. Considering that the reference model and physical plant have the same signals of reference and output, the virtual error in the physical plant is given by

$$\tilde{e}(k) = \tilde{r}(k) - y(k) \tag{2.2}$$

With the input ($\tilde{e}(k)$) and output ($u(k)$) signals of the controller ($C(z;\theta)$), the parameters of the controller (θ) are obtained by solving of the following optimization criterion problem:

$$J^{VR}(\theta) \triangleq \bar{E}[u(k) - C(k,\theta)\tilde{e}(k)]^2. \tag{2.3}$$

2.3.2 Mathematical Formulation

The transfer function of the linearly parameterized controller can be written as follows

$$C(z;\theta) = \theta^T \bar{C}(z), \tag{2.4}$$

where, θ is the vector of parameters, $\bar{C}(z)$ is a vector which represents the controller class, and $C(z;\theta)$ is the controller transfer function.

The VRFT aims to minimize the cost function of the reference tracking criterion $J_y(\theta)$, which takes into account only the closed loop system response $y(k,\theta)$, as follows:

$$y(k,\theta) \triangleq T(z,\theta)r(k), \tag{2.5}$$

where $T(z, \theta)$ is the closed loop transfer function system with the controller $C(z; \theta)$, and $r(k)$ is the reference signal applied in the system input.

The control objective is to make the process output as close as possible to the input to be tracked. Thus, the goal is to minimize the performance criterion of the reference tracking error, given by

$$J(\theta) = \bar{E}[r(k) - y(k, \theta)]^2. \tag{2.6}$$

Here, the $\bar{E}[.]$ is defined as

$$\bar{E}(x^2(k)) \triangleq \lim_{N\to\infty} \frac{1}{N}\sum_{k=1}^{N} \bar{E}[x^2(k)] \tag{2.7}$$

where $\bar{E}[x^2(k)]$ is the expectancy of aleatory variable $x^2(k)$.

Since perfect tracking is not possible, the tracking objective is usually relaxed into a specification of how close a tracking would be satisfactory. For that, a reference model for the $M(z)$ system is defined, which represents the desired behavior of the closed loop system, obtained from criteria such as overshoot and settling time. Thus, the desired output of the $y_d(k)$ system, given by

$$y_d(k) = M(z)r(k), \tag{2.8}$$

must be as close as possible to the real output system $y(k, \theta)$.

In this way, the control design comprises finding a set of parameters θ for the controller that, when added to the closed loop system, will make the output obtained $y(k; \theta)$ as close as possible to the desired output $y_d(k)$. Therefore, the performance criterion of the reference tracking is defined as

$$\begin{aligned} J_y(\theta) &\triangleq \bar{E}[y(k, \theta) - y_d(k)]^2 \\ &= \bar{E}[(T(z, \theta) - M(z))r(k)]^2. \end{aligned} \tag{2.9}$$

The VRFT becomes the problem of minimizing the $J_y(\theta)$ function, related to the reference tracking performance, into a problem of minimizing another cost function $J^{VR}(\theta)$, related to an ideal controller identification problem. Thus, under some conditions, the minimum of $J_y(\theta)$ is the same minimum of $J^{VR}(\theta)$ and, since $J^{VR}(\theta)$ is a quadratic function, finding the minimum of this function is simpler than finding the minimum of $J_y(\theta)$. The conditions for the global minimum of the two cost functions, $J_y(\theta)$ and $J^{VR}(\theta)$, to coincide, are translated into what is called the ideal case.

In the ideal case it is considered that the system is not affected by noise. In practice, no physical system is completely noise-free, however, when the noise level is considered small when compared to the signals generated by the system, this does not become a major problem and can be neglected. In addition to the absence of noise, in the ideal case two other assumptions must be satisfied.

Assumption 1 *The ideal controller belongs to the controller class, $C_d(z) \in \zeta$, i.e., $\exists \theta_d : C(z, \theta_d) = C_d(z)$.*

The first assumption affirms that there is a vector of desired parameters θ_d that will make the closed-loop system behave as desired, that is, there is an ideal controller $C_d(z)$ that will make the closed-loop system have the transfer function defined by $M(z)$.

Assumption 2 *The controller is linearly parameterized, i.e., $C(z, \theta) = \theta^T \bar{C}(z)$.*

This assumption affirms that it is possible to represent the controller equation in the form of a vector of parameters multiplied by the class of controllers. The vector of parameters θ is a vector of real numbers and the class of controllers $\bar{C}(z)$ is a vector formed by rational transfer functions in z. It is assumed that the rational functions of $\bar{C}(z)$ must be linearly independent on the field of real numbers, that is, it is assumed that the parameterization is minimal. There are infinite representations for the class of controllers $\bar{C}(z)$ where the rational functions of $\bar{C}(z)$ are linearly independent, which means that for each representation of $\bar{C}(z)$ the controller is determined by the respective parameter vector θ.

Therefore, assuming that the system is not affected by noise and that the two assumptions above are true, the parameters of the controller can be estimated using the VRFT method for the ideal case, as described in subsection 2.3.1.

As, in the ideal case, the controller is parameterized linearly (Assumption 2 is satisfied) the equation 2.3 can be rewritten as:

$$\begin{aligned} J^{VR}(\theta) &= \bar{E}[u(k) - \theta^T \bar{C}(z)\tilde{e}(k)]^2 \\ &= \bar{E}[u(k) - \theta^T \varphi(k)]^2. \end{aligned} \tag{2.10}$$

where, $\varphi(k)$ is the regressor vector, i.e.,

$$\begin{aligned} \varphi(k) &= \bar{C}(z)\tilde{e}(k) \\ &= \bar{C}(z)\frac{1 - M(z)}{M(z)} y(k). \end{aligned} \tag{2.11}$$

The problem of finding the global minimum of the equation (2.10) can be seen as a problem of least squares (BAZANELLA; CAMPESTRINI; ECKHARD, 2011), to solve this problem the normal equation is solved, that is, the controller parameters can be estimated as follows:

$$\theta^* = \left[\sum_{k=1}^{N} \varphi(k)\varphi^T(k)\right]^{-1} \sum_{k=1}^{N} \varphi(k)u(k). \tag{2.12}$$

In the ideal case, where the system is not affected by noise, the estimated value for θ^* is the exact value that will cause the closed loop system to have the desired behavior, defined by the transfer function $M(z)$.

However, if the input data $u(k)$ and output $y(k)$ of the process present non-neglect noise, the controller obtained will be biased; the controller found will not be an optimal controller. In these cases in which the noise present in the system is more pronounced, the VRFT method with instrumental variable can be used, but this approach will not be detailed in this work. A detailed explanation of this methodology can be found in (BAZANELLA; CAMPESTRINI; ECKHARD, 2011).

2.3.3 The Mismatched Case

In the mismatched case, the assumption 2 is not satisfied, that is, the ideal controller does not belong to the class of controllers, and the other two assumptions remain, the system is not affected by noise, and the controller is linearly parameterized.

When the controller has full order the ideal case works correctly. In the mismatched case the controller does not have full order, that is, the ideal controller does not belong to the class of controllers. It so happens that the minimum of $J^{VR}(\theta)$ can be quite different from the minimum of $J_y(\theta)$, however this problem can be mitigated by properly filtering the data to be used to calculate the parameters of the controller (BAZANELLA; CAMPESTRINI; ECKHARD, 2011).

In order to find the filter $L(e^{jw})$ that will solve the problem of the mismatched case, first the two criteria $J_y(\theta)$ and $J^{VR}(\theta)$ will be compared through their expressions in the frequency domain.

The equation (2.9) can be rewritten, using Parseval´s theorem, as follows, :

$$\begin{aligned} J_y(\theta) = \frac{1}{2\pi} \int_{-\pi}^{\pi} &|G(e^{jw})|^2 |S(e^{jw}, \theta)|^2 |S_d(e^{jw})|^2 \\ &\times |C(e^{jw}, \theta) - C_d(e^{jw})|^2 \Phi_r(e^{jw})\, d\omega \end{aligned} \tag{2.13}$$

where $S(e^{jw})$ is the sensitivity function of the system, and $S_d(e^{jw})$ is the desired sensitivity function, i.e., the sensitivity function that results from adding the ideal controller $C_d(z, \theta)$ to the process.

To obtain an expression for $J^{VR}(\theta)$, first, the signals $u(k)$ and $\widetilde{e}(k)$ are filtered through a filter defined as $L(z)$, obtaining the following expression for the cost function in question

$$\begin{aligned} J^{VR}(\theta) &= \bar{E}[L(z)(u(k) - C(z,\theta)\widetilde{e}(k))]^2 \\ &= \bar{E}\left[L(z)\left(u(k) - \left(C(z,\theta)\frac{1-M(z)}{M(z)}\right)y(k)\right)\right]^2 \end{aligned} \tag{2.14}$$

The equation (2.14) can be rewritten as

$$\begin{aligned} J^{VR}(\theta) = \frac{1}{2\pi}\int_{-\pi}^{\pi} &|L(e^{jw})|^2\frac{|G(e^{jw})|^2|S_d(e^{jw})|^2}{|M(e^{jw})|^2} \\ &\times |C_d(e^{jw}) - C(e^{jw},\theta)|^2\Phi_u(e^{jw})\, d\omega \end{aligned} \tag{2.15}$$

A detailed explanation of how to find these expressions can be found at (BAZANELLA; CAMPESTRINI; ECKHARD, 2011).

The core idea is to make the two cost functions $J_y(\theta)$ and $J^{VR}(\theta)$ equal, making the overall minimum of these two functions coincide. For this, the filter $L(e^{jw})$ must respect the following equation.

$$|L(e^{jw})|^2 = |M(e^{jw})|^2|S(e^{jw},\theta)|^2\frac{\Phi_r(e^{jw})}{\Phi_u(e^{jw})}, \quad \forall\omega \in [-\pi;\pi]. \tag{2.16}$$

However, $S(e^{jw},\theta)$ is unknown, since the transfer function of the $G(z)$ system is unknown, so an estimate for $S(e^{jw},\theta)$ must be found. The estimate used by the VRFT method is given by

$$|S(e^{jw},\theta)|^2 \approx |S_d(e^{jw}|^2 = |1 - M(e^{jw})|, \tag{2.17}$$

which is probably not the only possible approach. However, this approximation is quite reasonable because it is expected that the two sensitivity functions $S(e^{jw},\theta)$ and $S_d(e^{jw})$ are very close to each other around the global minimum. Based on this, the equation (2.20) for the filter $L(e^{jw})$ can be rewritten as

$$|L(e^{jw})|^2 = |M(e^{jw})|^2|1 - M(e^{jw})|^2\frac{\Phi_r(e^{jw})}{\Phi_u(e^{jw})}, \quad \forall\omega \in [-\pi;\pi]. \tag{2.18}$$

When the input signal $u(k)$ is selected by the designer, then $\Phi_u(e^{jw})$ is known, otherwise it must be estimated (CAMPI; LECCHINI; SAVARESI, 2002). When it is possible to choose that the input signal of an open loop experiment is the same signal that is usually applied to the process as a reference signal, the spectra $\Phi_r(e^{jw})$ and $\Phi_u(e^{jw})$ are the same, which provides

$$\frac{\Phi_r(e^{jw})}{\Phi_u(e^{jw})} = 1, \tag{2.19}$$

resulting in

$$L(e^{jw}) = M(e^{jw})(1 - M(e^{jw})). \tag{2.20}$$

Thus, the vector of parameters can be computed as

$$\widetilde{\theta} = \bar{E}\left[\varphi_L(k)\varphi_L^T(k)\right]^{-1}\bar{E}[\varphi_L(k)u_L(k)], \tag{2.21}$$

where $\varphi_L(k)$ and $u_L(k)$ are, respectively, the vector $\varphi(k)$ and the signal $u_L(k)$ filtered through the filter $L(e^{jw})$.

In this case, θ^* is equal to the value of $\widetilde{\theta}$ and the controller parameters can be estimated by solving the following equation:

$$\theta^* = \left[\sum_{k=1}^{N} \varphi_L(k)\varphi_L^T(k)\right]^{-1} \sum_{k=1}^{N} \varphi_L(k)u_L(k). \tag{2.22}$$

2.4 Model-Free Adaptive Control

Model Free Adaptive Control (MFAC), as its name indicates, is an adaptive control which does not need any information of system model, and it uses I/O data of the controlled system to design a controller, even without any information of the system (HOU; JIN, 2013). In this section, the fundamental tool for the MFAC system design, and the dynamic linearization data modeling method are presented.

2.4.1 Universal Process Model

Consider a class of nonlinear discrete-time systems described by

$$y(k+1) = f[U_k^{k-n}, u(k), Y_{k-1}^{k-m}, k+1] \tag{2.23}$$

where $u(k) \in R$ and $y(k) \in R$ are the control input and the system output at time instant k, respectively, n and m are unknown orders of input and output respectively, $f(.)$ is a general nonlinear function, Y_{k-1}^{k-m} is $y(k), \ldots, y(k-m)$, U_k^{k-n} is $u(k), \ldots, u(k-n)$, and R is a real number set.

The system in (2.23) needs to meet the following assumptions:

1. It is generalized Lipschitz, that is to say, $\Delta y(k+1) \leq b\Delta u(k)$, is reasonable for any k and $\Delta u(k) \neq 0$. Where $\Delta y(k+1) = y(k+1) - y(k)$, $\Delta u(k) = u(k) - u(k-1)$, and b is a constant.

2. Regarding to control input $u(k)$, the partial derivative of $f(.)$ is considered as smooth (so-called derivatives of function are continuous and available for all orders around its domain).

3. It is observable and controllable.

Considering the nonlinear system (2.23) and the proposed assumptions (1) and (2), there exists a time-varying parameter as Pseudo Partial Derivative (PPD) $\varphi(k)$ at each time interval. Generally, PPD can be considered as a slow time-varying parameter in the case of small sampling time and $\Delta u(k)$. It is worth mentioning that the PPD is theoretically determined for nonlinear systems using rigorous analysis (see proof 1). The definition of PPD considering a simple nonlinear system as $y(k+1) = f(u(k))$ is illustrated in Figure 4. Accordingly, Figure 4 clearly shows the PPD representation as a derivative value of the nonlinear function $f(.)$ between $u(k-1)$ and $u(k)$ at a certain sample time.

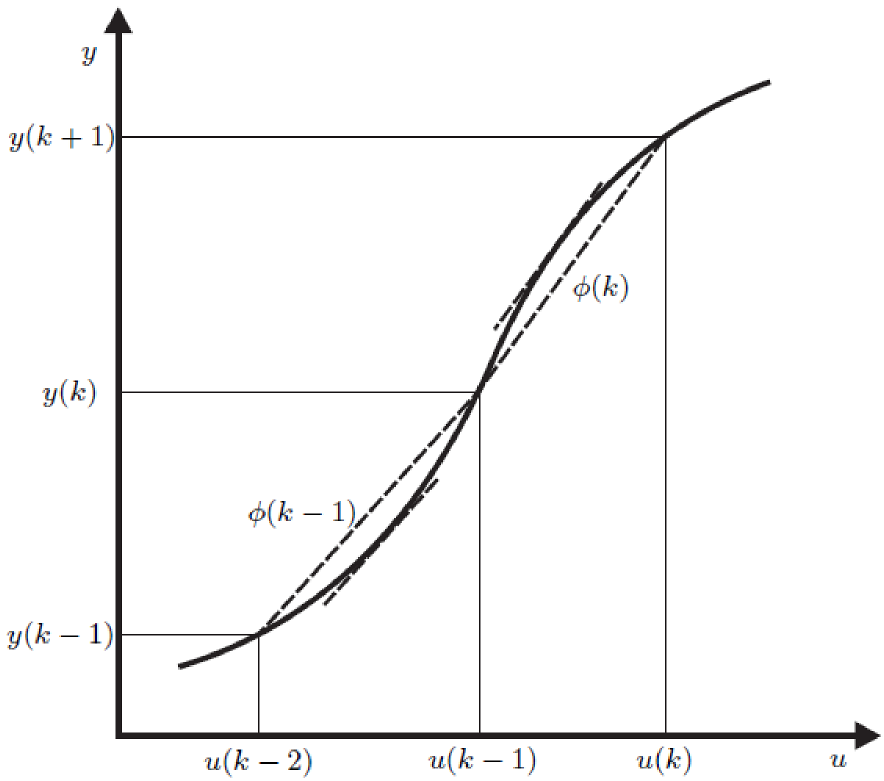

Figure 4 – Geometric Interpretation of PPD concept from (HOU; JIN, 2013).

Using PPD, a Compact Form Dynamically Linearization (CFDL) model can be written as

$$\Delta y(k+1) = \varphi(k)\Delta u(k) \tag{2.24}$$

where $|\varphi(k)| \leq b$ is bounded for any time interval k, $\varphi(k)$ are time-varying parameters, and $\Delta y(k) = y(k) - y(k-1)$. The proposed CFDL method uses only one step of previous input and output data.

Proof 1. Considering the nonlinear system (2.23) and defining $\Delta y(k) = y(k) - y(k-1)$, the change of system output can be obtained as (HOU; JIN, 2013)

$$\begin{aligned}
\Delta y(k+1) = {} & f(y(k), \cdots, y(k-n), u(k), \cdots, u(k-m)) \\
& - f(y(k), \cdots, y(k-n), u(k-1), u(k-1), \cdots, u(k-m)) \\
& + f(y(k), \cdots, y(k-n), u(k-1), u(k-1), \cdots, u(k-m,)) \\
& - f(y(k-1), \cdots, y(k-n-1), u(k-1), \cdots, u(k-m-1)).
\end{aligned} \tag{2.25}$$

According to assumption 2 and the differential mean value theorem, the dynamically linearization description (2.25) can be rewritten as

$$\Delta y(k+1) = \frac{\partial f}{\partial u(k)} \Delta u(k) + \Upsilon, \tag{2.26}$$

where $\frac{\partial f}{\partial u(k)}$ denotes the partial value of $f(.)$ considering $(n+2)th$ variable at a certain point between

$$[y(k), \cdots, y(k-n), u(k-1), u(k-1), \cdots, u(k-m)]^T,$$

and

$$[y(k), ..., y(k-n), u(k), u(k-1), ..., u(k-m)]^T.$$

Here $\Upsilon(k)$ denotes

$$\begin{aligned}
\Upsilon = {} & f(y(k), \cdots, y(k-n), u(k-1), u(k-1), \cdots, u(k-m)) \\
& - f(y(k-1), \cdots, y(k-n-1), u(k-1), \cdots, u(k-m-1)).
\end{aligned}$$

For every fixed time k, the following equation can be considered using a scalar variable $\Gamma(k)$ as

$$\Upsilon(k) = \Gamma(k)\Delta u(k). \tag{2.27}$$

With considering the condition $|\Delta u(k)| \neq 0$, equation (2.27) has at least one solution for $\Gamma(k)$. Consequently, the obtained structure (2.26) can be written as

$$\Delta y(k+1) = \underbrace{\left(\frac{\partial f}{\partial u(k)} + \Gamma(k)\right)}_{\varphi(k)} \Delta u(k). \tag{2.28}$$

According to the assumption 1 ($|\Delta y(k+1)| \leq b|\Delta u(k)|$) it can be concluded that $|\varphi(k)| \leq b$. It is worth mentioning that all variables and definitions used in proof 1 are considered as scalar.

Considering the condition $|\Delta u(k)| \neq 0$ in the procedure of MFAC algorithm, it is assumed that in the case of $|\Delta u(k)| = 0$, a slightly different dynamic linearization is considered by shifting $\sigma_k \in Z^+$ time instants to ensure $u(k) \neq u(k - \sigma_k)$ (further information about the proposed assumption refer to (HOU; JIN, 2013)).

According to the properties and conditions of model-free approaches, the states and state space model of the system are completely unknown. Therefore, the existence of appropriate control inputs cannot be guaranteed using non-singularity of the controllability matrix. To prove controllability of the unknown nonlinear system (2.23), the authors (HOU; JIN, 2013) assume that the system is controllable if PPD is neither zero nor infinite for all sample times. Therefore, the boundedness of PPD is determined considering the generalized Lipschitz condition (see proof 1).

Remark 1. It is worth noting that to satisfy the conditions mentioned in assumption 1, some adjustable parameters should be considered in designing the control law and estimation of the PPD to obtain suitable change rate of the control input signal (HOU; JIN, 2013).

2.4.2 Model-Free Adaptive Control Algorithm

To obtain the control law, the one-step-ahead controller idea is used, which generally leads to steady-state tracking error. In particular, one of the usual objective functions to estimate the time-varying parameters is to minimize the square of the error between real system output and model output. Considering the estimation algorithm derived from this kind of objective function, the estimated parameter value is often sensitive to some inaccurate data, which may be caused by disturbance or faulty sensors. Therefore, the following objective function has to be considered as

$$J(u(k)) = |y^*(k+1) - y(k+1)|^2 + \lambda|u(k) - u(k-1)|^2 \tag{2.29}$$

where $y^*(k+1)$ is the desired output and λ is the penalty weighted factor.

In (2.29), $|y^*(k+1) - y(k+1)|^2$ can reduce the steady tracking error and $\lambda|u(k) - u(k-1)|^2$ can restrict the change in control input.

If the case $\Delta u(k) = 0$ comes forth at certain sampling time, equation (2.23) can be transformed into Compact Form Dynamic Linearization (CFDL) model as

$$y(k+1) - y(k-\sigma+1) = \varphi(k)[u(k) - u(k-\sigma)] \tag{2.30}$$

and

$$y(k+1) = y(k) + \varphi(k)\Delta u(k) \tag{2.31}$$

By substituting equation (2.31) to equation (2.29) and solving $\frac{\partial J(u(k))}{\partial u(k)} = 0$, the control law $u(k)$ is obtained as follows

$$u(k) = u(k-1) + \frac{\rho\hat{\varphi}(k)}{\lambda + ||\hat{\varphi}(k)||^2}[y^*(k+1) - y(k)] \tag{2.32}$$

where ρ is the step factor. This control law (2.32) thus obtained is model-free, order-free and only I/O data-related.

In the control law defined by (2.32), the only unclear parameter is the characteristic parameters $\varphi(k)$, so the main task is to find it. There are several ways for estimating this parameter such as recursive least square approach. The necessary condition that the universal model (2.24) could be used in practice is that the estimation of $\varphi(k)$, denoted $\hat{\varphi}(k)$, is available in real-time, and is sufficiently accurate.

Consider the estimation criterion function as

$$J(\varphi(k)) = |y^*(k+1) - y(k+1) - \varphi(k)\Delta u(k)|^2 + \mu|\varphi(k) - \hat{\varphi}(k-1)|^2 \tag{2.33}$$

The equation (2.33) can be estimated as given by

$$\hat{\varphi}(k) = \hat{\varphi}(k-1) + \frac{\eta\Delta u(k-1)}{\mu + ||\Delta u(k-1)||^2}[\Delta y(k) - \hat{\varphi}(k-1)\Delta u(k-1)] \tag{2.34}$$

$$\hat{\varphi}(k) = \hat{\varphi}(1) \quad \text{if} \quad |\hat{\varphi}(k)| \leq \varepsilon \quad \text{or} \quad |\Delta u(k-1)| \leq \varepsilon \tag{2.35}$$

where $\lambda > 0$, $\mu > 0$, $\rho \in (0, 1]$, $\eta \in (0, 2]$, and ε is a small positive constant.

Remark 2. Regarding Remark 1, the step size constant η is added to obtain a general algorithm and to analyze the stability analytically.

Remark 3. For the nonlinear system in the proposed model-free concept (2.24), a suitable $\varphi(k)$ exists when $|\Delta u(k)| \neq 0$. To satisfy the condition $|\Delta u(k)| \neq 0$ noted in assumption 1 and to improve tracking time-varying performance regarding parameter estimation, a sufficient measurement of estimation algorithm is considered (2.35).

The equations (2.32), (2.33) and (2.34) are the MFAC laws which do not need to specify a particular controlled system, are unrelated with the mathematical model and the order of the controlled system.

2.4.3 Stability Analysis

Assumption 4. It is assumed that for a given bounded desired output signal $y^*(k+1)$, there exists a bounded control input $u(k)$. Briefly, the nonlinear system (2.23) is assumed as controllable.

Theorem 1. Suppose that assumptions 1, 2, and 4 are satisfied for the considered nonlinear system (2.23). If the weighting factor in control law (2.32) is designed as $\lambda > \lambda_{min}$ with $\lambda_{min} > 0$ as a positive value, the control-loop system with CFDL MFAC is asymptotically stable.

Proof 2. Assume that one of the conditions $|\varphi(k)| \leq \varepsilon$ or $|\Delta u(k)| \leq \varepsilon$ is satisfied. Then the boundedness of $\hat{\varphi}(k)$ is straightforward. By using PPD estimation error as $\varphi_{est}(k) = \hat{\varphi}(k) - \varphi(k)$ and parameter estimation algorithm (2.34), the PPD estimation error $\varphi_{est}(k)$ is achieved as (HOU; JIN, 2013)

$$\varphi_{est}(k) = \left(1 - \frac{\eta|\Delta u(k-1)|^2}{\mu + |\Delta u(k-1)|^2}\right)\varphi_{est}(k-1) + \varphi(k-1) - \varphi(k). \tag{2.36}$$

By taking absolute value on both sides of (2.36) yields

$$|\varphi_{est}(k)| \leq \left|\left(1 - \frac{\eta|\Delta u(k-1)|^2}{\mu + |\Delta u(k-1)|^2}\right)\right| |\varphi_{est}(k-1)| + |\varphi(k-1) - \varphi(k)|. \tag{2.37}$$

Therefore, the term $\frac{\eta|\Delta u(k-1)|^2}{\mu+|\Delta u(k-1)|^2}$ is monotonically increasing based on $|\Delta u(k-1)|^2$ and its minimum value is $\frac{\eta\varepsilon^2}{\mu+\varepsilon^2}$. Considering $0 < \eta \leq 2$ and $\mu > 0$, there exists a constant d_1 that leads to

$$0 \leq \left|\left(1 - \frac{\eta|\Delta u(k-1)|^2}{\mu + |\Delta u(k-1)|^2}\right)\right| \leq 1 - \frac{\eta\varepsilon^2}{\mu + \varepsilon^2} = d_1 < 1. \tag{2.38}$$

Furthermore, assuming $|\varphi(k)| \leq b$ in proof 1 yields $|\varphi(k-1) - \varphi(k)| \leq 2b$. Therefore, by combining (2.37) and (2.38) implies that

$$|\varphi_{est}(k)| \leq d_1|\varphi_{est}(k-1)|+2b \leq d_1^2|\varphi_{est}(k-2)|+2d_1b+2b \leq \cdots \leq d_1^{k-1}|\varphi_{est}(1)|+\frac{2b(1-d_1^{k-1})}{1-d_1} \tag{2.39}$$

which denotes that $\varphi_{est}(k)$ is bounded.

By defining the output tracking error as $e(k+1) = y^* - y(k+1)$ and substituting CFDL model (2.24), the absolute value is achieved as

$$\begin{aligned} |e(k+1) = |y^* - y(k+1)| &= |y^* - y(k) - \varphi(k)\Delta u(k)| \\ &\leq \left|1 - \frac{\rho\varphi(k)\hat{\varphi}(k)}{\lambda + |\varphi(k)|^2}\right| |e(k)|. \end{aligned} \tag{2.40}$$

According to the mentioned assumptions and (2.35), let assume $\lambda_{min} = b^2/4$. Considering the boundedness of $\hat{\varphi}(k)$, there exists a constant value as $0 < M < 1$ yielding

$$0 < M \leq \frac{\varphi(k)\hat{\varphi}(k)}{\lambda + |\hat{\varphi}(k)|^2} \leq \frac{b\hat{\varphi}(k)}{\lambda + \hat{\varphi}(k)} \leq \frac{b\hat{\varphi}(k)}{2\sqrt{\lambda}\hat{\varphi}(k)} < \frac{b}{2\sqrt{\lambda_{min}}} = 1 \tag{2.41}$$

Based on (3.22) and $\lambda > \lambda_{min}$, there exists a positive constant $d_2 < 1$ as

$$\left|1 - \frac{\rho\varphi(k)\hat{\varphi}(k)}{\lambda + |\varphi(k)|^2}\right| = 1 - \frac{\rho\varphi(k)\hat{\varphi}(k)}{\lambda + |\varphi(k)|^2} \leq 1 - \rho M = d_2 < 1 \tag{2.42}$$

Combining (2.40) and (2.42), the reference tracking error converges to zero under the proposed model-free adaptive CFDL control law as follows

$$|e(k+1)| \leq d_2|e(k)| \leq d_2^2|e(k-1)| \leq \cdots \leq d_2^k|e(1)|. \tag{2.43}$$

2.5 Summary

In this chapter, the concepts of DDC and the main methods were presented. Besides, a literature review of its application in power system showed the vast opportunity in this field, mainly in coordinate voltage problems. The mathematical formulation and the steps to design a controller using VRFT and MFAC algorithm were discussed. In the next Chapter, it will be presented a description of the SVC control scheme in power systems.

3 SVC Control Scheme

3.1 Introduction

The main goal of this chapter is to show the physical characteristics involved in a SVC scheme. The processed signals involved and its generators are described in details. Besides, a real scheme is presented, in order to compare its performance with the DDC methods designed in this work.

3.2 Control Scheme

The multilevel control scheme used in this work is composed of the PVC (only local measurements) and the SVC (remote pilot bus measurements). This hierarchical control structure is presented in Figure 5. Practically, the PVC assures the minimum performance level required for the system, and it is located close to the generator plants. The SVC is located at a central level, such the Energy Management System (EMS), to be able to optimize the performance of the local controllers. To reach this goal, the SVC controller must be able to process real-time signals (voltage magnitudes) from selected pilot buses $(y_1(k), ..., y_n(k))$. The voltages of the pilot buses are measured by PMUs and processed by the SVC in order to provide the appropriate control signals to the AVR reference $(u_1(k), ..., u_n(k))$ at each local generator. These control signals must keep the power system voltage profile at a desired threshold.

According to previous works (SANCHA et al., 1996), (ARCIDIACONO, 1983) the structure of the SVC controller must take into account the capability of the generator to control the voltage in a selected pilot bus. This capability is clearly determined by the electrical distance of the generators from the pilot bus. As suggested in (SANCHA et al., 1996), (ARCIDIACONO, 1983) it is better to divide the power system in control areas following the selection of the pilot buses. Additionally, the SVC control design must be coordinated, otherwise some oscillations or even unstable oscillations may show up. These oscillations come from the iteractions between controllers of neighboring areas.

3.3 Italian Secondary Voltage Regulation

The Italian hierarchical voltage control consists of a tertiary and secondary voltage regulation added to generator (PVC) to improve the voltage stability (Figure 6). An optimization criterion is used to provide the optimal voltage set points for the pilot buses in the National Voltage Regulator (NVR). The secondary level (RVR - Regional Voltage Regulators) includes the reactive power regulator, which is basically integral controls, able

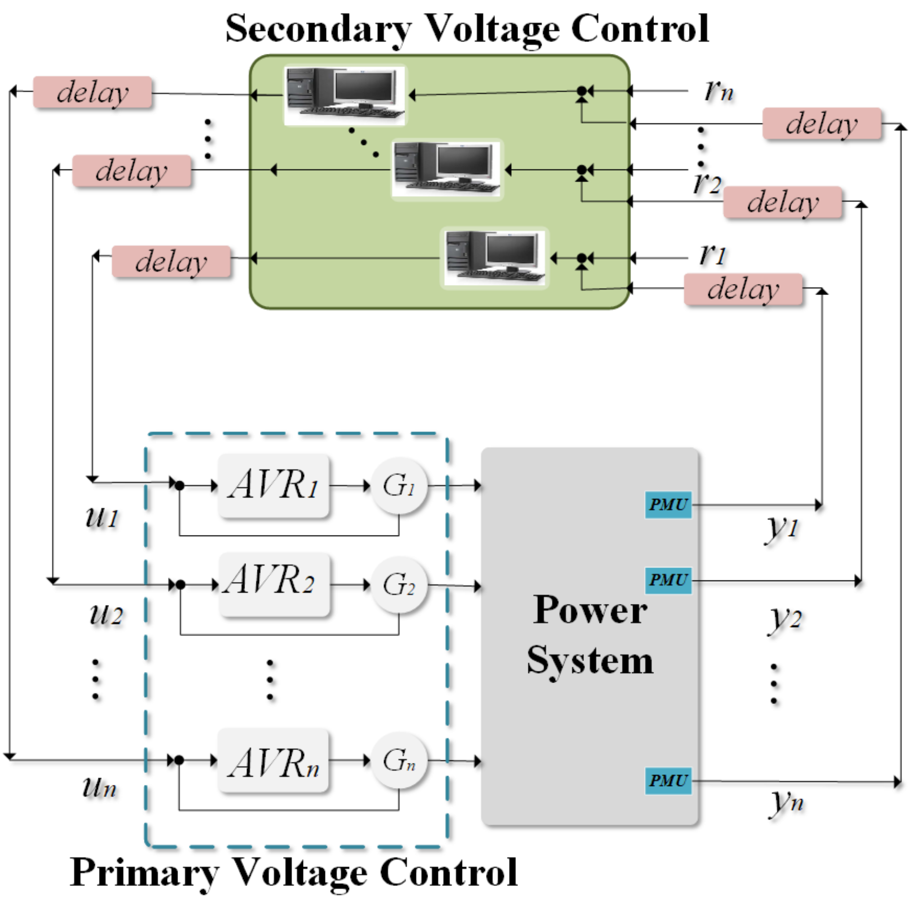

Figure 5 – SVC control structure.

to operate to achieve SVR. The primary level includes the classical AVR units already operating in the power plants. The Italian hierarchical voltage control regulates pilot node voltages in closed loop through real-time control of the reactive resources that influence those buses most. Regional voltage regulators close the control loops of pilot node voltages, providing each area with a specific reactive power level, one which controls the local power plant's voltage and reactive power regulators. The generators that control each pilot node are then chosen through a sensitivity analysis (CAñIZARES et al., 2005).

Figure 7 presents the control blocks used to model the various regulators, where in terms of time constants it is assumed that AVR (ms) < PQR ($T_{vsc} = 5s$) < RVR ($T_{qsc} = 50s$), to establish the hierarchical characteristics of these controllers. Observe that the limits on the PQR control block set the limits on the AVR input to 15% and -20%.

The controllers parameters are computed as follow.

$$K_{psc} = \frac{1}{Q_{g_{M/n}} X_t} \tag{3.1}$$

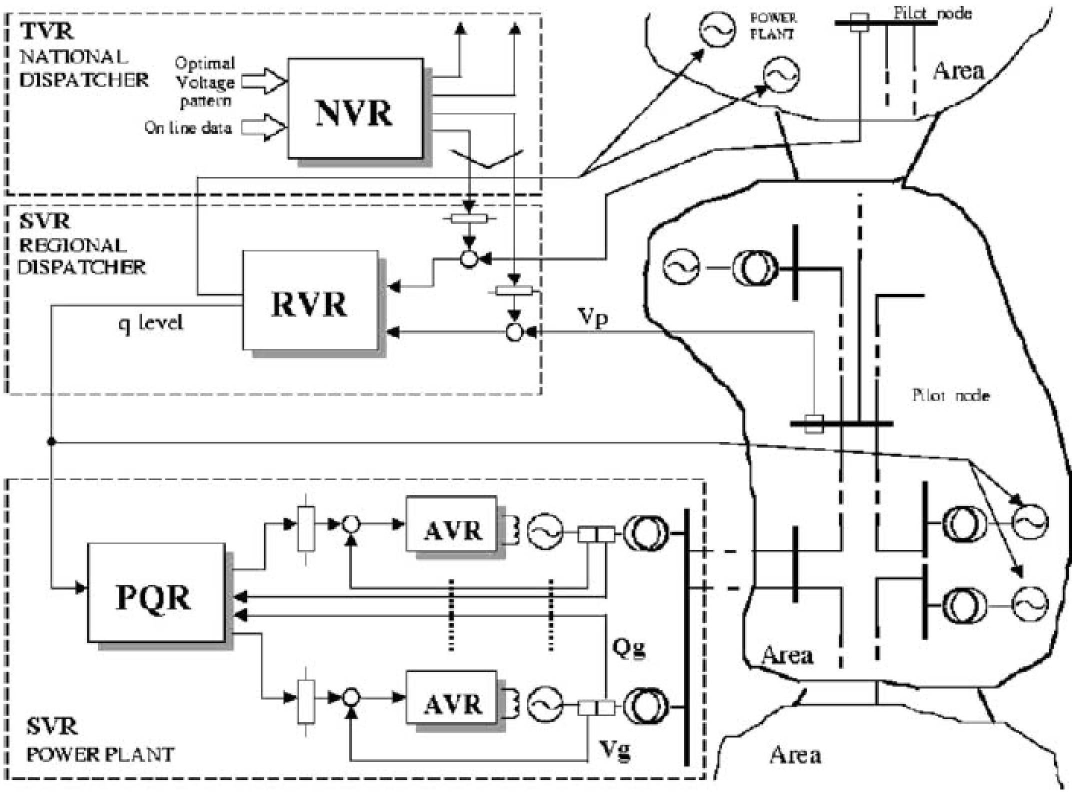

Figure 6 – Italian Hierarchical Voltage Control Structure (CAñIZARES et al., 2005).

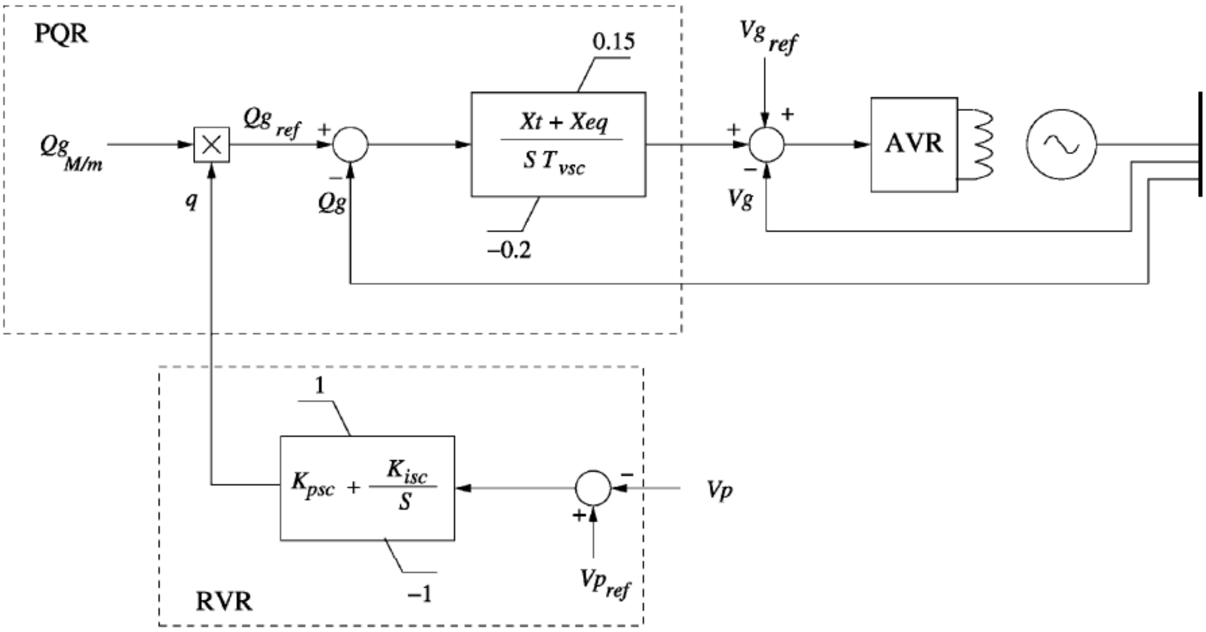

Figure 7 – Generator SVR controller (CAñIZARES et al., 2005).

$$
\begin{aligned}
K_{isc} &= \frac{1 + K_{psc} Q_{g_{M/n}} X_{eq}}{T_{qsc} Q_{g_{M/n}} X_{eq}} \\
T_{qsc} &= 50s \\
T_{vsc} &= 5s \\
&\begin{cases} Q_{g_{ref}} = q Q_{g_M} \quad for \quad 0 < q < 1 \\ Q_{g_{ref}} = -q Q_{g_M} \quad for \quad -1 < q < 0 \end{cases}
\end{aligned}
\tag{3.2}
$$

where X_t and X_{eq} are the generator's transformers reactance and the equivalent reactance from the generator terminals to the pilot bus, respectively. Q_g represents the generator reactive power, and its maximum and minimum limits, Q_{g_M} and Q_{g_m}. V corresponds to the bus voltage magnitudes, and K_{psc} and K_{isc} are the PI gains of the RVR controller.

In this work, the Italian SVC system is used to compare the performance with the proposed DDC methods.

3.4 Summary

In this chapter, the SVC control scheme was presented. The Italian coordinate scheme showed that a PI controller leads the SVC control. Real SVCs control systems were discussed and they will the basis of comparisons for further developments. In the next Chapter, two data-driven methodologies will be presented to design SVC control schemes.

4 Methodology

4.1 Introduction

The aim of this chapter is to present the detailed steps to design an entire secondary voltage scheme using the VRFT and MFAC algorithm. Some guidelines are presented to choose the reference model in VRFT algorithm. In the MFAC algorithm, the choice of parameters is not described in details in literature, but some methods are discussed in this chapter, and a proposal using a complete data-driven MFAC initialization is presented.

4.2 VRFT Methodology

4.2.1 Select pilot buses and generators

Selecting the pilot buses is an important part of the SVC design. One of the first methodologies for determining pilot bars and choosing control zones was proposed in (LAGONOTTE et al., 1989) using network structural analysis, and electrical distance concepts. Another methodology, quite simple and with low computational effort, is based on the concept of buses that have high levels of short circuit power, as these buses impose the voltage value on the electrically close buses. This method proved to be efficient when applied to the Italian system (CAñIZARES et al., 2005). In this work, the choice of pilot buses was based on the methodologies presented in (ZHAO; LU, 2018) and (CAñIZARES et al., 2005).

As generators are readily available reactive power sources, additional equipment as static and synchronous compensator, is not required for the proposed application. In (CAñIZARES et al., 2005), the generators that control each pilot node are then chosen through a sensitivity analysis based on the sensitivity matrix $\frac{\partial V_p}{\partial Q_g}$, where V_p corresponds to the pilot node voltages and Q_g are the system generator powers. The largest inputs on this matrix define the generators that should be associated with the pilot nodes.

4.2.2 Probing Signal

Once the pilot buses and generators have been chosen, a probing signal must be applied to obtain the dynamics between the system's inputs (generators) and outputs (pilot buses). The core idea is that the dynamics of pilot bus voltage, under any change in generator reference, should be modeled from the data. In this work, a step signal with controlled amplitude is applied to the AVR of each generator, and then the voltages in the pilot buses are collected by the PMU measurements.

4.2.3 Choice of Controller Structure

The VRFT belongs to the class of methods in which the controller design is based only on the input and output data of the system, with a fixed and pre-specified controller structure. Thus, the problem of the controller design is summarized in a problem of parametric identification, where the structure of the controller is known, and its parameters are linear. The main issue in this kind of methods is how to determine controller structure for a given controlled plant. Obtaining good controller structure with unknown parameters, especially for general nonlinear systems, is quite difficult. It can be as hard as modeling a plant (HOU; WANG, 2013).

In this work, the PI controller is chosen, since its structure is linear in the parameters, and for this reason can be tuned by VRFT approach. Besides, in the SVC problems this structure is widely used, as presented in (CAñIZARES et al., 2005).

The control law of an ideal PI controller is given by

$$u(t) = K_p e(t) + K_i \int_0^t e(\tau) d\tau \tag{4.1}$$

where K_p and K_i are the proportional and integral gains, respectively. The signal $u(t)$ and $e(t)$ are the control signal, and the error between the reference signal and the output of the plant.

Applying the Euler method to (4.1)

$$\begin{aligned} C(z, K_p, K_i) &= K_p + K_i T_s \frac{1}{1 - z^{-1}}, \\ C(z, K_p, K_i) &= [K_p \quad K_i] \begin{bmatrix} 1 \\ \frac{T_s}{1 - z^{-1}} \end{bmatrix}, \\ C(z, \theta) &= \theta^T \bar{C}(z). \end{aligned} \tag{4.2}$$

where $\theta = [K_P \quad K_i]^T$ and T_s is the sampling time.

4.2.4 Reference Model

A closed-loop transfer function represents the desired system performance. The choice of parameters that make up the reference model should be driven by process constraints, and input constraints, etc. Fast controllers require high control effort, which can saturate them more easily, while slow controllers may not be efficient under disturbances. The SVC has a slower response when compared with the PVC. Therefore, the reference model $M(z)$ should be defined according to the dynamics expected for the SVC.

In (BAZANELLA; CAMPESTRINI; ECKHARD, 2011), the authors warn that some precautions must be taken when choosing reference models to avoid problems that may interfere with the proper behavior of the closed loop system. Therefore, two guidelines are presented by the authors:

Guideline 1. (Causality of the controller) The relative degree of the reference model cannot be smaller than the relative degree of the process.

Guideline 2. (Internal stability with non-minimum phase process) The non-minimum phase zeros of the process must be included in the reference model.

Based on this, a procedure to automatically determine the appropriate reference model is presented by (SILVA; CAMPESTRINI; BAZANELLA, 2014), using three different kind of reference models. Firstly, using the same data collected for the controller design, a model for the process with $G(z, \beta)$ is estimate by an identification process

$$\begin{aligned} G(z,\beta) &= \frac{(\beta_1 + \beta_2 z^{-1})z^{-nk}}{1+\beta_3 z^{-1} + \beta_4 z^{-2}} \\ &= \frac{K(1-fz^{-1})z^{-nk}}{(1-p_{z_1}z^{-1})(1-p_{z_2}z^{-1})}, \end{aligned} \tag{4.3}$$

which represents the open-loop behavior of the process. The second step is to vary nk from 1 to 10 and estimate models using these different values. The goal is to find the model which presents the minimum value of $\bar{E} = [y(k) - G(z,\beta)u(k)]$. The model with the minimum error presents important information, as the relative degree of the system (nk), identify the non-minimum phase zero, if it exists, and the presence or absence of overshoot (p_1 and p_2).

All three reference models are parametrized to present a desired response with zero steady-state error. The reference models are described below:

Model 1:

$$M_1(z) = \frac{1-a}{1-az^{-1}} z^{-nk}, \tag{4.4}$$

This model represents a desired behaviour with no overshoot, and depends on the process's time delay (nk), and the dominant discrete pole a, which can be computed as follow

$$a = e^{\frac{-4T_s}{t_s}} \tag{4.5}$$

where t_s is the desired settling time.

Model 2:

$$M_2(z) = \frac{(1-a)(1-b)}{(1-az^{-1})(1-bz^{-1})} z^{-nk}, \tag{4.6}$$

This model represents a desired behaviour with or without overshoot, and depends on the process's time delay (nk), and two poles a and b. These poles are chosen by performance criteria largely found in the literature, as maximum overshoot and settling time. The complete mathematical formulation can be found in (SILVA; CAMPESTRINI; BAZANELLA, 2014).

Model 3:

$$M_3(z) = \frac{\frac{(1-a)(1-b)}{(1-c)}}{(1-az^{-1})(1-bz^{-1})}(1-cz^{-1})z^{-nk}, \tag{4.7}$$

This model represents a desired behaviour with or without overshoot, may contain a non-minimum phase zero, depends on the process's time delay (nk), two poles a and b (which are chosen as in Model 2), and a zero c. If the zero of the identified process is nonminimum phase, then c is equal to this zero. If not, this zero is located in a position between the two poles of the model.

The algorithm below summarizes choosing the reference model, and Figure 8 summarizes the VRFT-SVC methodology:

Algoritmo 1: Reference Model Choice

Input: $U = u(k), \cdots, u(k-N)$
`// Collected input data`

Output: $Y = y(k), \cdots, y(k-N)$
`// Collected output data from the process`

Identify $G(z, \beta)$ according to (4.3)
if *Zero is non-minimum phase* **then**
    Use **Model 3**
else
    if *The identified poles are complex* **then**
        Use **Model 2**
    else
        if *Dominance does not exist between real poles* **then**
            Use **Model 3**
        else
            if *Overshoot is non-zero* **then**
                Use **Model 2**
            else
                Use **Model 1**

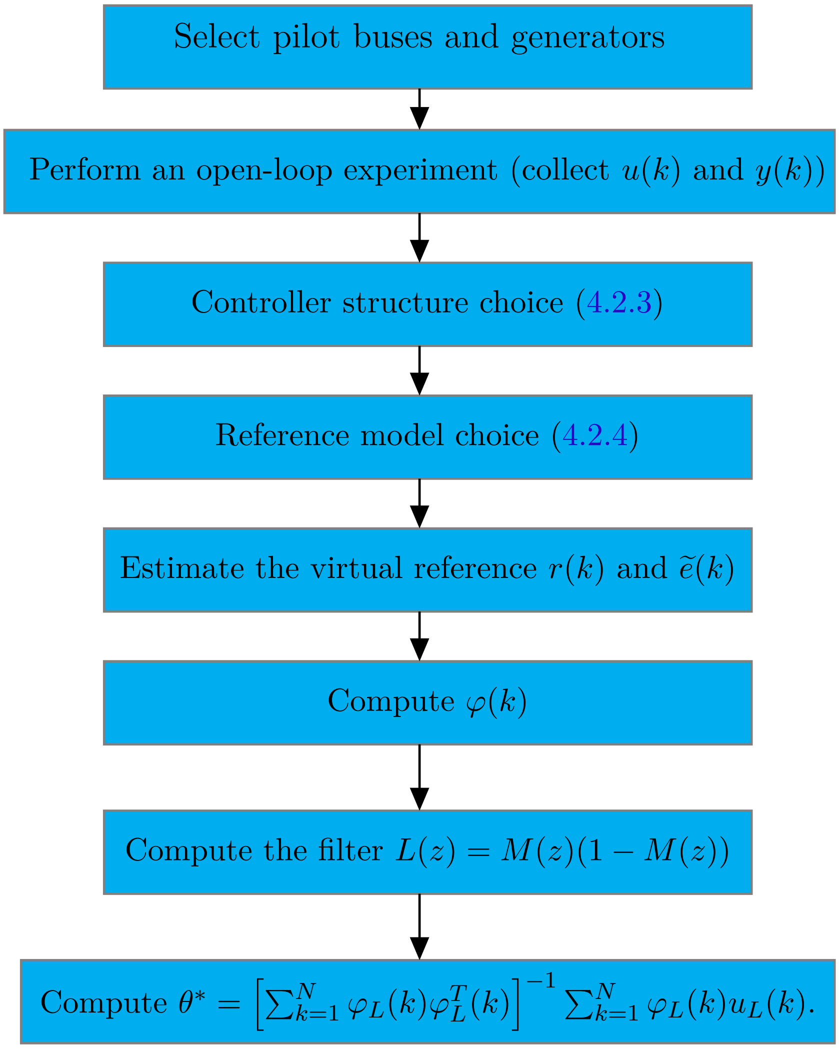

Figure 8 – VRFT-SVC steps.

4.3 MFAC Methodology

4.3.1 The Parameters Settings in Literature

There are no guidelines to choose the appropriate factors values (λ, μ, ρ, and η) in the MFAC algorithm. However, the penalty factor on the change of the control input λ is an important adjustable parameter for MFAC system design (HOU; JIN, 2013). The authors states that a proper selection of λ can guarantee the stability and output tracking performance of the controlled systems. The system initial operating conditions are determined by the values of $\hat{\varphi}(0)$ and λ, and must be stable at the initial operating point.

In (ZHAO; LU, 2018), the authors designed a MISO regional power system controller with MFAC using a full form dynamic linearization (FFDL). Their propose is to substitute the pre-existing traditional PI controller of SVC. Then, the designers rewrote the MFAC control law as discrete transfer function with a zero pole and nonzero zero as a PI controller. Thus, the MFAC parameters could be found by association with the parameters of traditional PI transfer function.

In (LU et al., 2015), to maintain the stability of the system with MFAC controller at the initial operating point, the initial parameters of MFAC are set to have the same compensation phase and gain as pre-existing model based controller. The values of $\hat{\varphi}(0)$ and λ can be calculated by solving a cost function, minimizing compensation phase, and under the restriction of the transfer functions gain set to be the same. Numerous optimisation techniques, such as ant colony optimisation, genetic algorithm and particle swarm optimisation, can be used to solve this problem. Genetic algorithm is adopted in this study. Considering that the solution is not unique, one solution is randomly selected as the values of $\hat{\varphi}(0)$ and λ in general. The above initial parameter calculation of MFAC algorithm involves only one running of system simulation and the offline computation is small.

4.3.2 The Proposed Parameters Settings

In both cases presented above, the initial setting parameters of MFAC needed the pre-existing model based controller of the process. The following method suggests a complete data-driven initial setting to MFAC controller using the VRFT idea, proposed in (ROMAN et al., 2016). Figure 9 shows the structure with MFAC-VRFT.

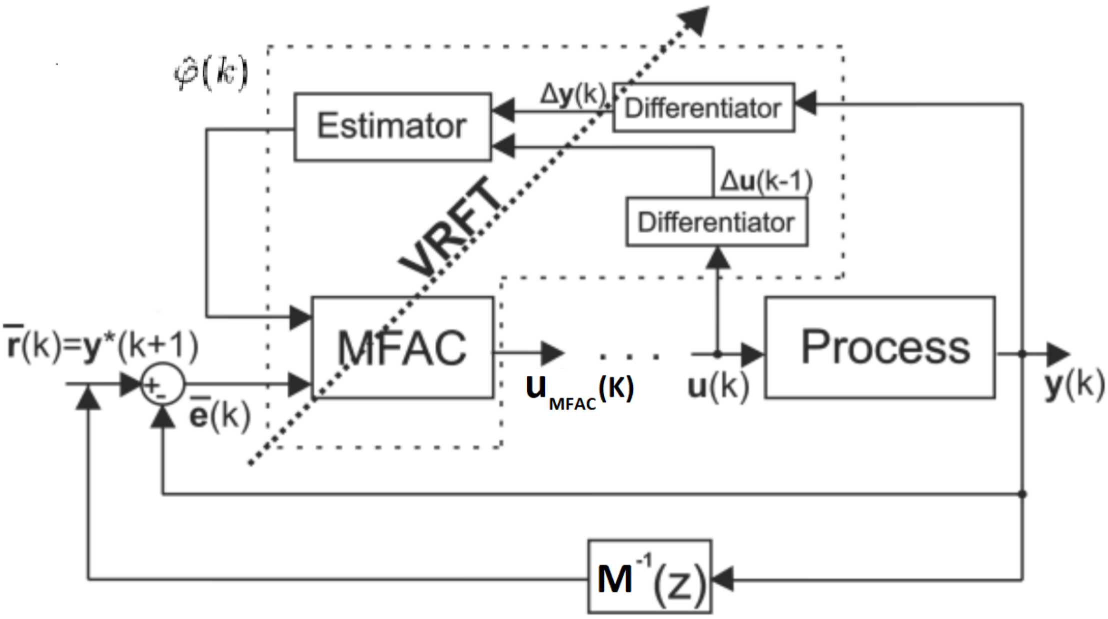

Figure 9 – Structure with mixed MFAC-VRFT (adapted from (ROMAN et al., 2016)).

If $\tilde{r}(k)$ specific to VRFT is considered to desired response $y^*(k+1)$ in MFAC, the MFAC controller structure can be considered in a closed-loop, thus the desired response can be estimates as follows

$$y^*(k+1) = M^{-1}y(k) \tag{4.8}$$

The law control in (2.32) at the initial point can be rewritten as

$$u_{MFAC}(k) = u_{MFAC}(k-1) + \frac{\hat{\varphi}(1)}{\lambda + ||\hat{\varphi}(1)||^2}[M^{-1} - 1]y(k) \tag{4.9}$$

where the weight factor ρ is set to be 1.

Thus, the goal is to minimize the performance criterion of the signal controller output error

$$\begin{aligned} J(\varphi(1), \lambda) &= \bar{E}[u_{MFAC}(k, \varphi(1), \lambda) - u(k)]^2 \\ &= \bar{E}\left[u(k-1) + \frac{\hat{\varphi}(1)}{\lambda + ||\hat{\varphi}(1)||^2}[M^{-1} - 1]y(k) - u(k)\right]^2 \\ &= \bar{E}\left[\frac{\hat{\varphi}(1)}{\lambda + ||\hat{\varphi}(1)||^2}[M^{-1} - 1]y(k) - \Delta u(k)\right]^2. \end{aligned} \tag{4.10}$$

where a nonlinear least-squares is used to solve this problem. To solve this problem was used the Matlab function *lsqnonlin*, based on trust-region-reflective algorithm.

Therefore, the proposed mixed MFAC-VRFT control approach translates the design of MFAC algorithm parameters ($\varphi(1)$ and λ) into easier to comprehend closed-loop characteristics described by the reference model M. Figure 10 shows the MFAC-VRFT SVC steps.

4.4 Summary

In this chapter, an entire methodology were presented to design the SVC using DDC methods, since the choice of pilot buses until the controller parameters tunning. A complete algorithm to each method is presented with all their particularities. The SVC-VRFT algorithm was used to initialize the MFAC parameters, keeping this last one a complete data-driven process.

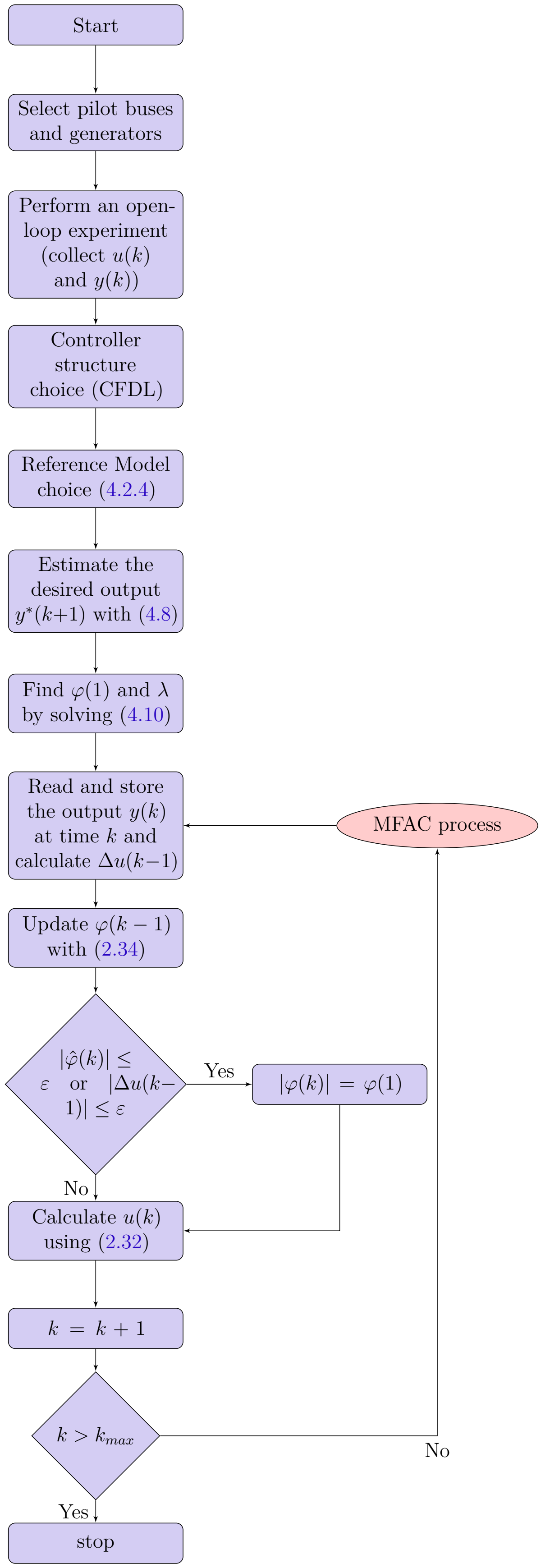

Figure 10 – MFAC-VRFT SVC steps.

5 Results

5.1 Introduction

In this chapter, the VRFT and MFAC algorithms are applied in the SVC problems and compared with the model based Italian method. A power system model used for the small signal stability and dynamic stability analysis is used to perform the simulations. The DDC methods parameters settings are explained, and four different cases of system disturbances are carried out to show the system efficiency.

5.2 System Description

The IEEE 39 bus power system, which contains 10 generators, is well known also as New England 39 bus and it is shown in Figure 11. This benchmark has 39 buses, 19 loads, and 10 generators. It is widely used for small signal stability studies and dynamic stability analysis. The nonlinear simulations are carried out using Matlab/Simulink software with the power system parameters are available in (MOEINI et al., 2015). The Matlab version used in this work was 8.8 R2016b 64bits, and the component libraries for modeling and simulating the electrical power systems was provided by Simscape Electrical 4.1. The computer used to run all simulations is Intel(R) Core(TM) i5-2410M CPU 2.3GHz, 8,00GB RAM, and 64bits.

5.3 VRFT-SVC Parameters Settings

In this work, the SISO VRFT-SVC approach was carried out using the Italian hierarchical voltage control structure, presented in subsection 3.3. The RVR (PI controller) is tunned by the VRFT algorithm. The VRFT-SVC performs a SISO control, where only one generator by region performs the voltage control in the pilot bus. Table 1 presents the pairs (bus/generator) of each region, chosen as in subsection 4.2.1. The transformer reactance located in each generator bus and the equivalent reactance of each pair (computed using the Thevenin principle) are presented in Table 2.

A step signal is applied to the generators, and the voltage at each pilot bus is collected. This procedure occurs individually to the pair (bus/generator) in each region. The Figure **??** show the signals collected from an open-loop experiment. As mentioned previously, the controller structure chosen in this work is a PI controller, which is linear in its parameters.

With the open-loop experiment data, the reference model choice is computed by using the Algorithm 1. The result is shown in Table 3, where each pair (bus/generator)

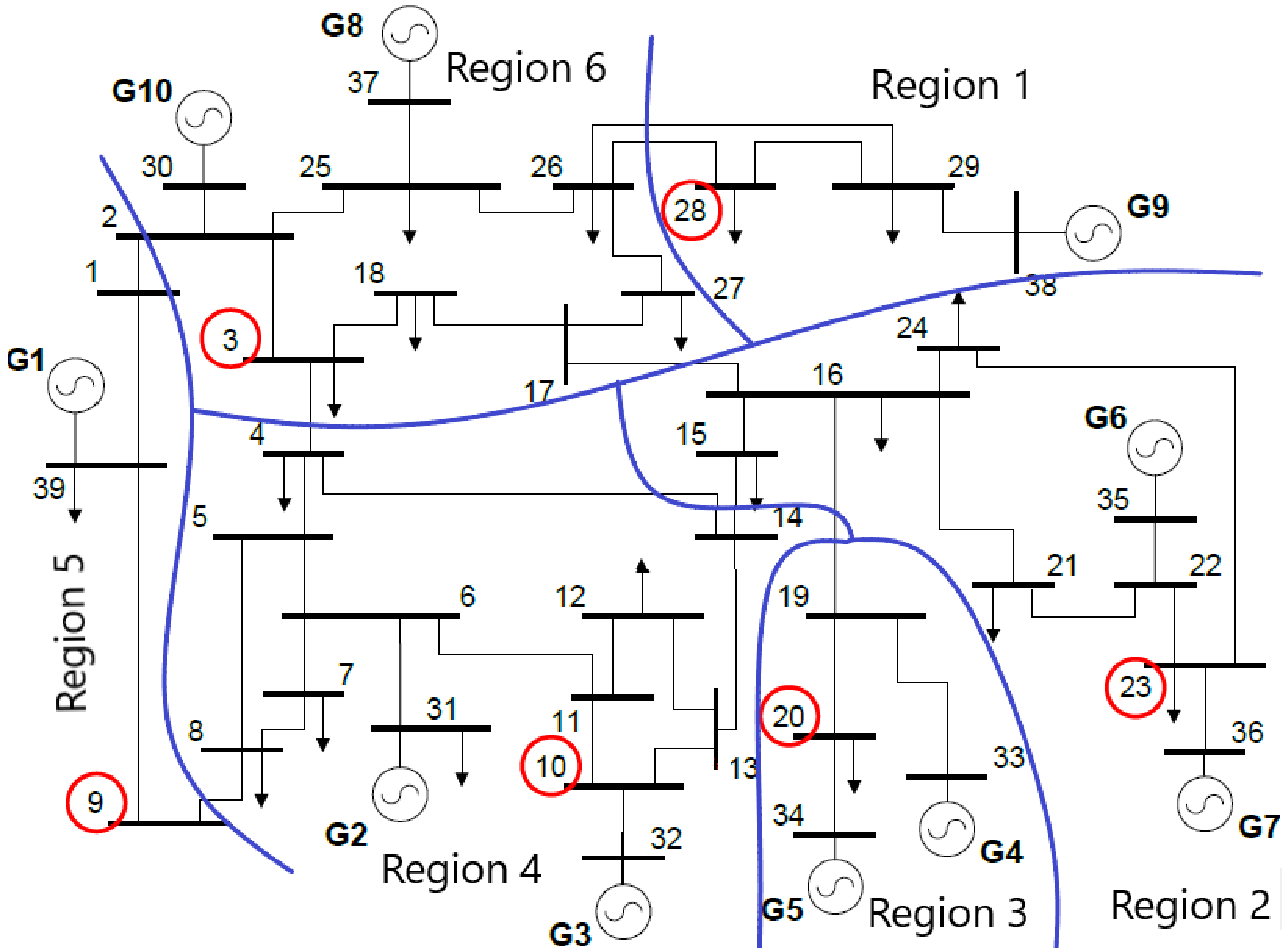

Figure 11 – IEEE 39 bus power system diagram.

Table 1 – Sensitive pairs (bus/generator).

Bus	**09**	**10**	**20**	**23**	**28**	**03**
Generator	01	03	05	07	09	10

reference model has the Model 1 structure, with the sampling time (T_s) chosen as $50ms$ and the desired settling time (t_s) is $50s$.

The estimated controller parameters using the VRFT algorithm and the traditional PI parameters are presented in Table 4.

Table 2 – Transformer and equivalent reactance of the pairs (bus/generator).

Bus|Generator	$X_T(p.u.)$	$X_{eq}(p.u.)$
03|10	0,1810	0,0311
09|01	0	0,0250
10|03	0,0200	0,0200
20|05	0,0180	0,0180
23|07	0,0272	0,0272
28|09	0,0156	0,0288

Table 3 – Reference models parameters.

Bus|Generator	Process time delay (nk)	dominant discrete pole (a)
03|10	2	0.996007989
09|01	2	0.996007989
10|03	2	0.996007989
20|05	2	0.996007989
23|07	2	0.996007989
28|09	2	0.996007989

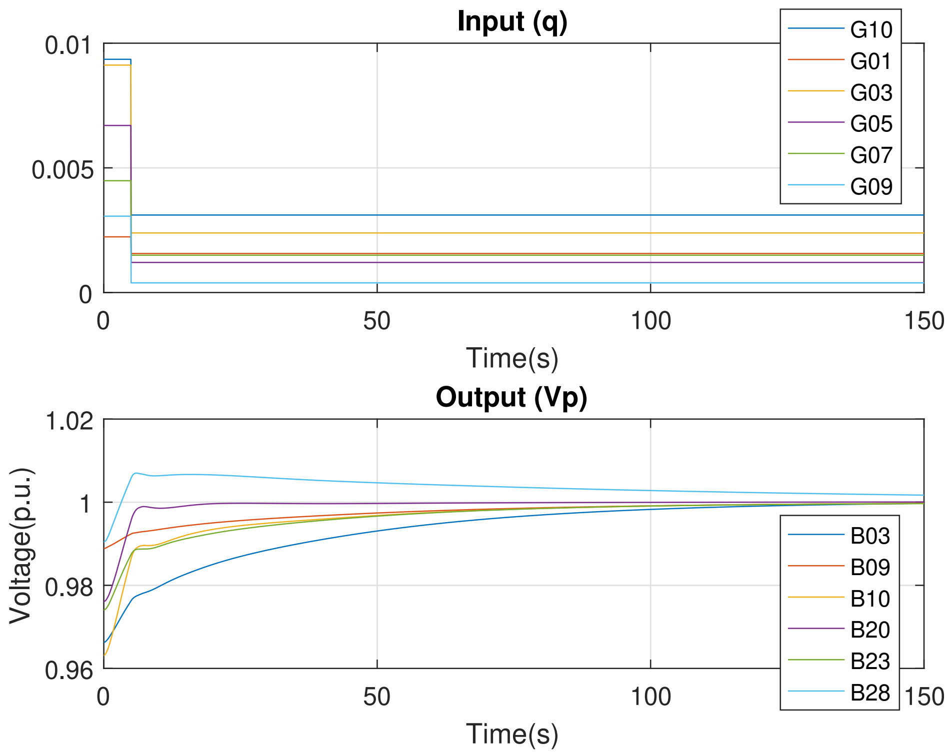

Figure 12 – VRFT open-loop experiment data.

Table 4 – PI controller parameters.

	VRFT		Traditional	
Bus|Generator	K_p	K_i	K_p	K_i
03|10	0.3190	0.0071	0.2760	0.0077
09|01	0.2470	0.0122	0.2000	0.0080
10|03	0.1301	0.0051	0.2500	0.0100
20|05	0.1098	0.0036	0.2777	0.0111
23|07	0.1186	0.0048	0.1838	0.0073
28|09	0.0666	0.0024	0.3205	0.0099

5.4 MFAC-SVC Parameters Settings

In this work, the MFAC controller is designed to substitute the entire PVR and RVR in the traditional controller. Thus, an open-loop experiment is carried out, where a step signal (0.02 p.u.) is applied in the AVR' s reference (Vg_{ref}), and the all pilot buses voltage is collected, as presented in Figure 13. The reference model choice is computed by using the algorithm 1. The result is shown in Table 3, where each pair (bus/generator) reference model has the Model 1 structure, with the sampling time (T_s) chosen as $50ms$ and the desired settling time (t_s) is $50s$. The initial parameters $\varphi(1)$ and λ are obtained by solving the equations (4.8) and (4.10), and it is shown in Table 5. The other MFAC-VRFT controller parameters (μ, ρ, and η) can make better the controller performance, but in this work, they are set to be 1.

Table 5 – MFAC-VRFT controller parameters.

Bus|Generator	$\varphi(1)$	λ
03|10	0.2664	7.4217
09|01	0.0860	9.2111
10|03	0.1504	8.5975
20|05	0.0936	9.1402
23|07	0.1621	8.4836
28|09	0.0714	9.3481

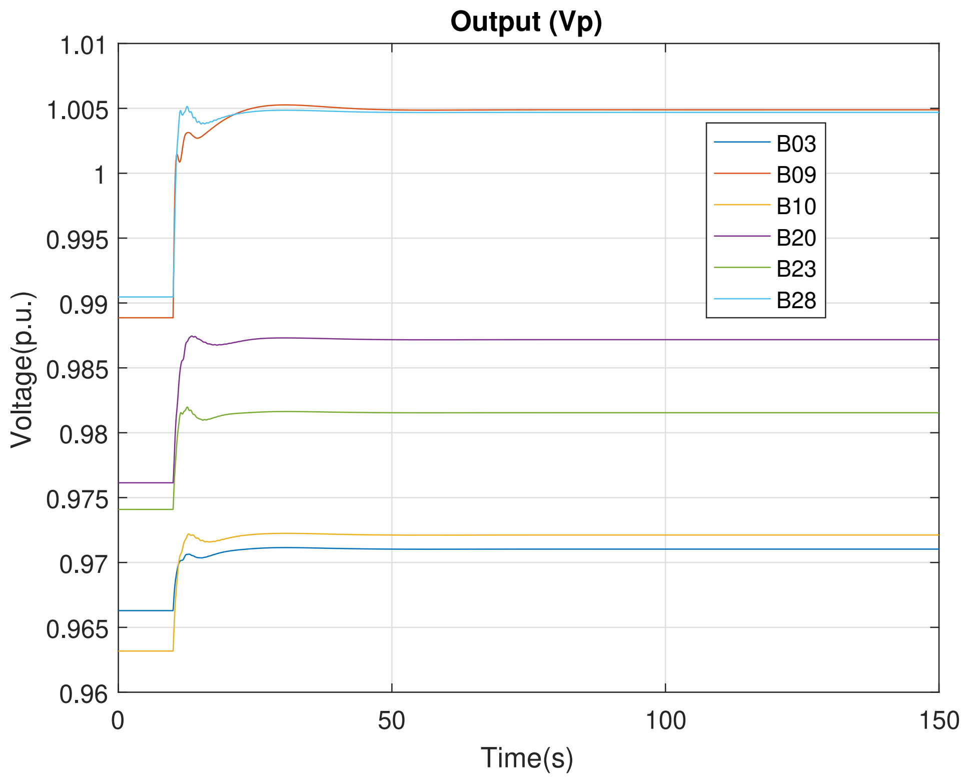

Figure 13 – MFAC-VRFT open-loop experiment data.

5.5 Simulation Results

In this section a set of cases are simulated in order to demonstrate the VRFT and MFAC SVC efficiency.

- **Case 1**

In the first case, all the pilot buses are in steady state, and the SVC is turned on to lead the voltage to reference, which set to be 1, as shown in Figure 14-43. Figure 14 shows the output voltage in pilot Bus 03. Note the VRFT and traditional approach present a similar response, while the MFAC approach is faster. Table 6 compares the settling time of each pilot bus in different controller design approaches.

Figure 15 shows the difference between the VRFT output and the desired response chosen by the desired transfer function. Note the pilot Bus 03 response is similar to the desired response. Figure 16 shows the RVR signal control efforts to generator 10 in the VFRT and Traditional approach, and the Figure 17 represents the reference signal to generator 10. The adaptive parameter signal in MFAC approach is shown in Figure 18.

Figure 39 shows the output voltage in pilot bus 28. Traditional approach presents a faster performance, while the VRFT approach is slower. The Section 5.6 will discuss about this performance difference, caused by the influence of the electrical distance, between the pilot bus and the generator, in the Traditional approach. Figure 40 shows the VRFT output and the desired response chosen by the desired transfer function. Note the pilot bus 28 response is similar to the desired response. Figure 41 shows the RVR control signal efforts to generator 09 in the VFRT and Traditional approaches. Note the signal control effort in Traditional approach increase as closer the generator is to the pilot bus . Figure 42 represents the reference signal to generator 09. The adaptive parameter signal in MFAC approach is shown in Figure 43. The same figures sequence is shown to the other sensitive pairs, as follow:

Table 6 – Settling Time (Case 01).

Bus|Generator	Traditional (s)	VRFT (s)	MFAC (s)
03|10	24.55	23.75	11.35
09|01	48.00	33.70	10.75
10|03	13.65	27.40	10.90
20|05	10.40	30.80	13.90
23|07	16.80	26.65	12.20
28|09	12.25	37.87	14.85

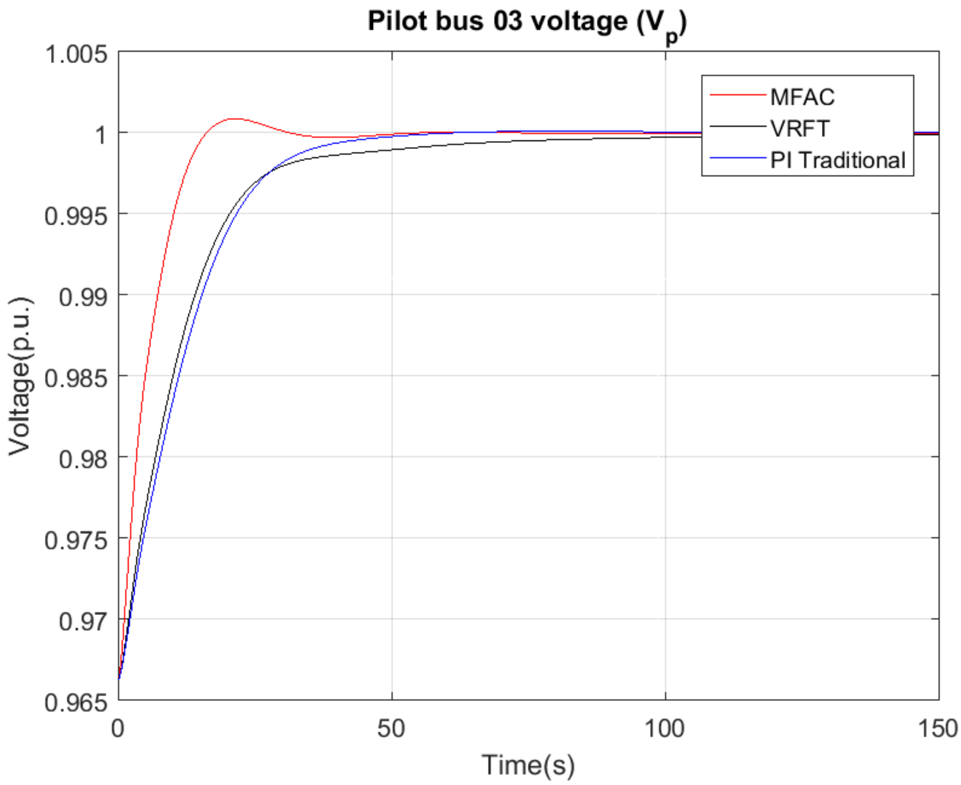

Figure 14 – Pilot bus voltage (Bus_{03}).

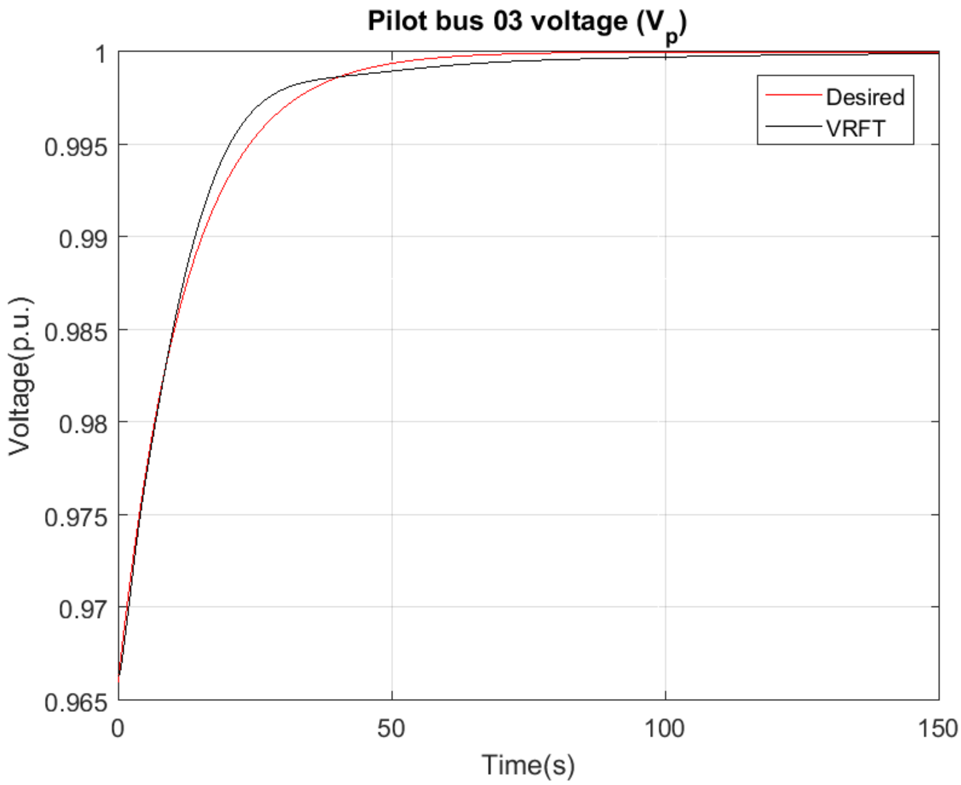

Figure 15 – Pilot bus voltage desired response (Bus_{03}).

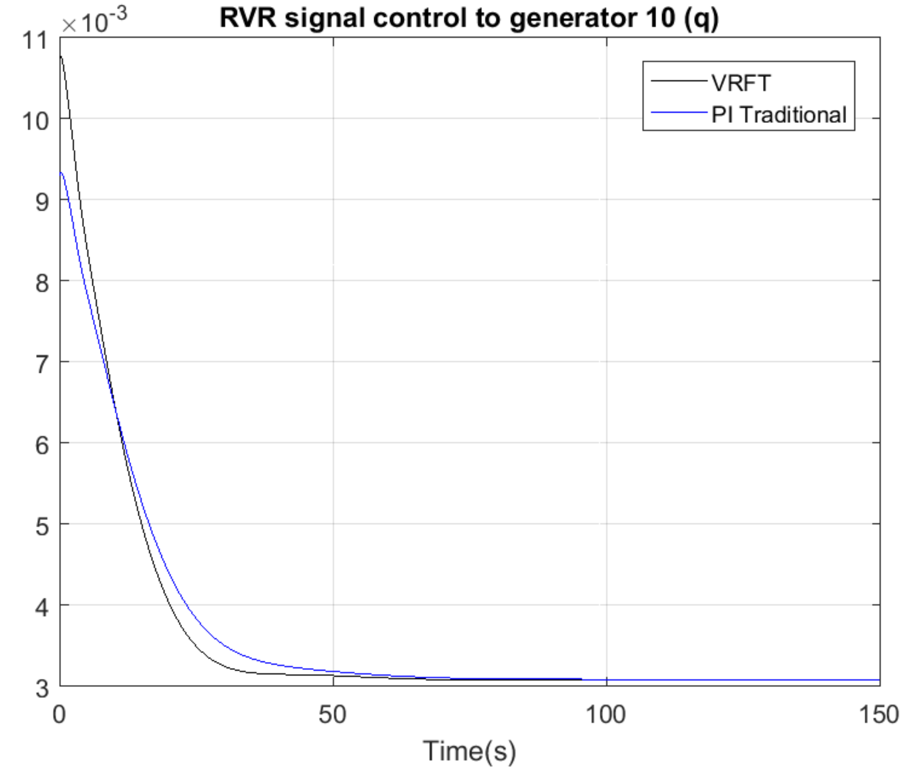

Figure 16 – RVR signal control (q) to generator 10.

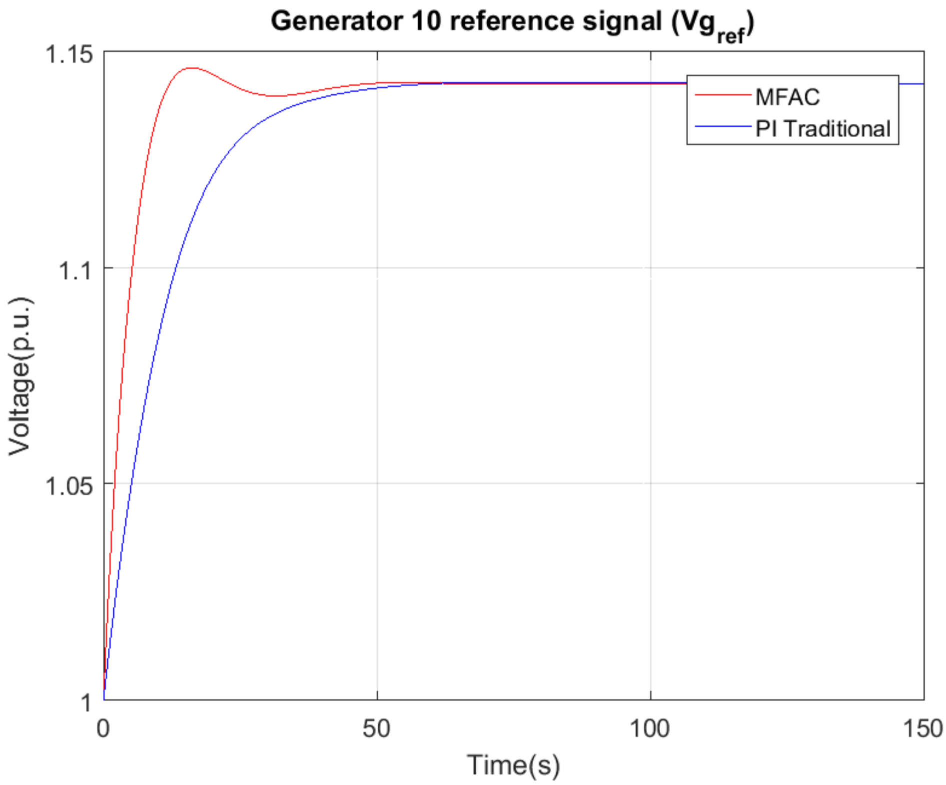

Figure 17 – Reference signal (Vg_{ref}) to generator 10.

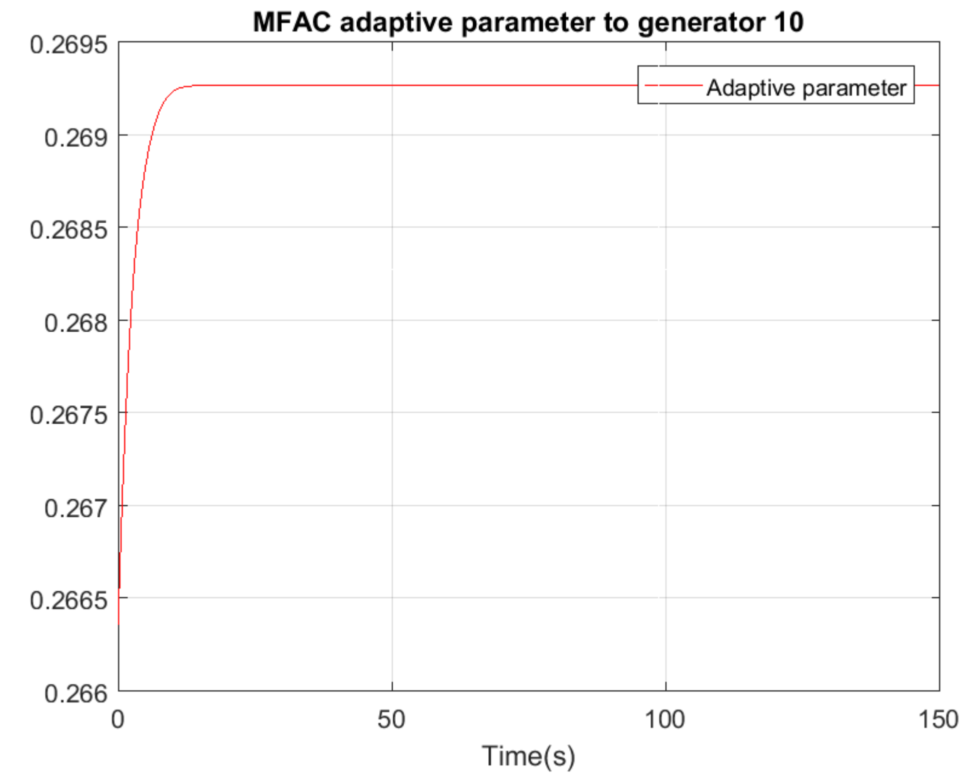

Figure 18 – MFAC adaptive parameter ($B_{03}G_{10}$).

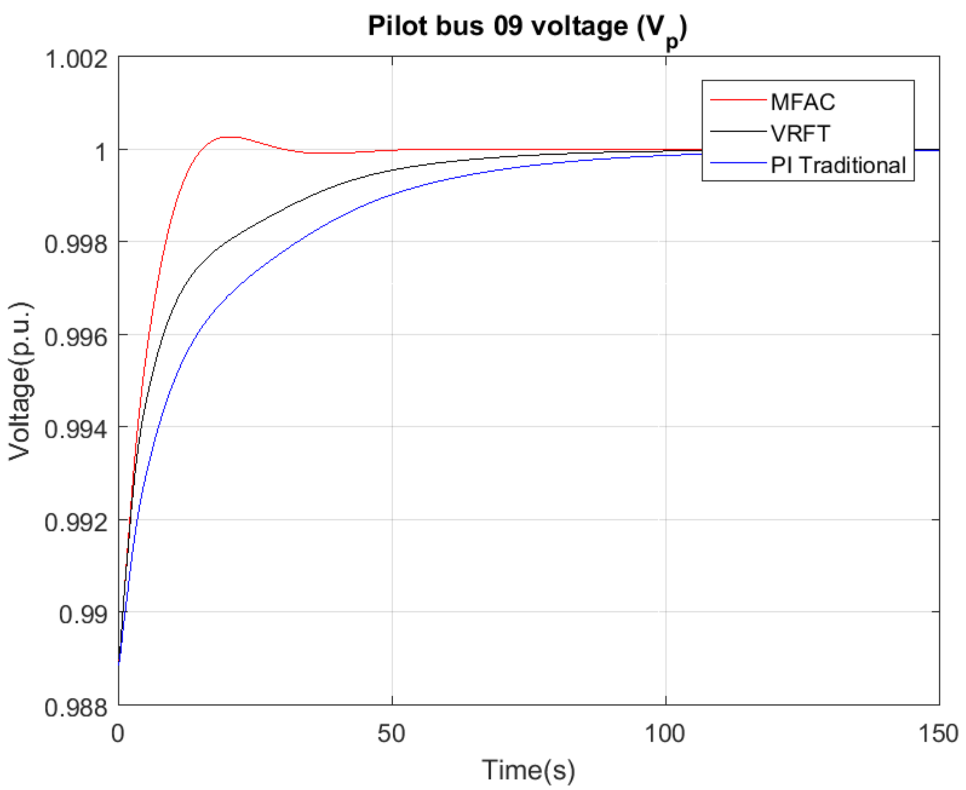

Figure 19 – Pilot bus voltage (Bus_{09}).

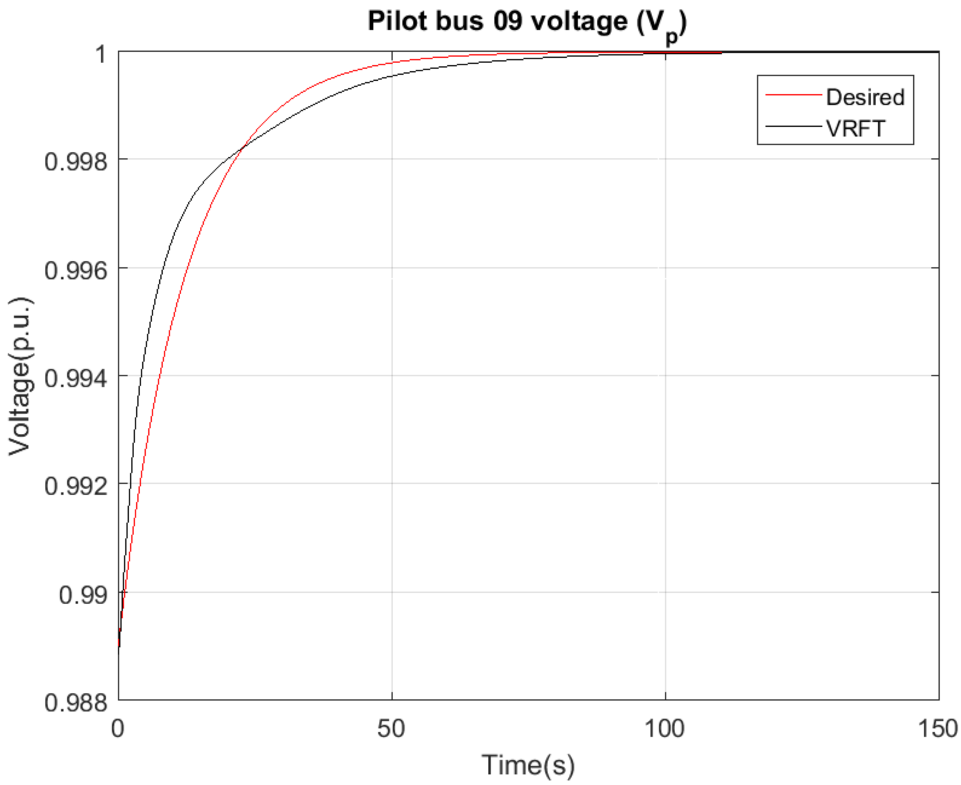

Figure 20 – Pilot bus voltage desired response (Bus_{03}).

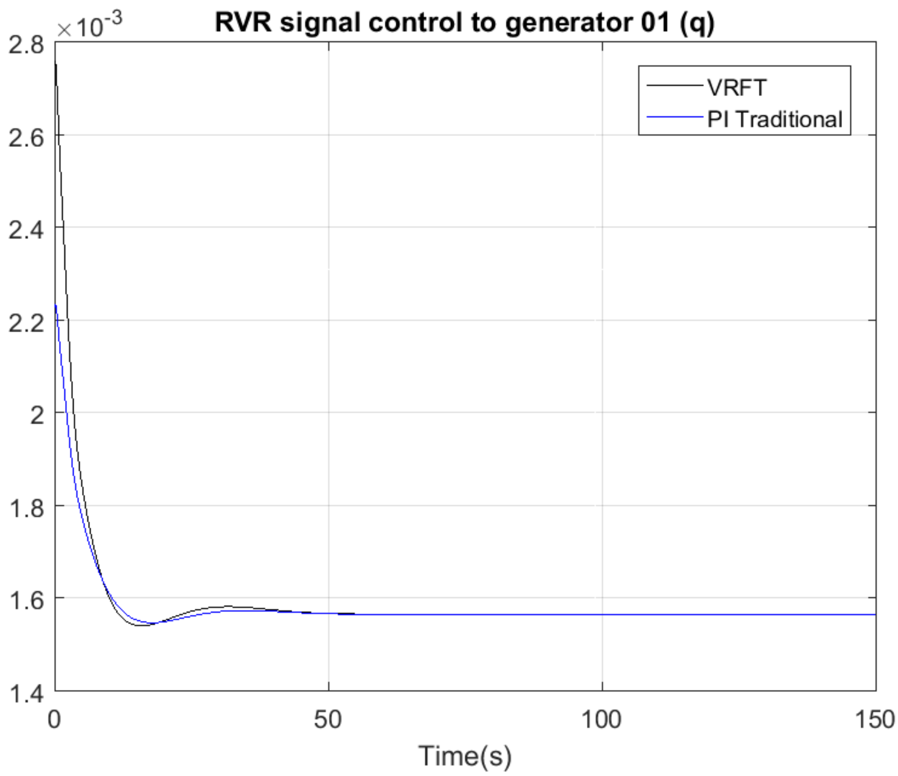

Figure 21 – RVR signal control (q) to generator 01.

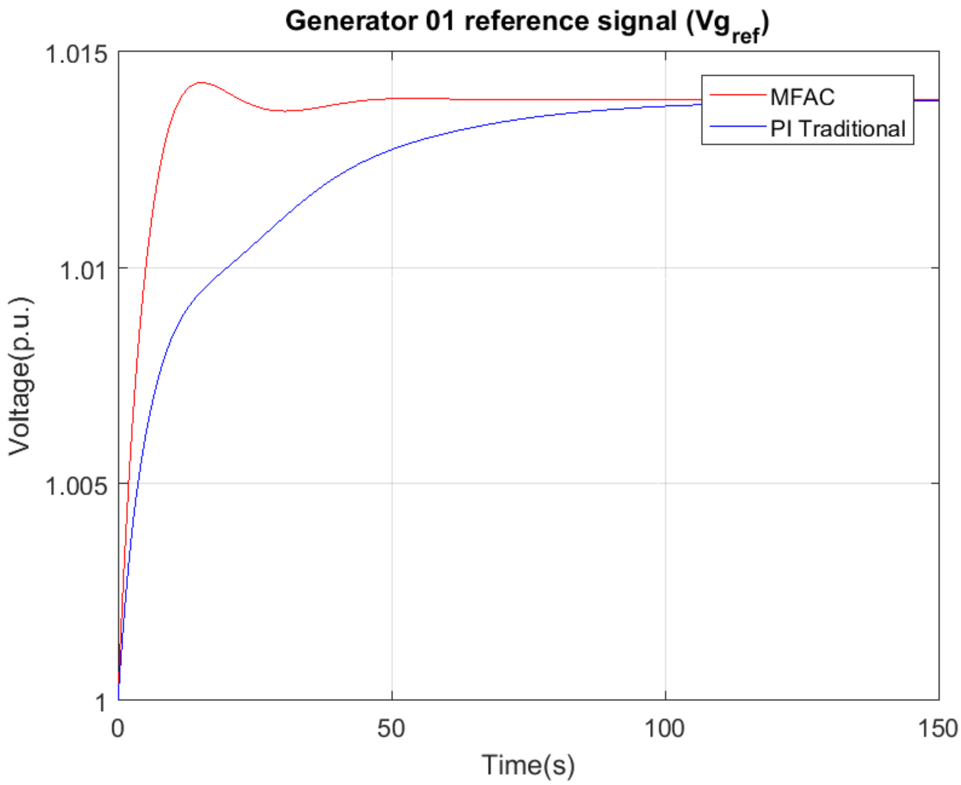

Figure 22 – Reference signal (Vg_{ref}) to generator 01.

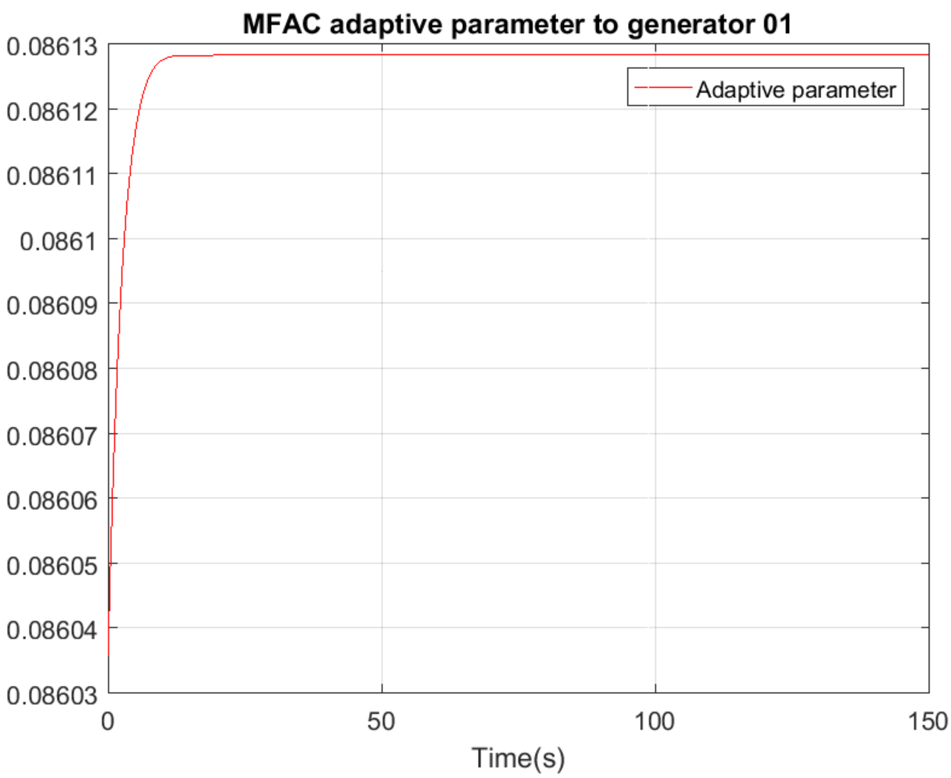

Figure 23 – MFAC adaptive parameter ($B_{09}G_{09}$).

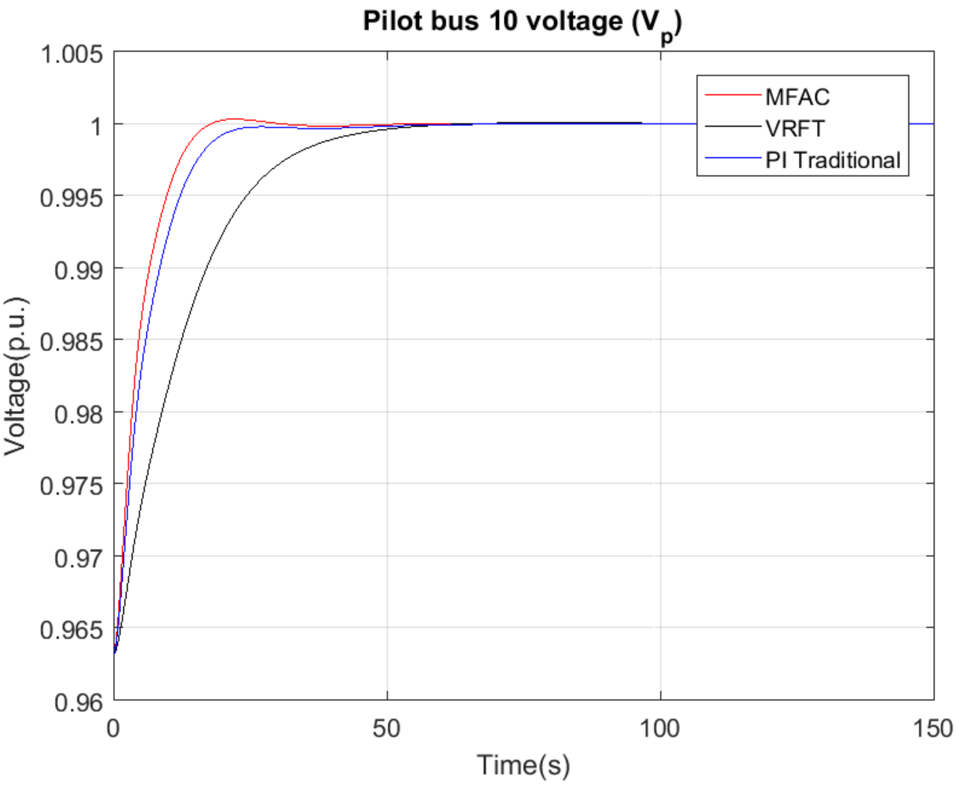

Figure 24 – Pilot bus voltage (Bus_{10}).

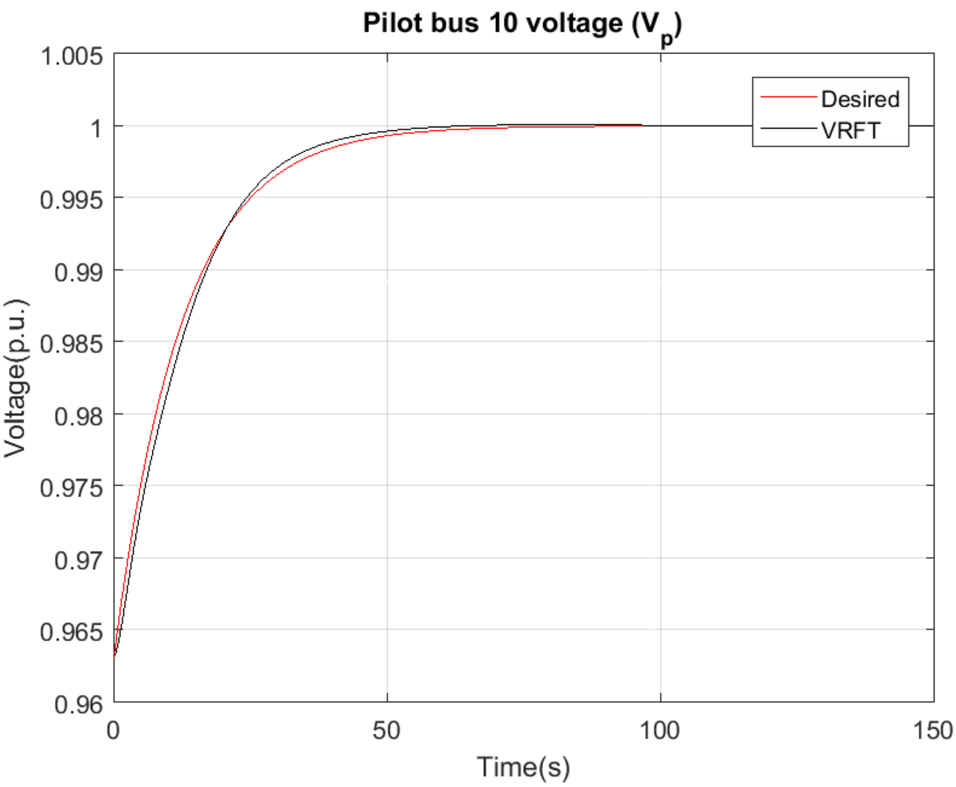

Figure 25 – Pilot bus voltage desired response (Bus_{10}).

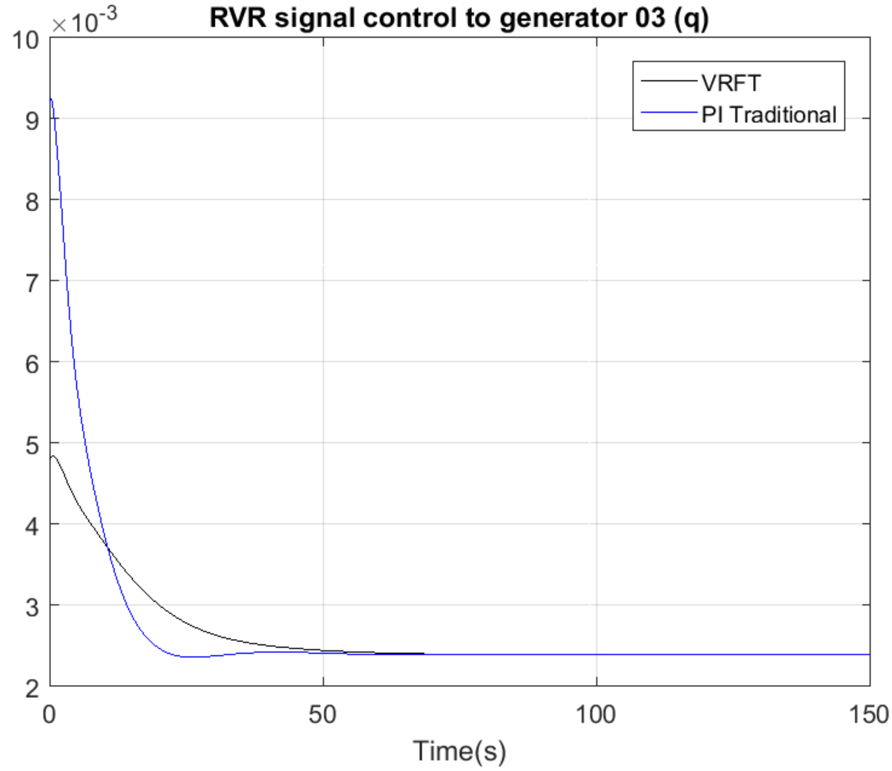

Figure 26 – RVR signal control (q) to generator 03.

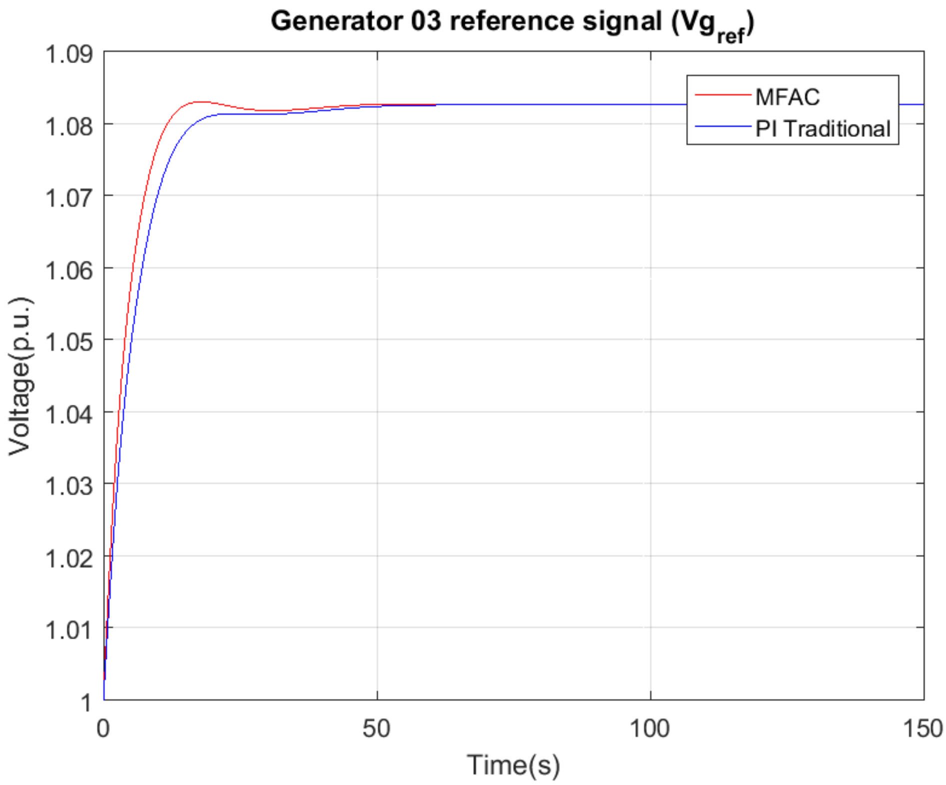

Figure 27 – Reference signal (Vg_{ref}) to generator 03.

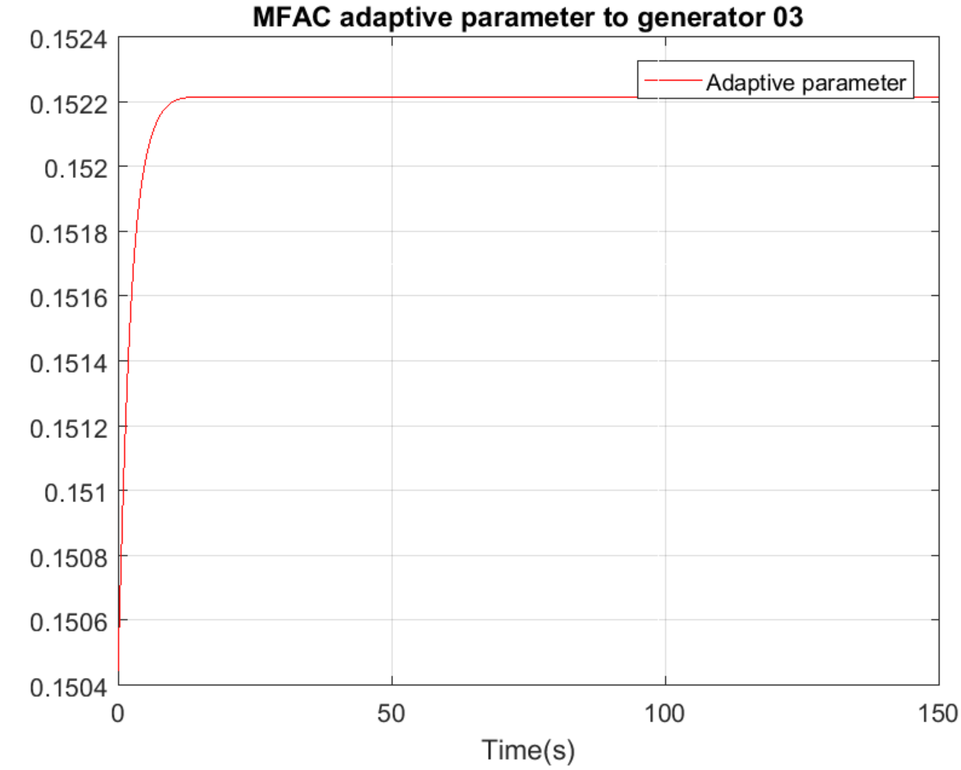

Figure 28 – MFAC adaptive parameter ($B_{10}G_{03}$).

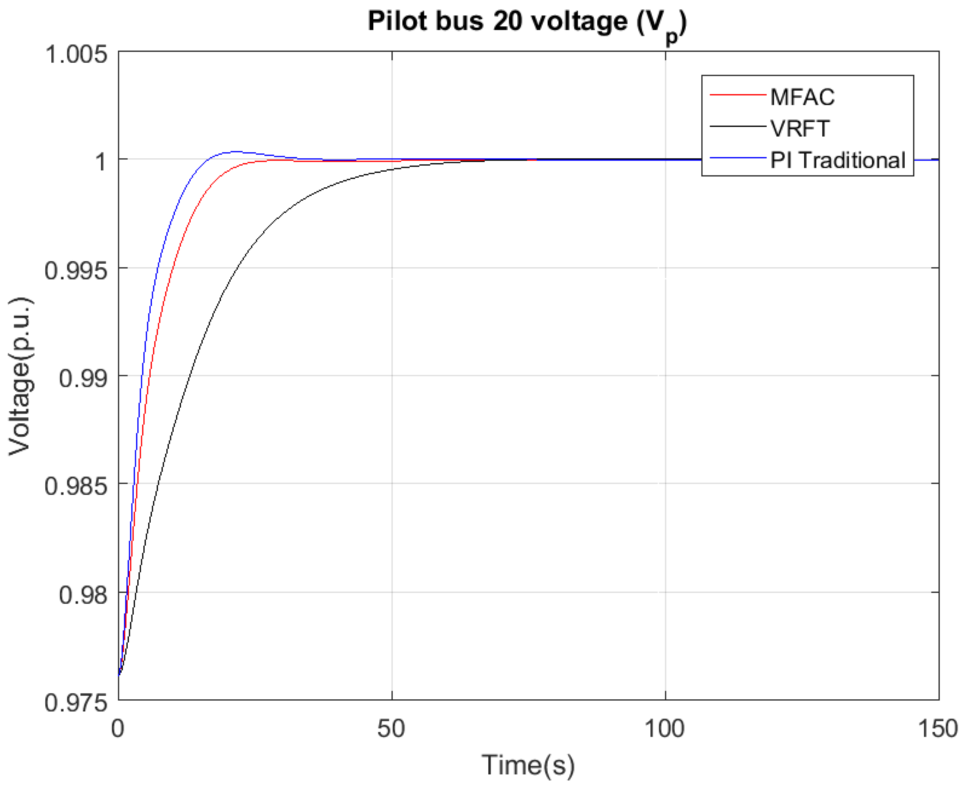

Figure 29 – Pilot bus voltage (Bus_{20}).

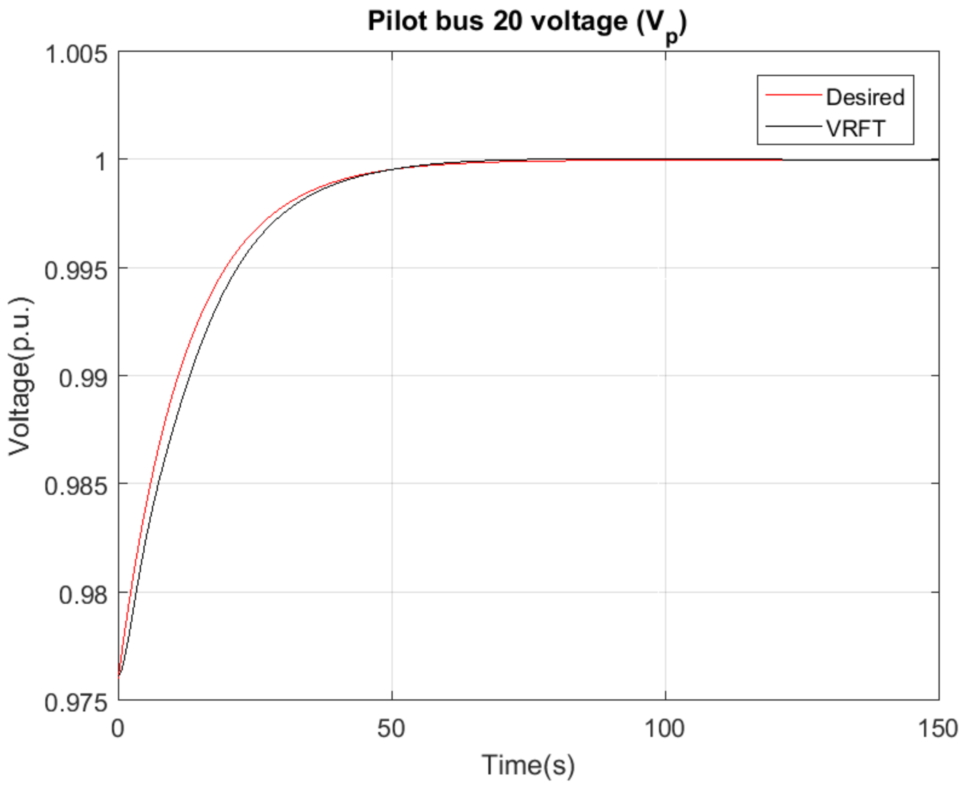

Figure 30 – Pilot bus voltage desired response (Bus_{20}).

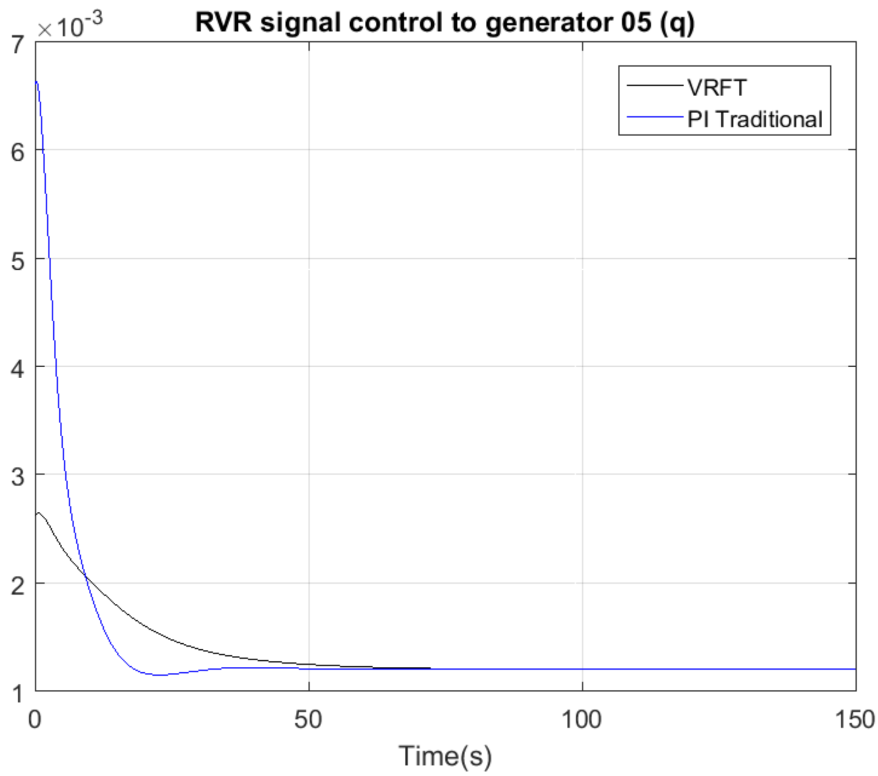

Figure 31 – RVR signal control (q) to generator 05.

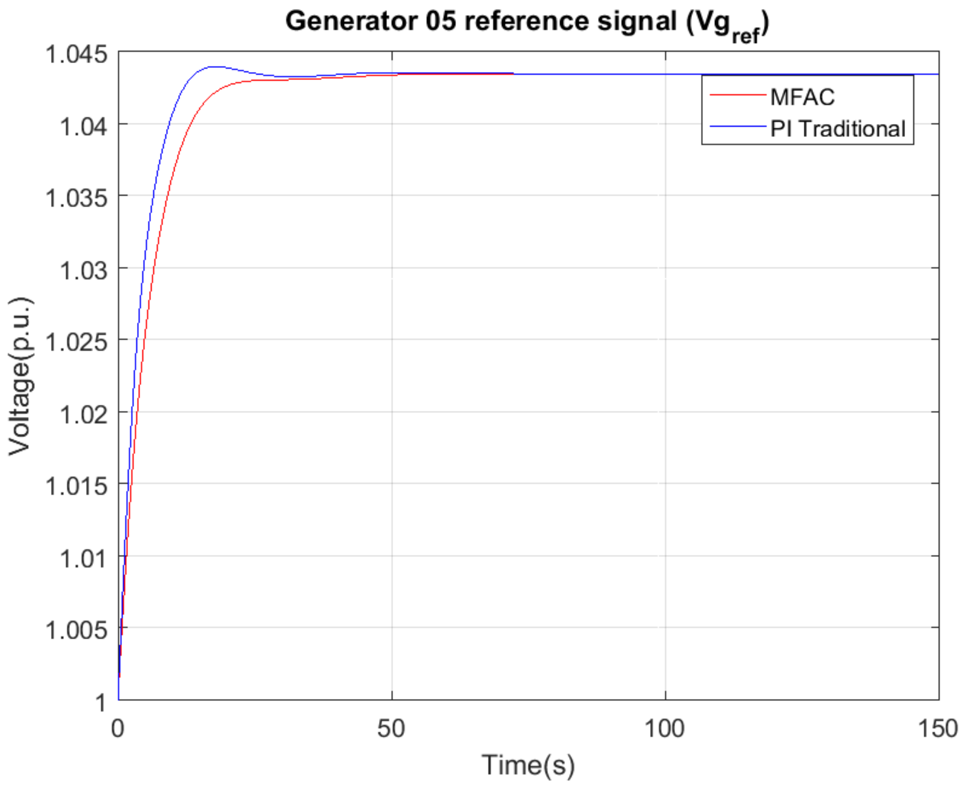

Figure 32 – Reference signal (Vg_{ref}) to generator 05.

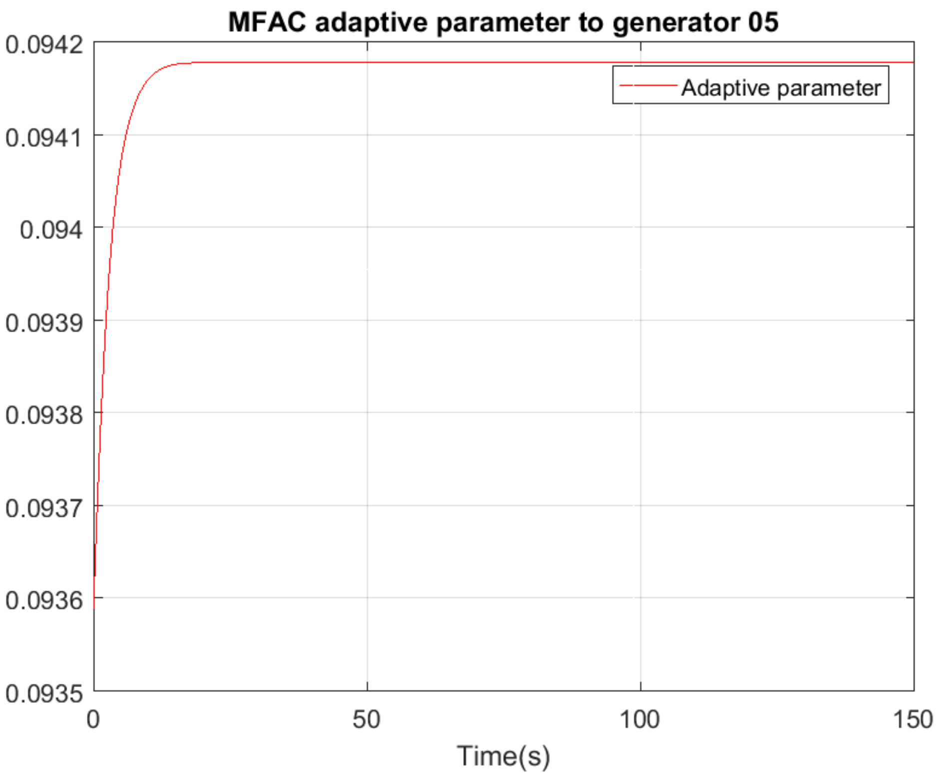

Figure 33 – MFAC adaptive parameter ($B_{20}G_{05}$).

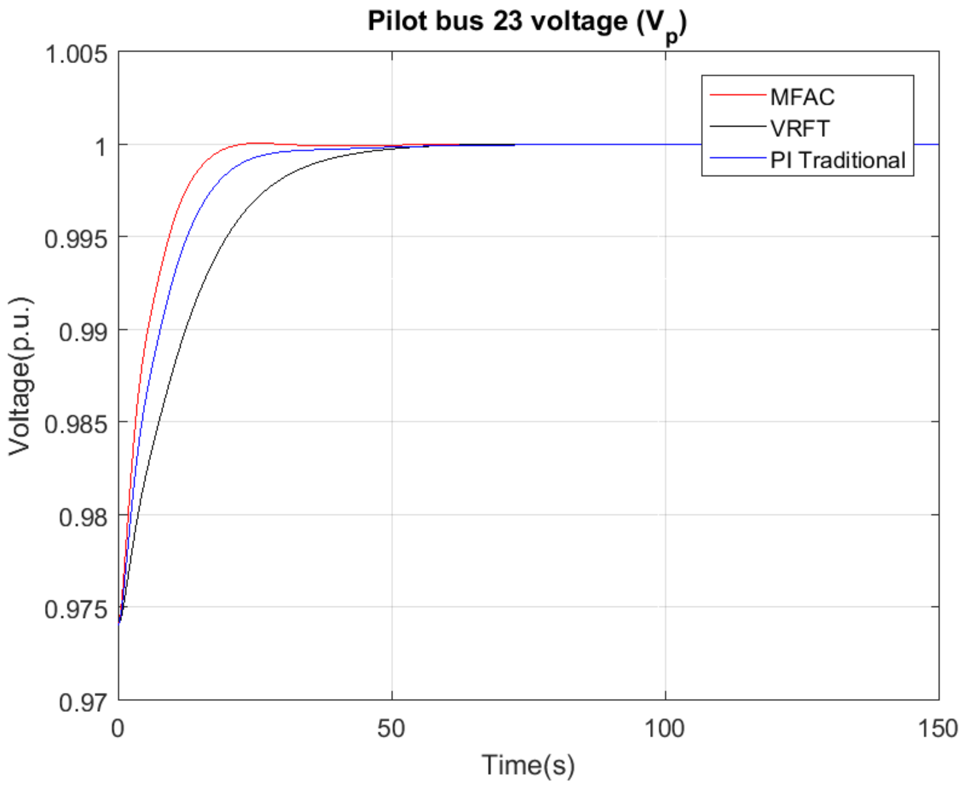

Figure 34 – Pilot bus voltage (Bus_{23}).

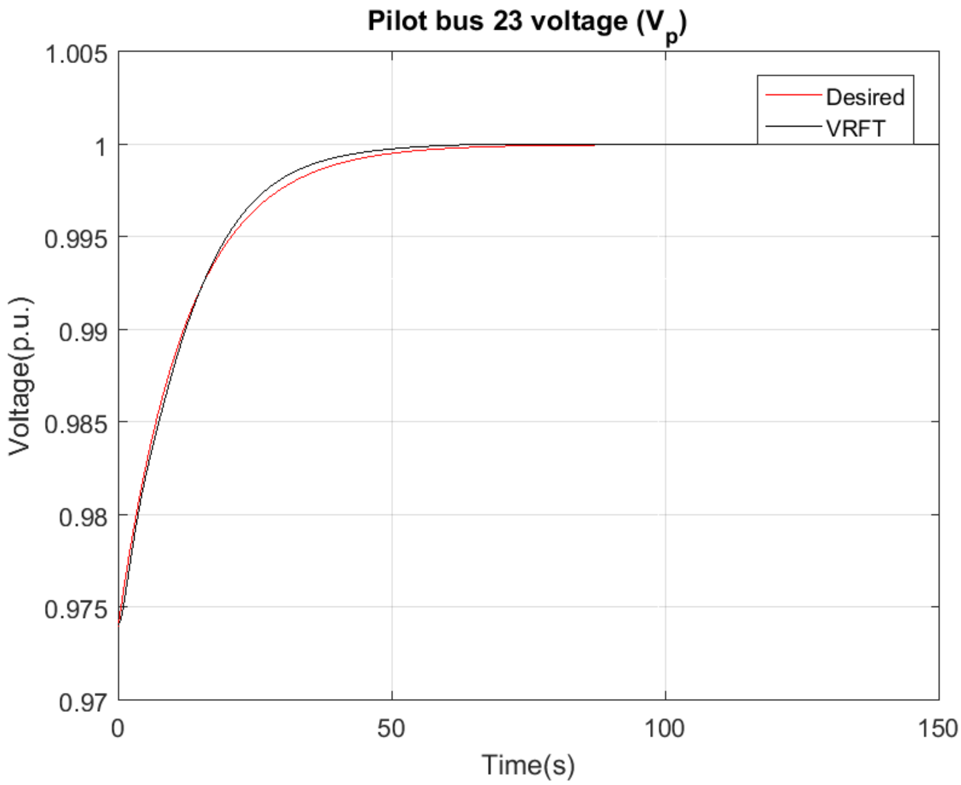

Figure 35 – Pilot bus voltage desired response (Bus_{23}).

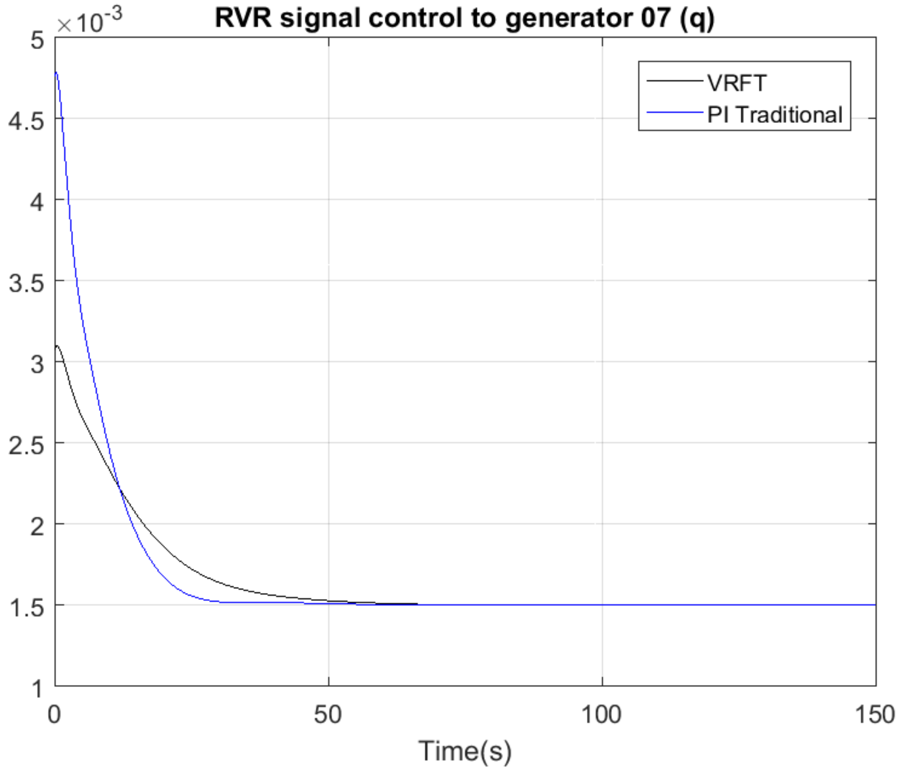

Figure 36 – RVR signal control (q) to generator 07.

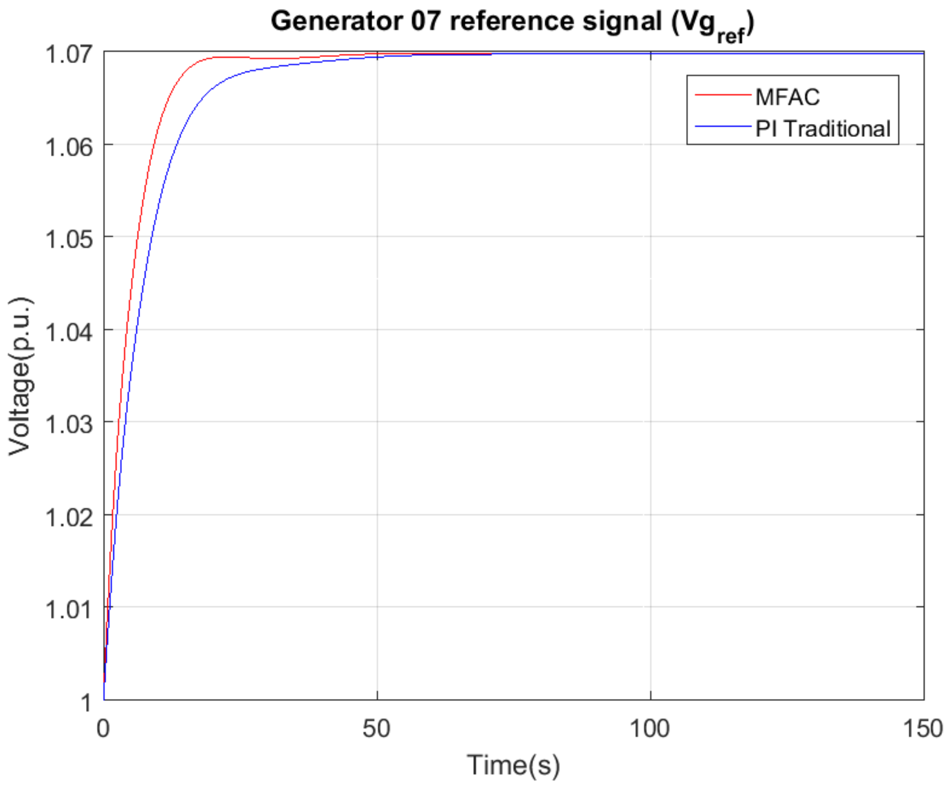

Figure 37 – Reference signal (Vg_{ref}) to generator 07.

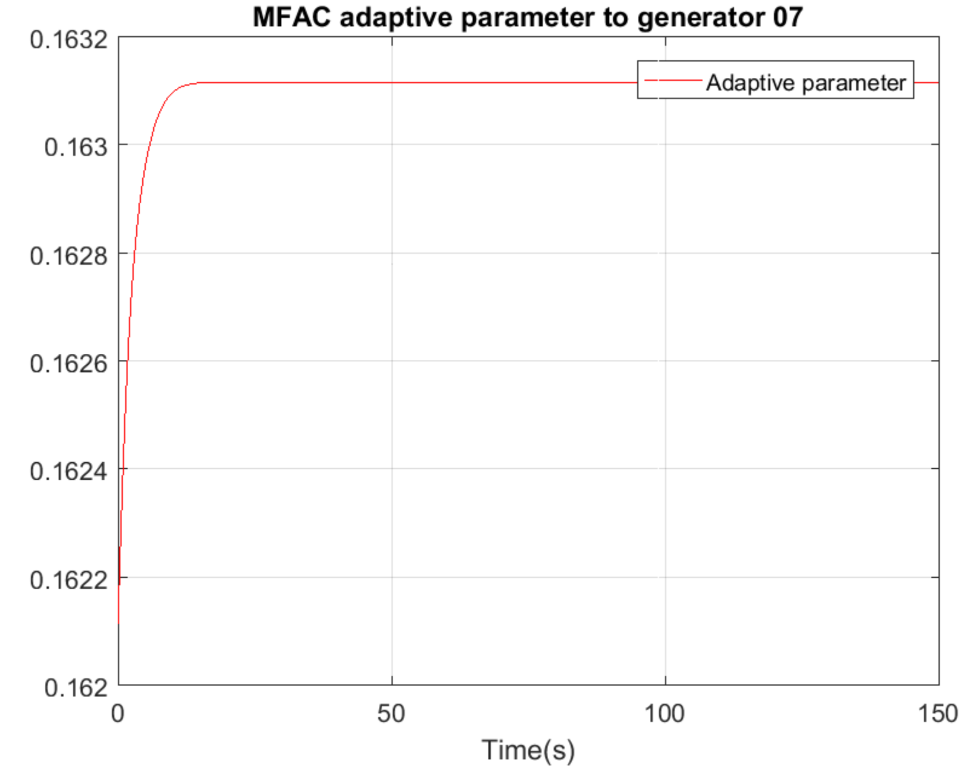

Figure 38 – MFAC adaptive parameter ($B_{23}G_{07}$).

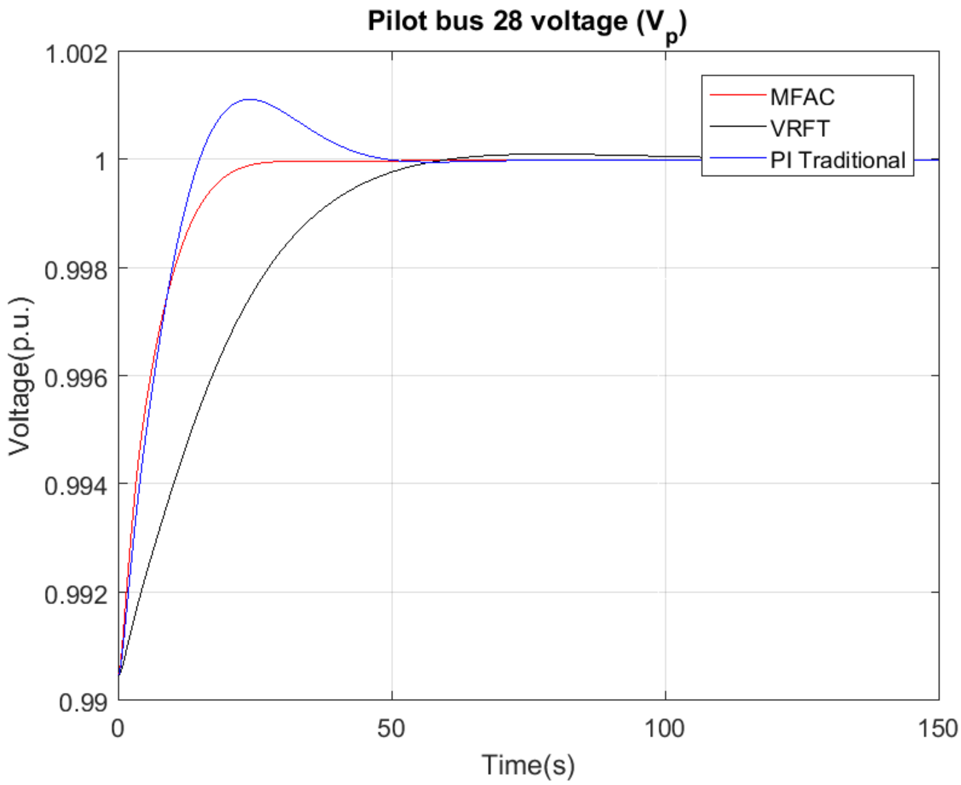

Figure 39 – Pilot bus voltage (Bus_{28}).

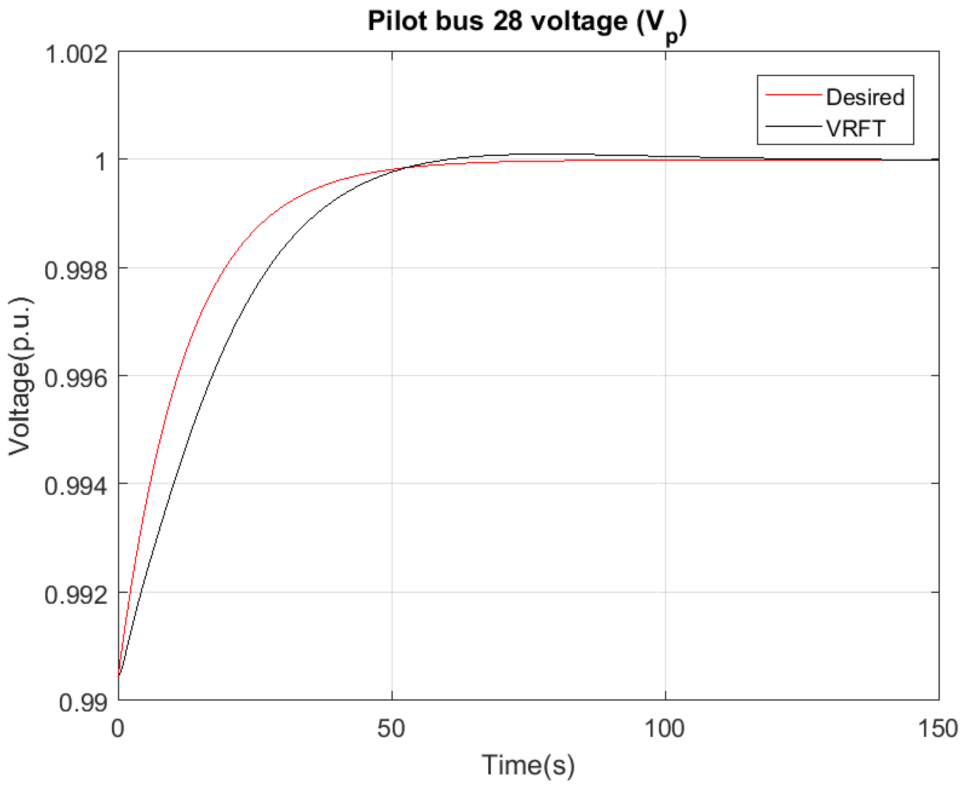

Figure 40 – Pilot bus voltage desired response (Bus_{28}).

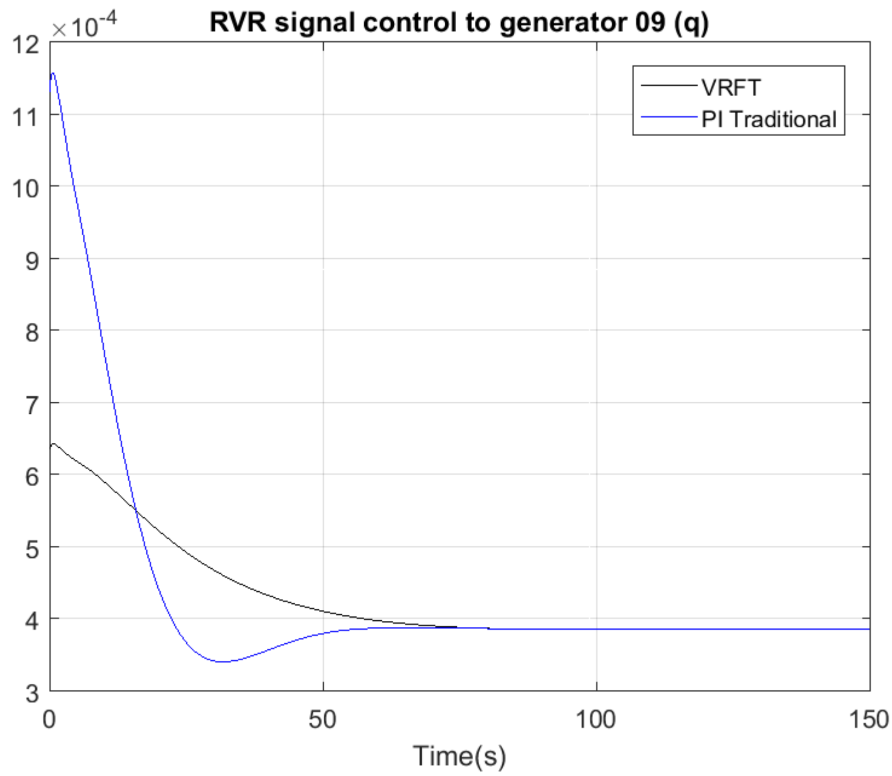

Figure 41 – RVR signal control (q) to generator 09.

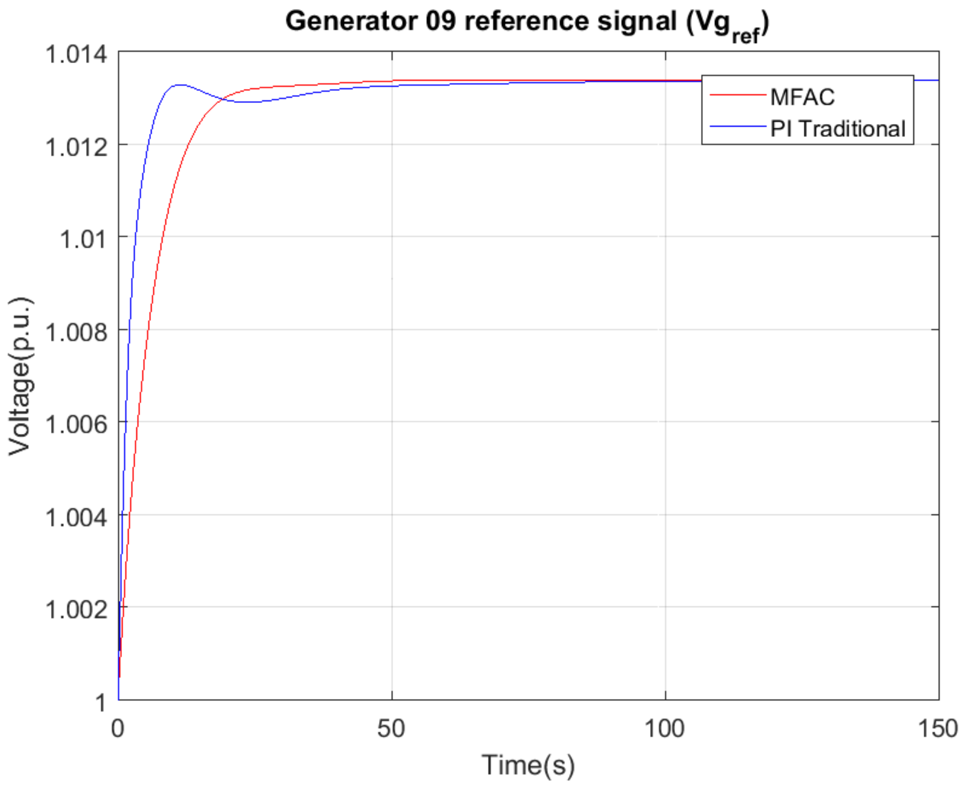

Figure 42 – Reference signal (Vg_{ref}) to generator 09.

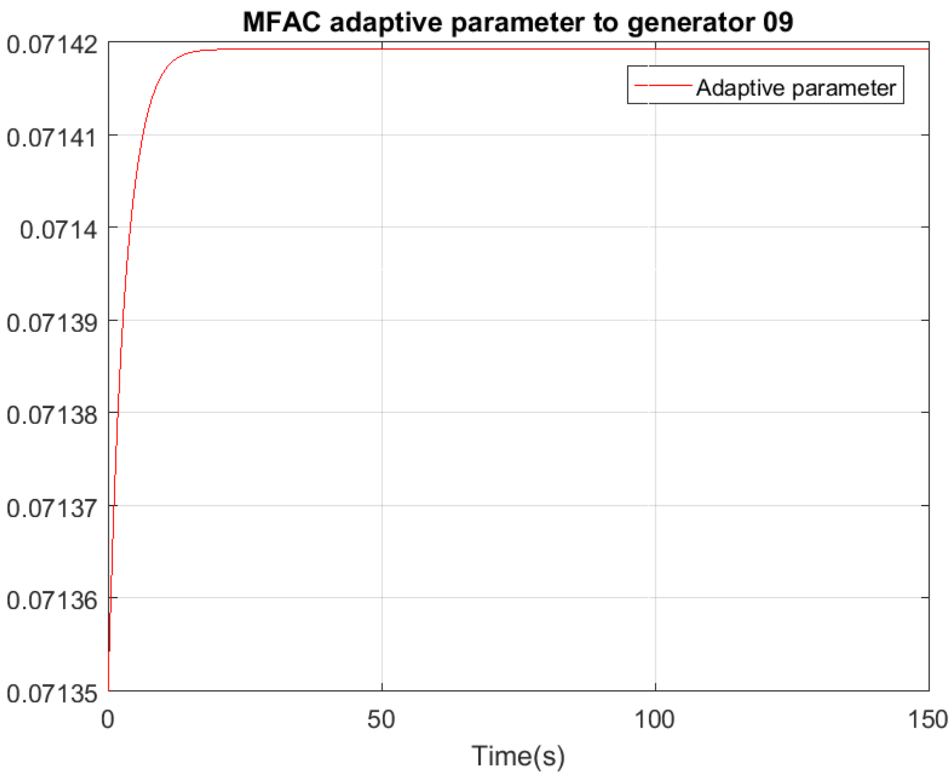

Figure 43 – MFAC adaptive parameter ($B_{28}G_{09}$).

- **Case 2**

To demonstrate the SVC efficiency, simulations are carried out using a step of load at the selected pilot buses. The reference voltage magnitude is set to 1 p.u. in all pilot buses. The power system voltage requirement is 4%. To preserve the terminal bus of generators against over voltage, a limiter is specified in the AVR output $u(k)$ (20%). Initially, the power system is stable with all buses attending the 4% requirement for voltage magnitude using the PVC (AVRs are set to 1 p.u.) and SVC. Suddenly, a load disturbance with a constant power factor (100% in the active and reactive power) is applied at Bus 27, as shown in Figure 44-67 . Table 7 compares the settling time of each pilot bus in different controller design approaches.

Figure 44 shows the load disturbance effect in the pilot bus 03 using the three different controller approaches. Figure 45 represent the control signal to generator 10 in VRFT and Traditional approach. Figure 46 shows the reference signal to generator 10. Note that under disturbance effects, the MFAC approach presents a higher reference signal, due to its derivative effect, and its adaptive parameter that changes to reach a faster response, as shown in Figure 47. The same figures sequence is shown to the other sensitive pairs, as follow:

Table 7 – Settling Time (Case 02).

Bus|Generator	Traditional (s)	VRFT (s)	MFAC (s)
03|10	8.53	8.97	6.98
09|01	5.82	4.95	7.22
10|03	7.05	8.63	6.78
20|05	6.80	9.22	8.12
23|07	8.35	9.40	8.10
28|09	6.02	10.33	8.62

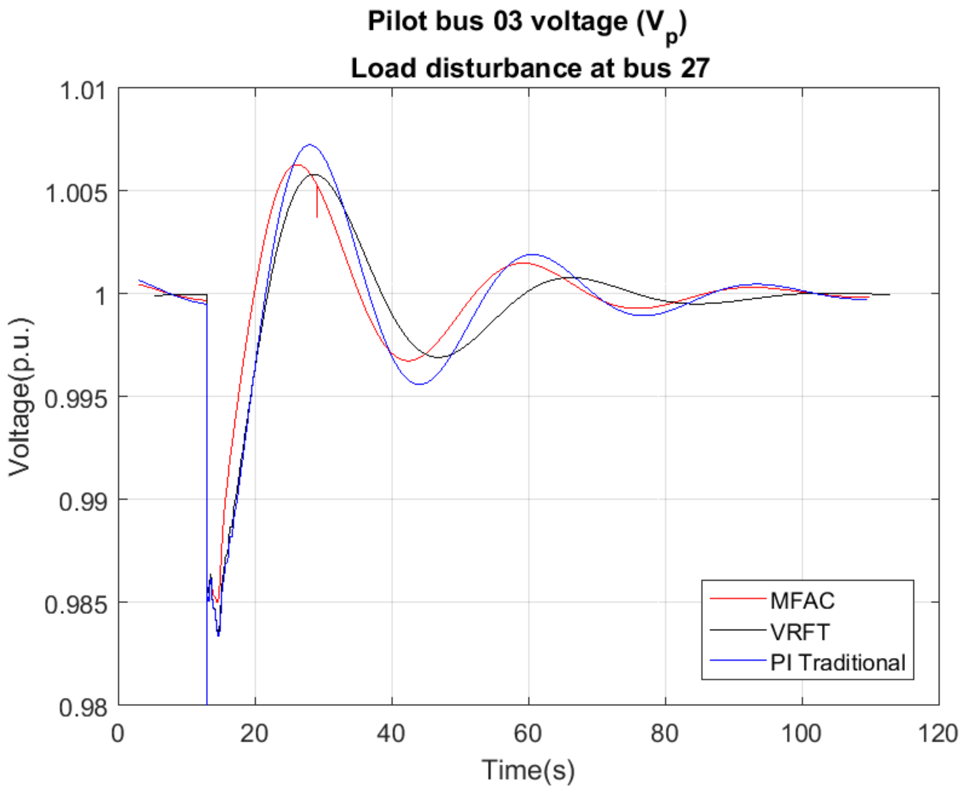

Figure 44 – Pilot bus voltage during load disturbance (Bus_{03}).

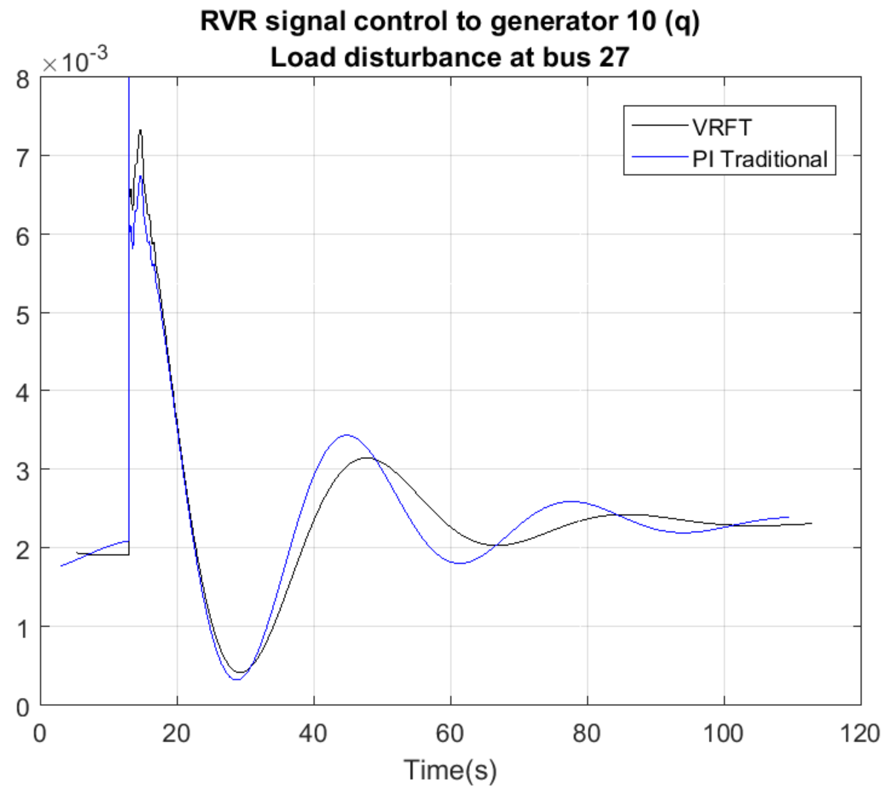

Figure 45 – RVR signal control (q) to generator 10 during load disturbance.

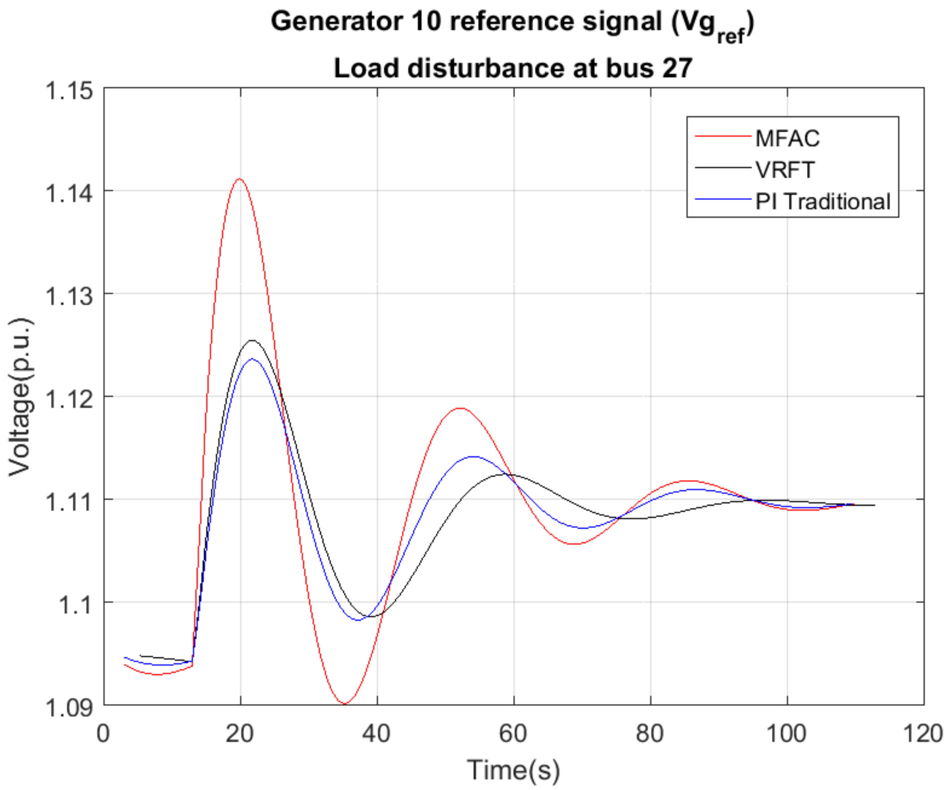

Figure 46 – Reference signal (Vg_{ref}) to generator 10 during load disturbance.

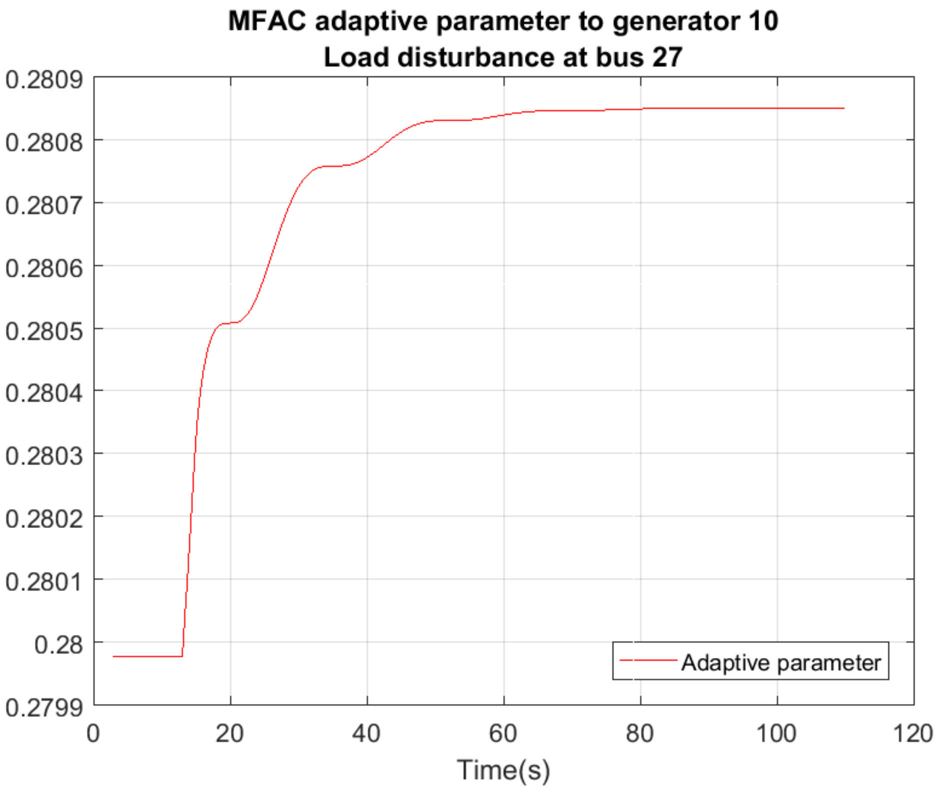

Figure 47 – MFAC adaptive parameter during load disturbance ($B_{03}G_{10}$).

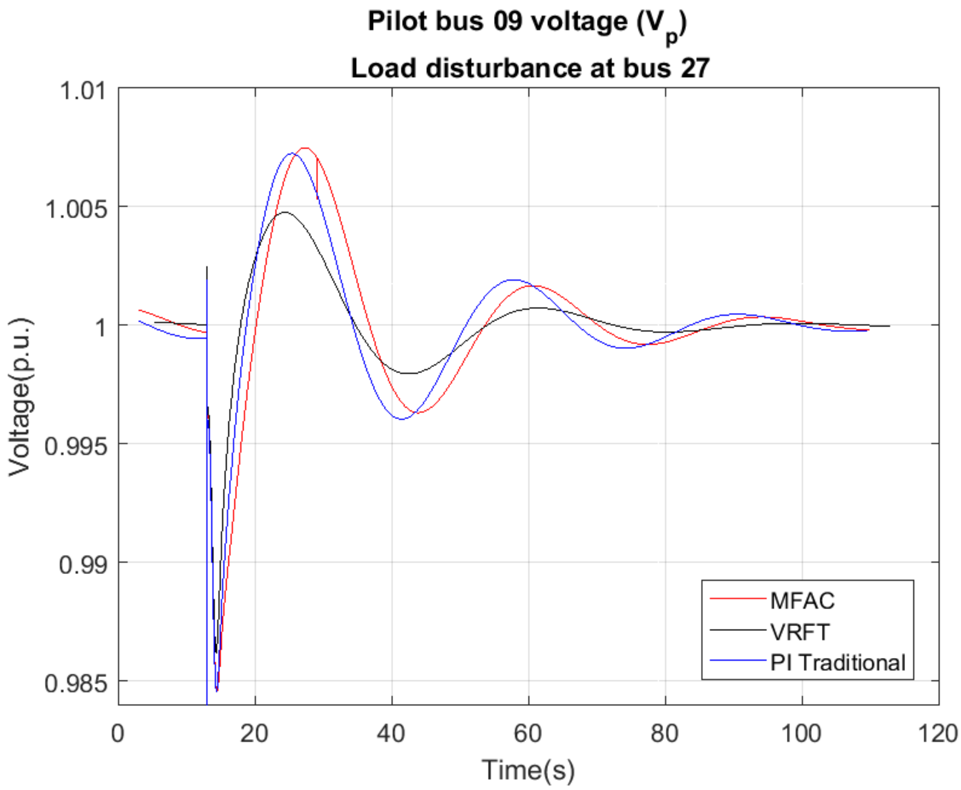

Figure 48 – Pilot bus voltage during load disturbance (Bus_{09}).

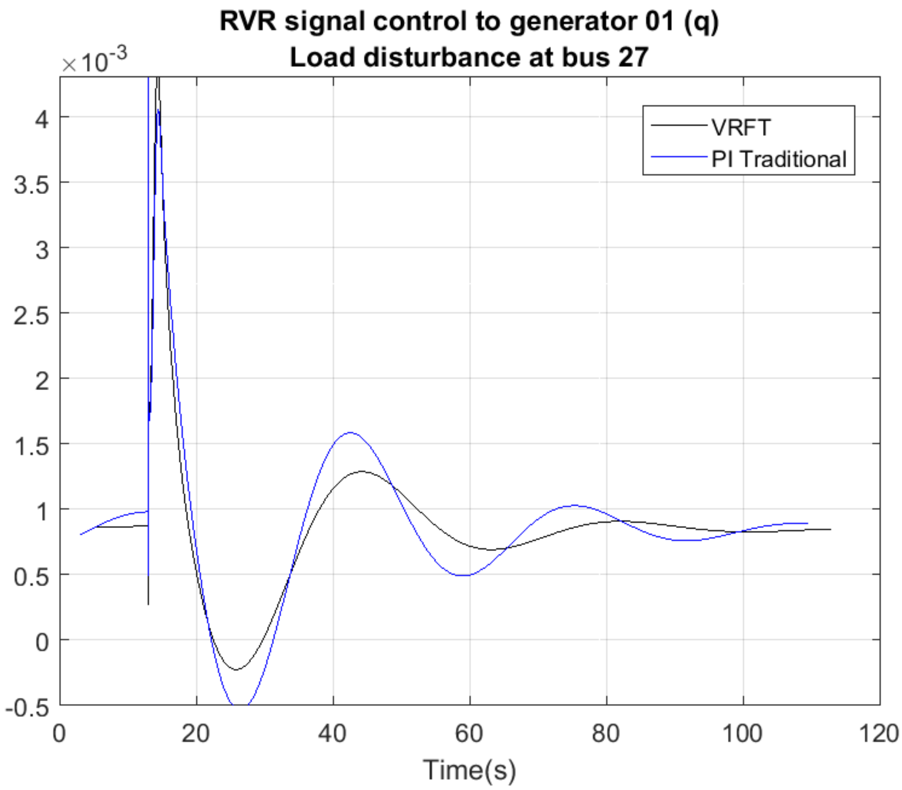

Figure 49 – RVR signal control (q) to generator 01 during load disturbance.

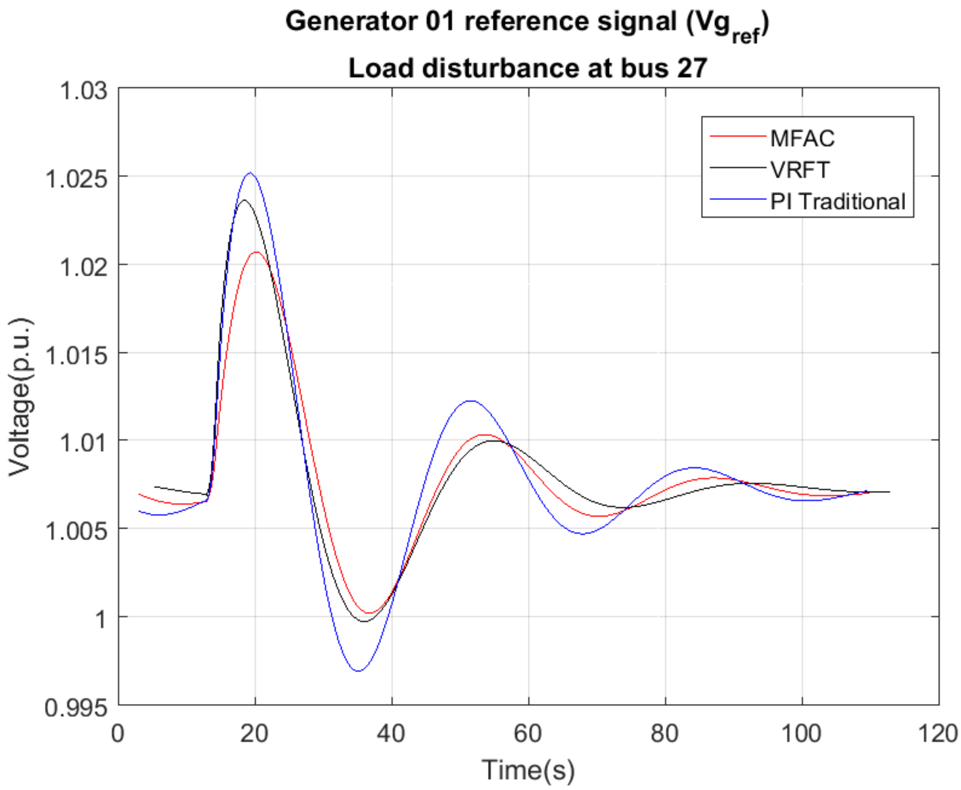

Figure 50 – Reference signal (Vg_{ref}) to generator 01 during load disturbance.

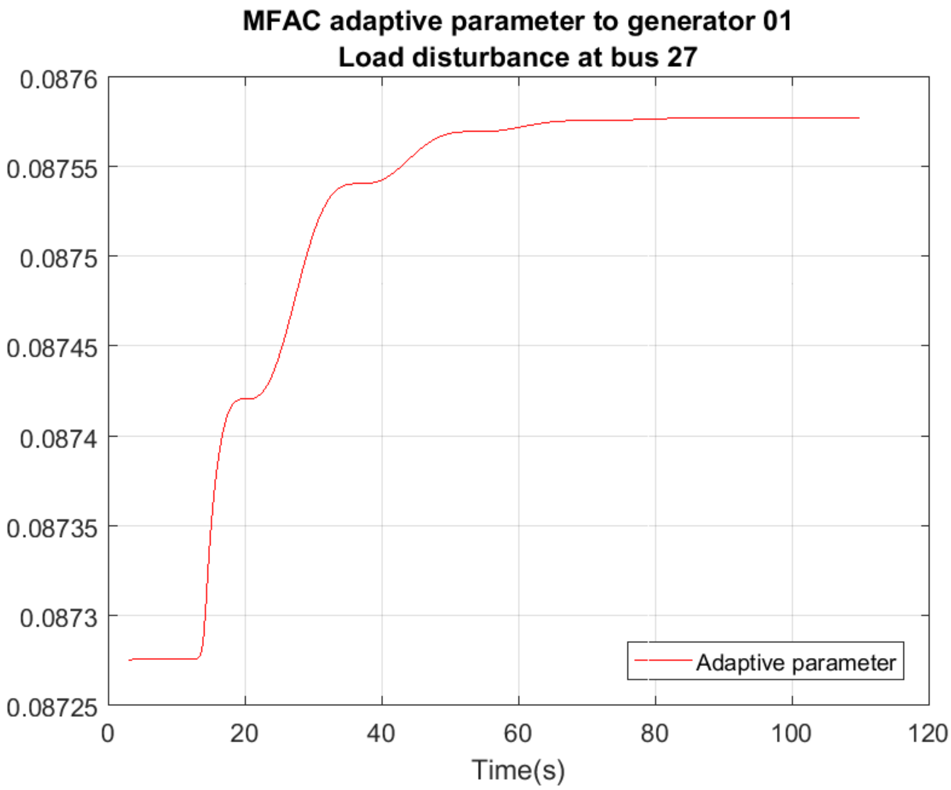

Figure 51 – MFAC adaptive parameter during load disturbance ($B_{09}G_{09}$).

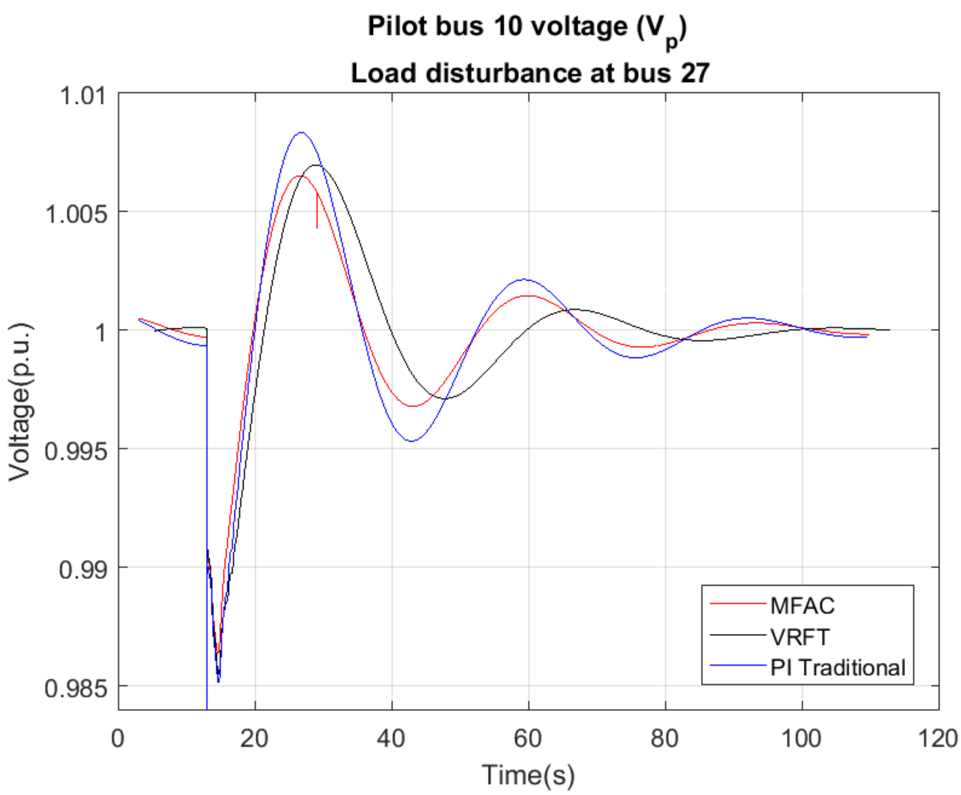

Figure 52 – Pilot bus voltage during load disturbance (Bus_{10}).

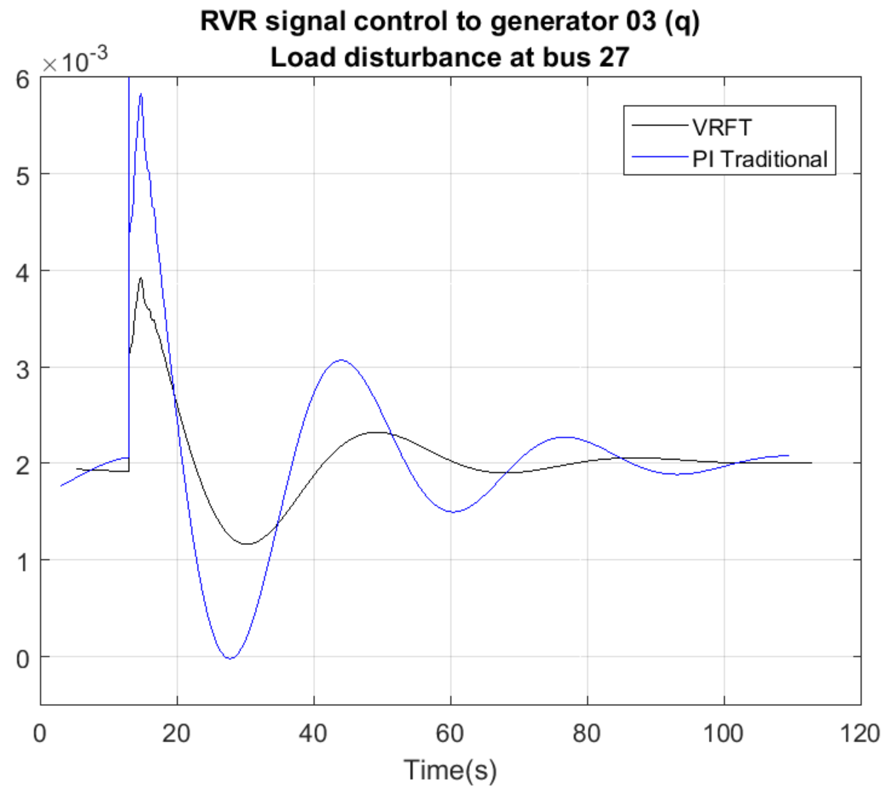

Figure 53 – RVR signal control (q) to generator 03 during load disturbance.

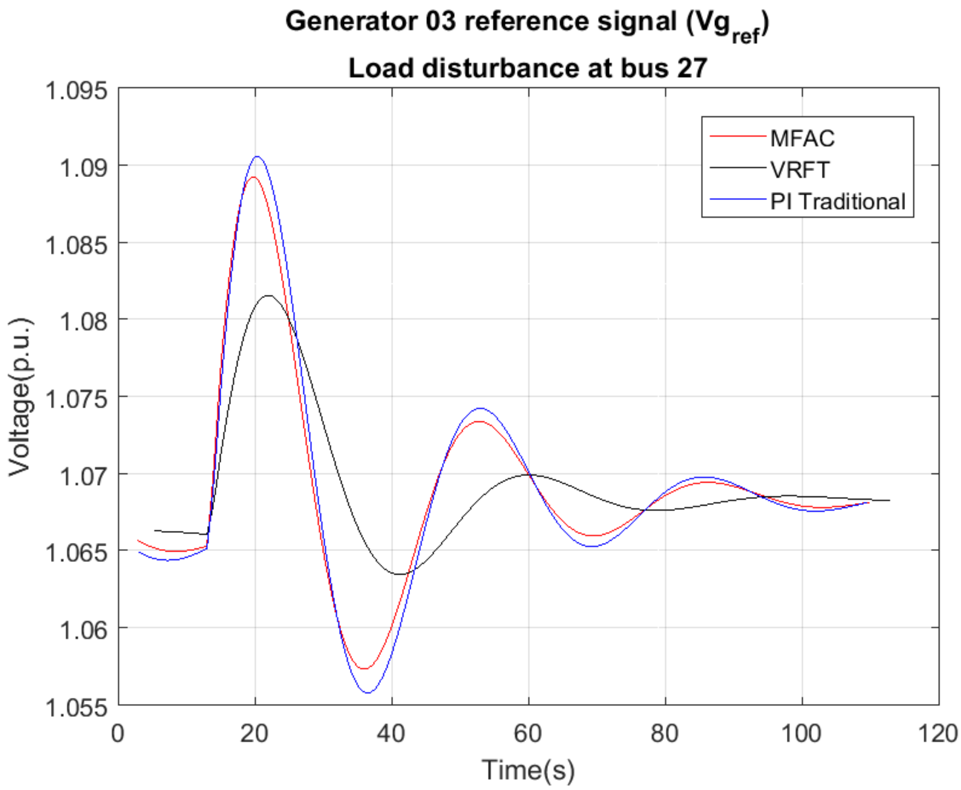

Figure 54 – Reference signal (Vg_{ref}) to generator 03 during load disturbance.

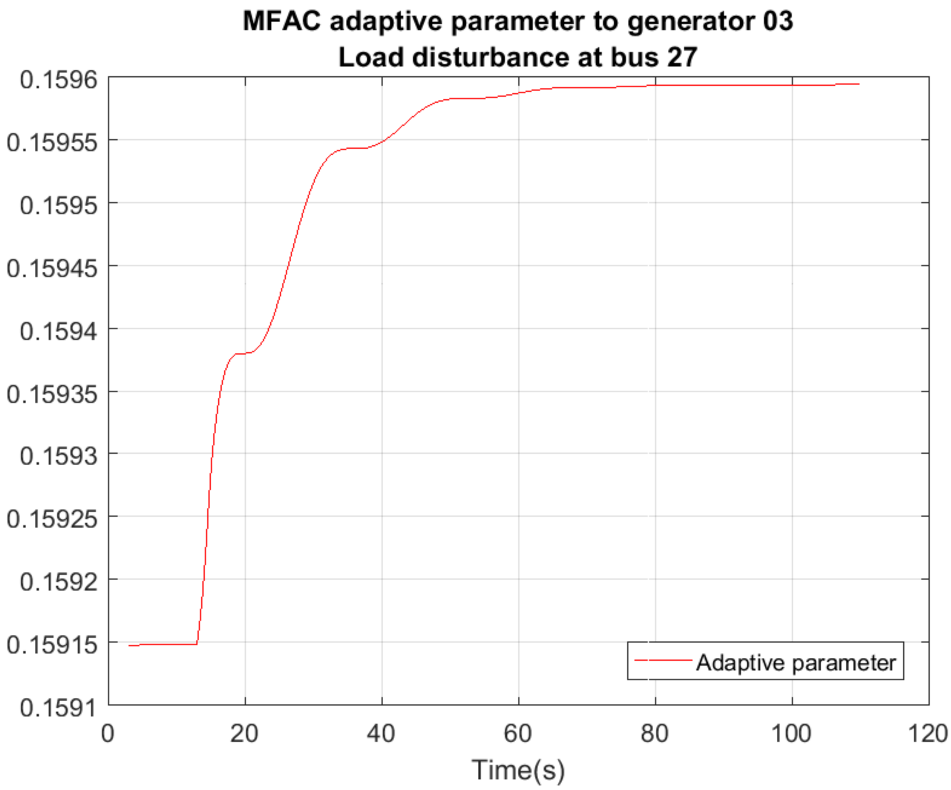

Figure 55 – MFAC adaptive parameter during load disturbance ($B_{10}G_{03}$).

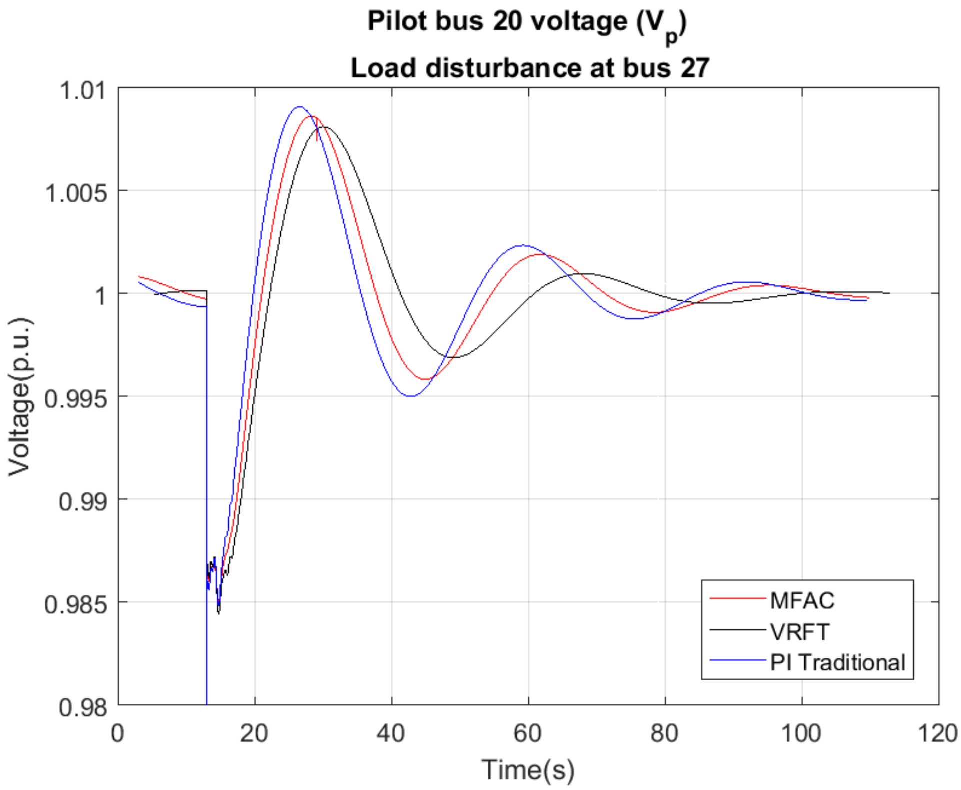

Figure 56 – Pilot bus voltage during load disturbance (Bus_{20}).

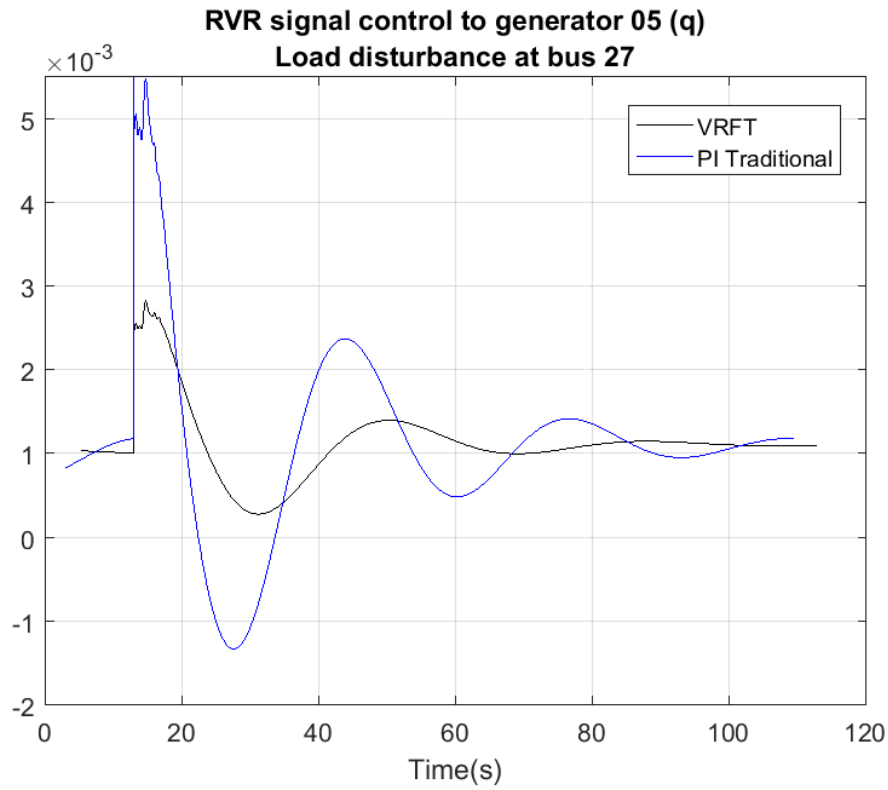

Figure 57 – RVR signal control (q) to generator 05 during load disturbance.

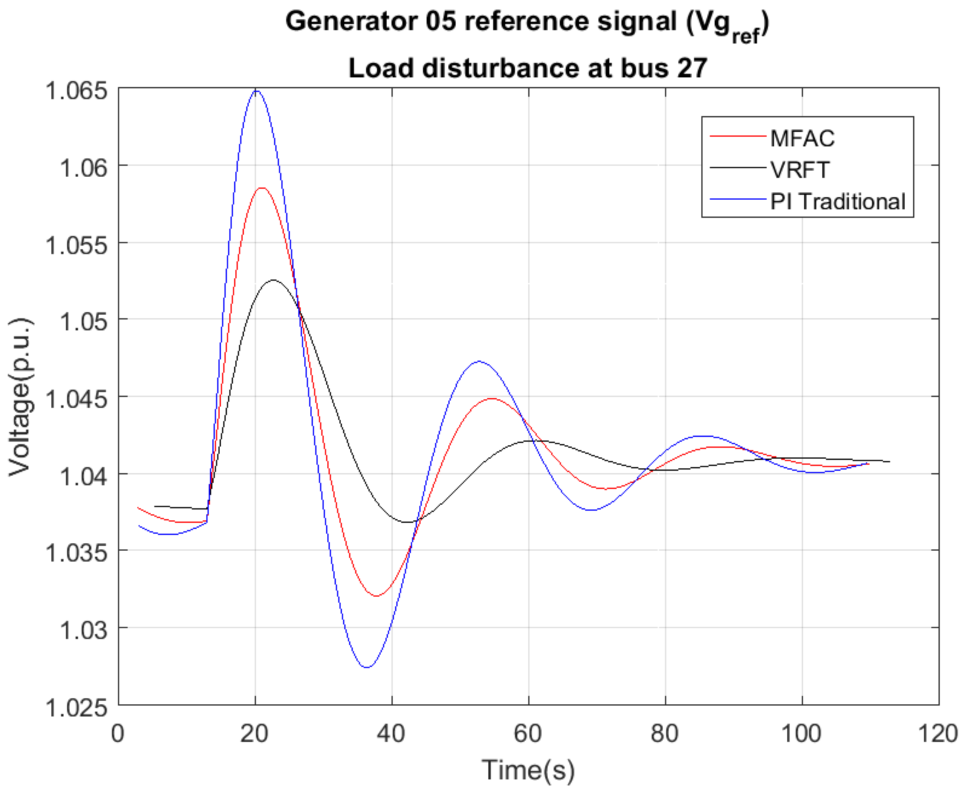

Figure 58 – Reference signal (Vg_{ref}) to generator 05 during load disturbance.

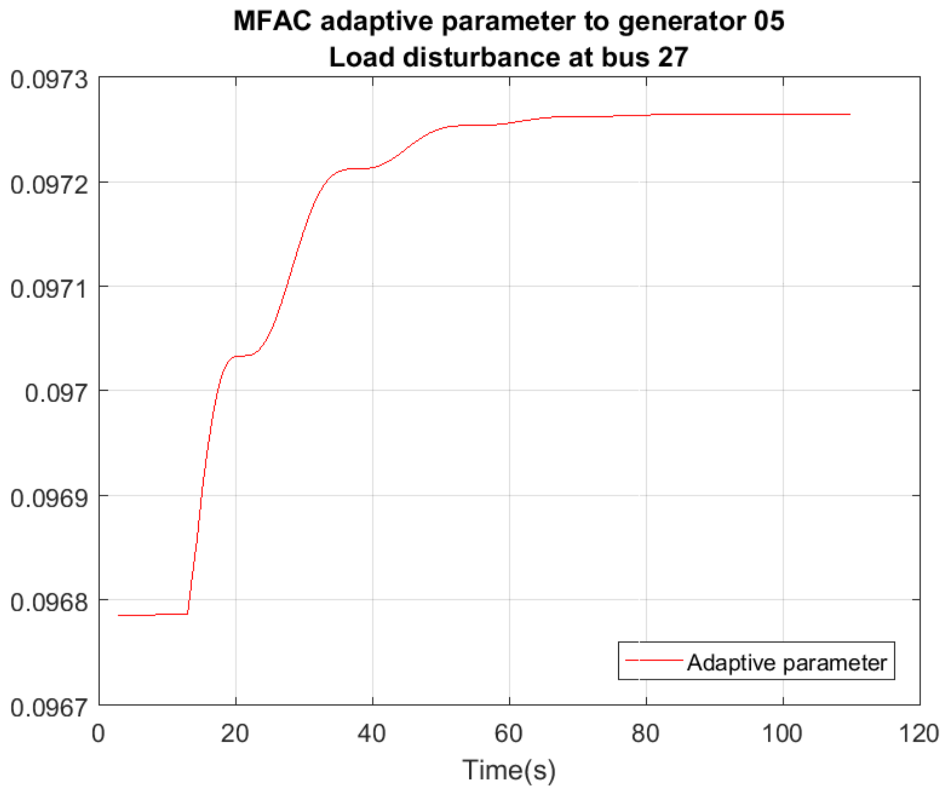

Figure 59 – MFAC adaptive parameter during load disturbance ($B_{20}G_{05}$).

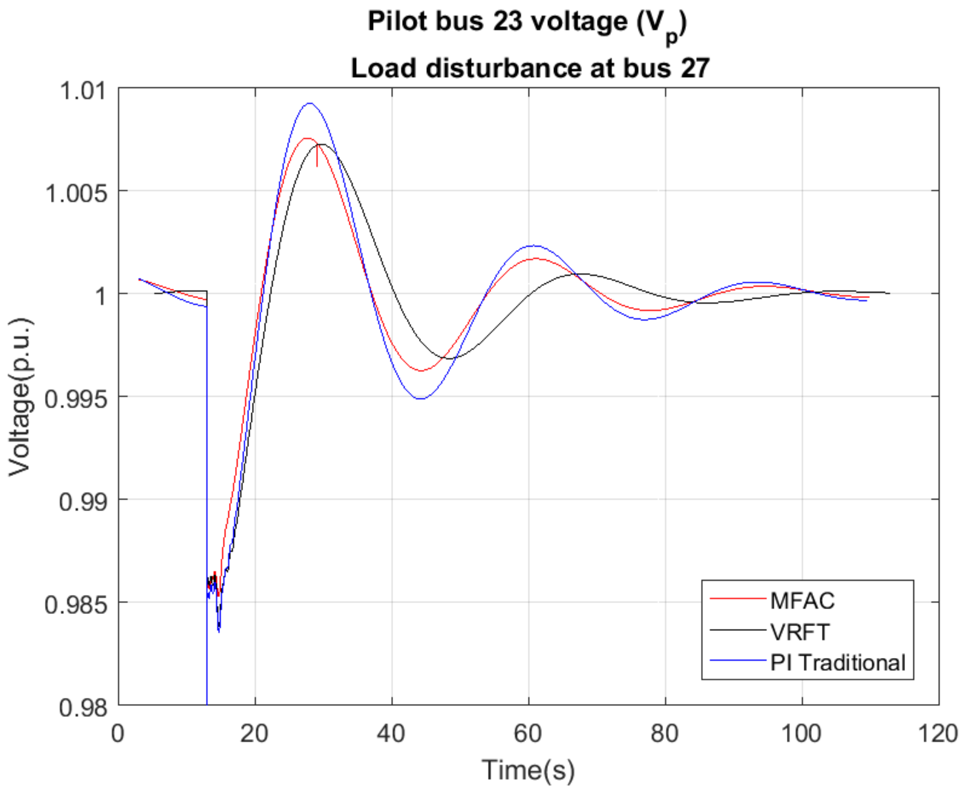

Figure 60 – Pilot bus voltage during load disturbance (Bus_{23}).

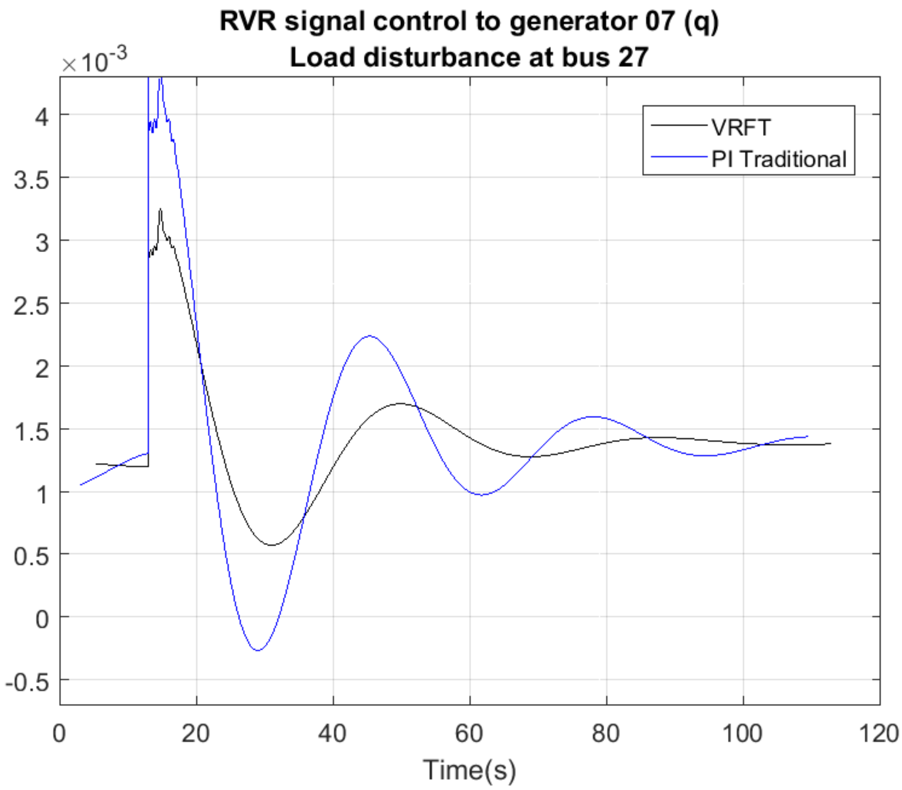

Figure 61 – RVR signal control (q) to generator 07 during load disturbance.

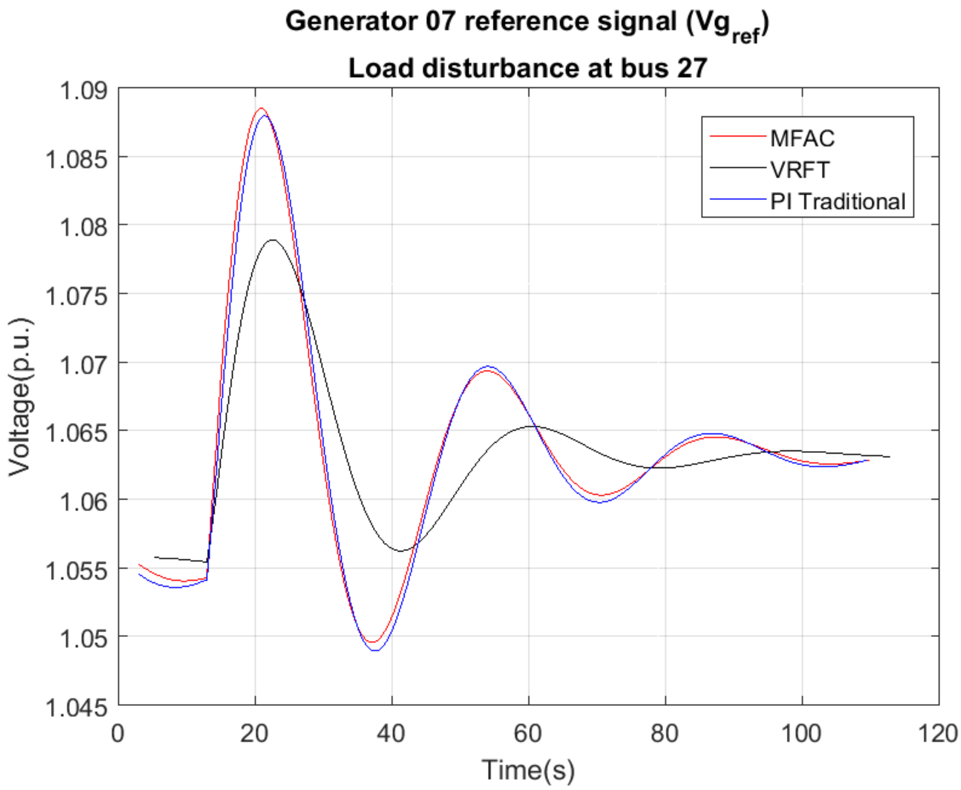

Figure 62 – Reference signal (Vg_{ref}) to generator 07 during load disturbance.

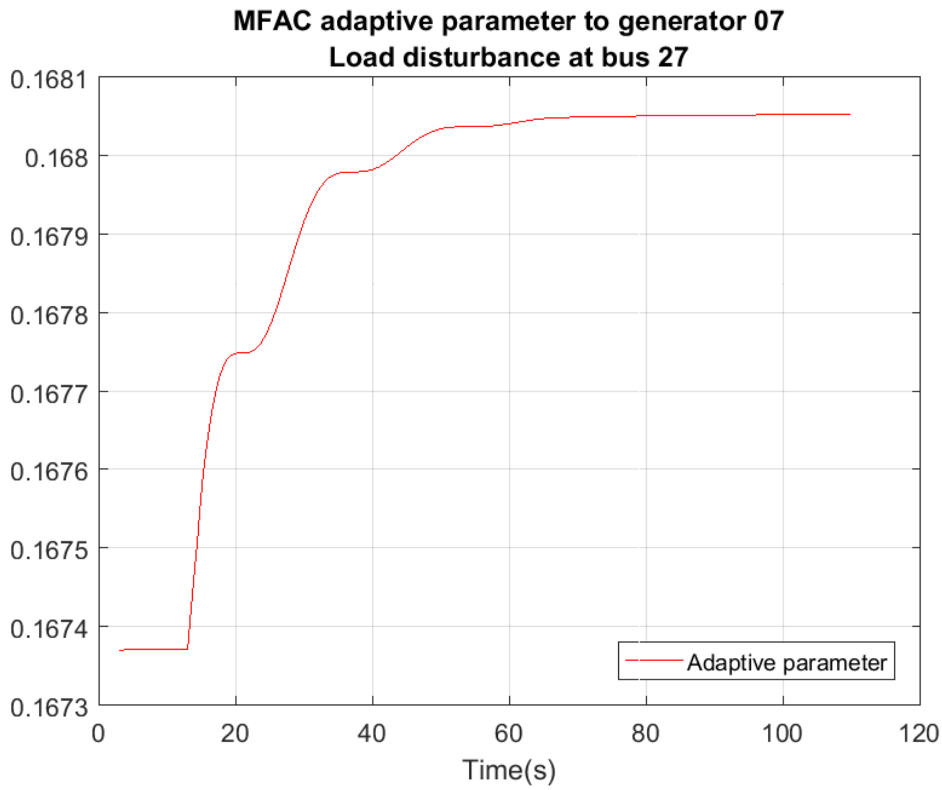

Figure 63 – MFAC adaptive parameter during load disturbance ($B_{23}G_{07}$).

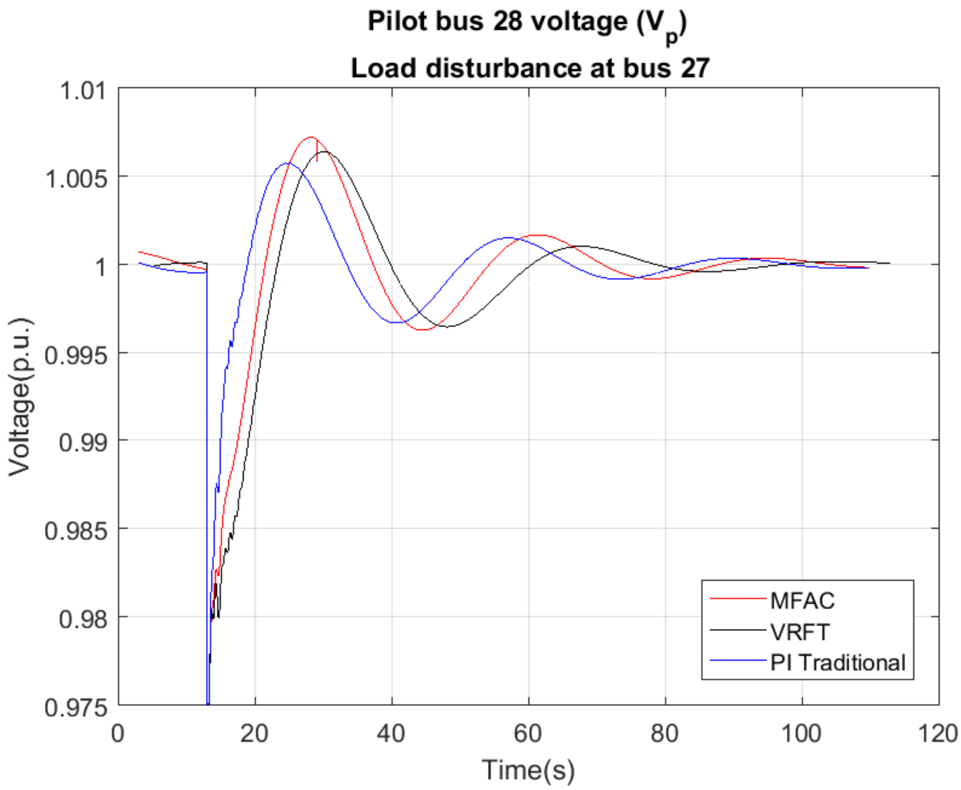

Figure 64 – Pilot bus voltage during load disturbance (Bus_{28}).

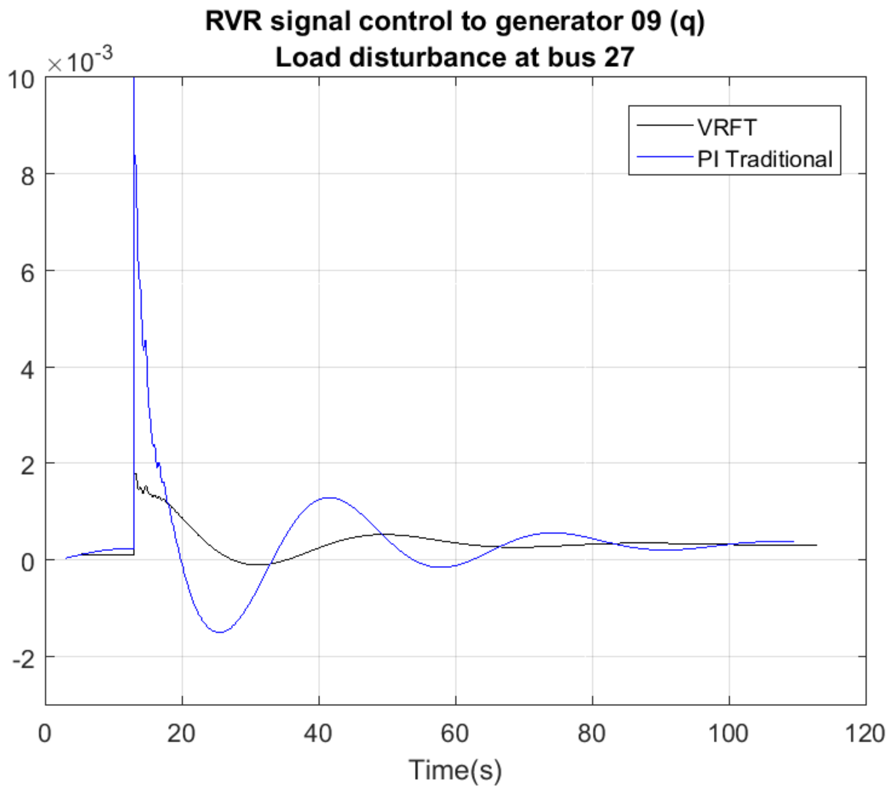

Figure 65 – RVR signal control (q) to generator 09 during load disturbance.

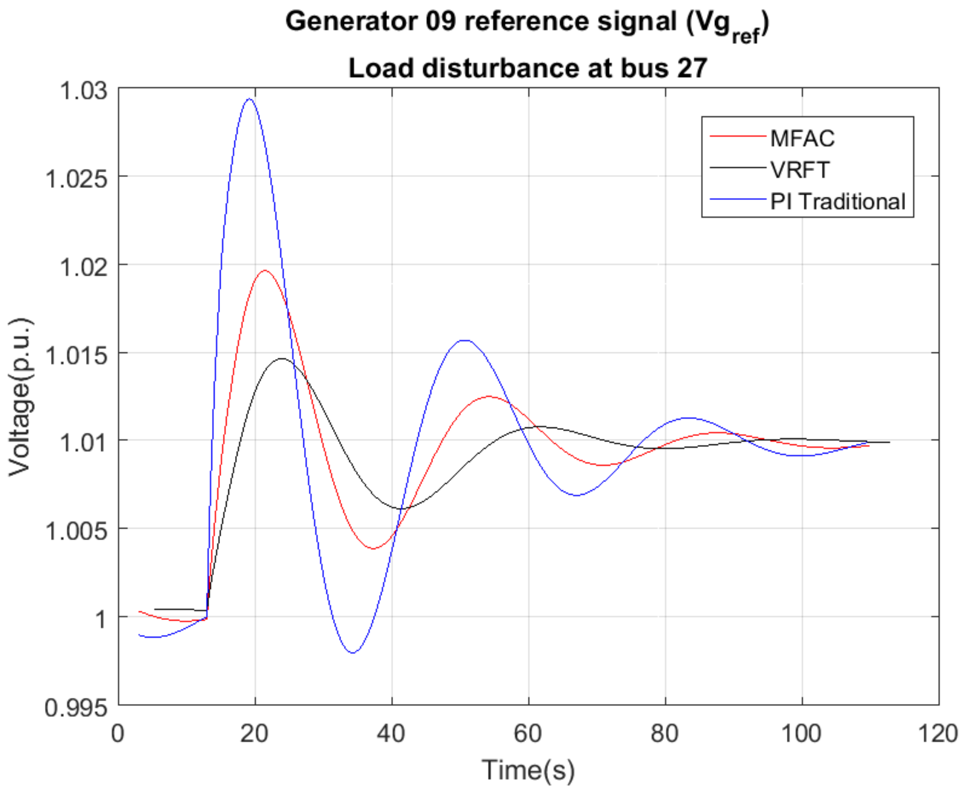

Figure 66 – Reference signal (Vg_{ref}) to generator 09 during load disturbance.

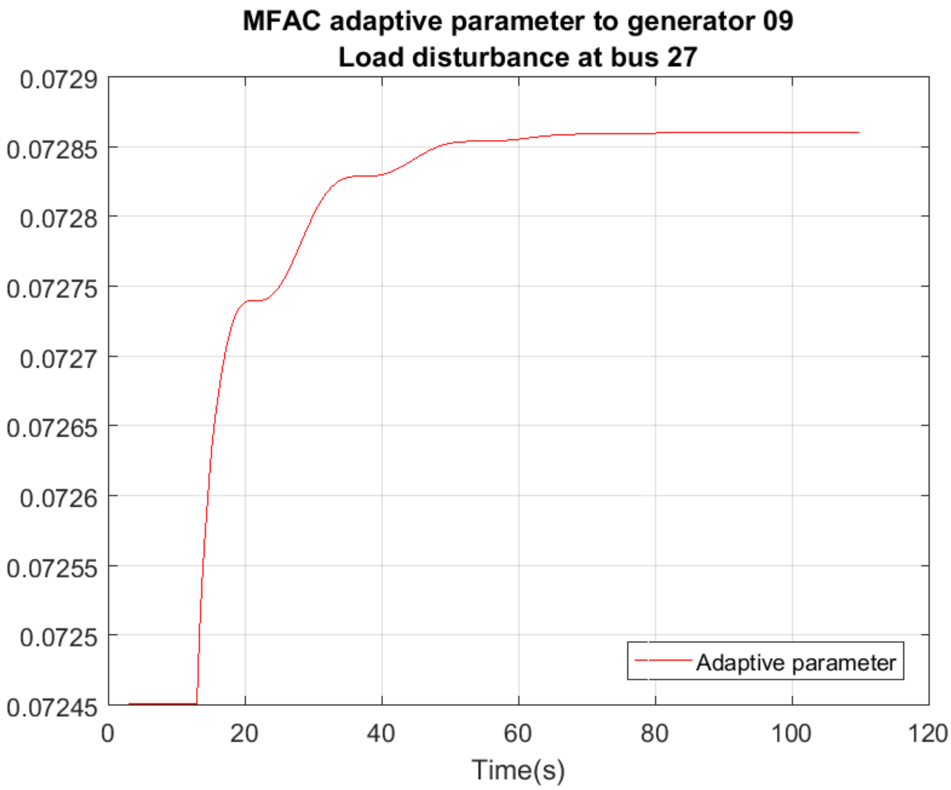

Figure 67 – MFAC adaptive parameter during load disturbance ($B_{28}G_{09}$).

- **Case 3**

Initially, all the pilot buses are in a steady state, with their values in 1p.u. Suddenly, a disturbance in the 3-4 transmission line occurs, leading to the opening of its circuit breakers, and the loss of this line. The Figure 68-91 shows the pilot buses voltage and the control signals behaviour. Table 8 compares the settling time of each pilot bus in different controller design approaches.

Figure 68 shows the load disturbance effect in the pilot bus 03 using the three different controller approaches. Figure 69 represents the signal control to generator 10 in VRFT and Traditional approach. Figure 70 shows the reference signal to generator 10. The adaptive parameter in the MFAC approach is presented in Figure 71. The same figures sequence is shown to the other sensitive pairs, as follow:

Table 8 – Settling Time (Case 03).

Bus|Generator	Traditional (s)	VRFT (s)	MFAC (s)
03|10	31.30	20.38	12.60
09|01	33.58	30.70	24.25
10|03	29.70	39.25	24.43
20|05	27.75	33.28	25.53
23|07	34.68	32.75	25.20
28|09	28.90	40.43	26.70

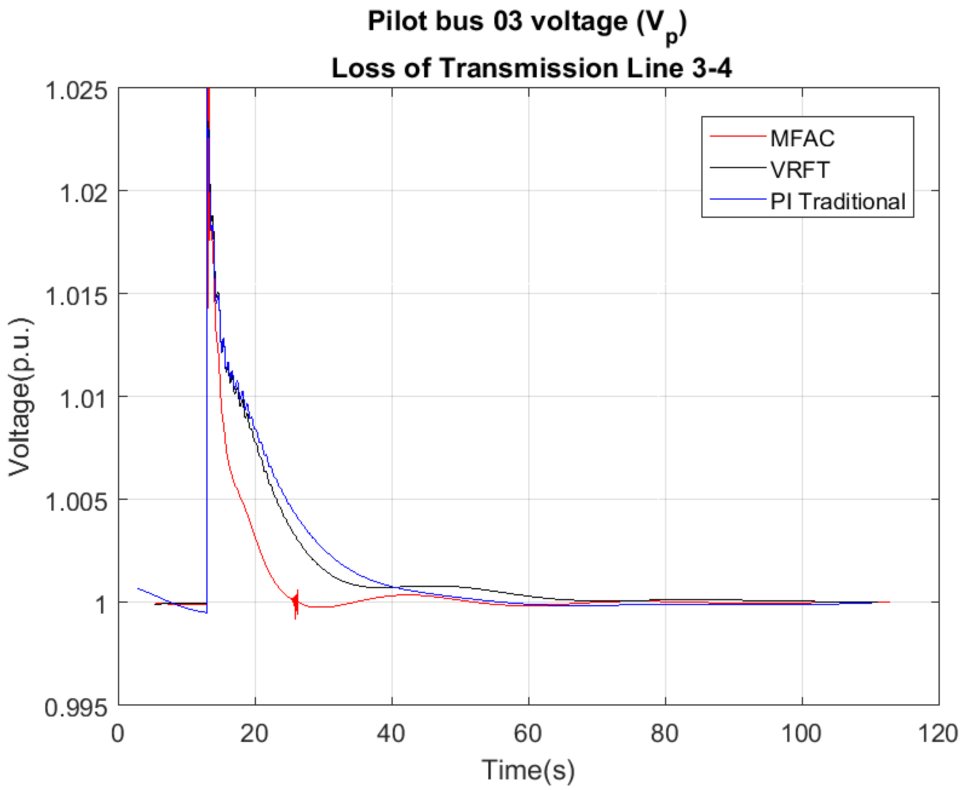

Figure 68 – Pilot bus voltage during Transmission Line 3-4 disturbance (Bus_{03}).

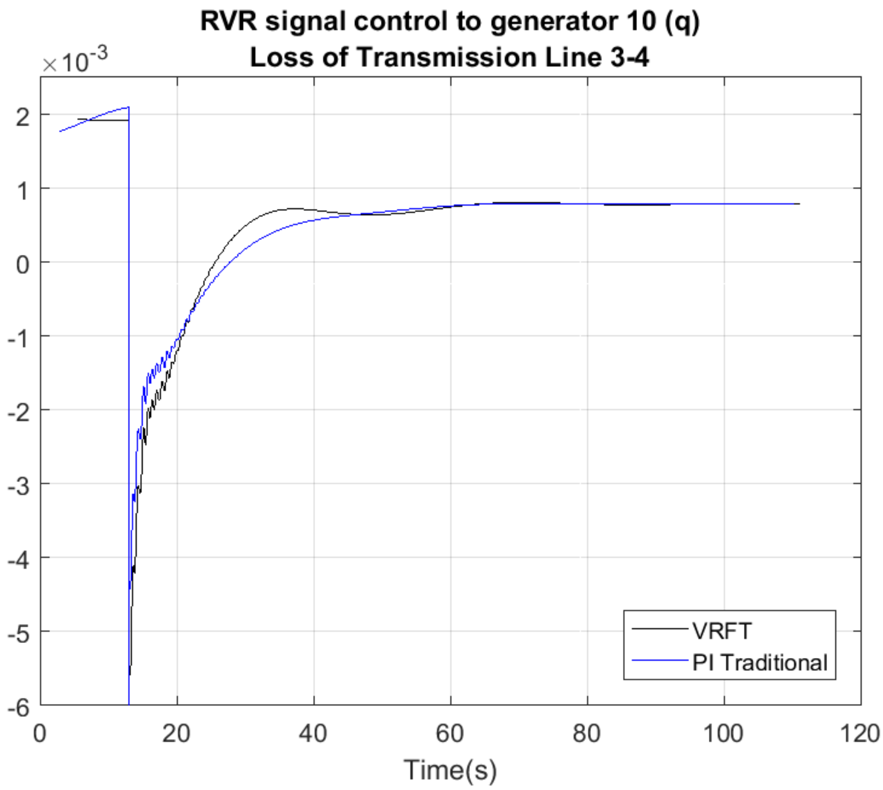

Figure 69 – RVR signal control (q) to generator 10 during Transmission Line 3-4 disturbance.

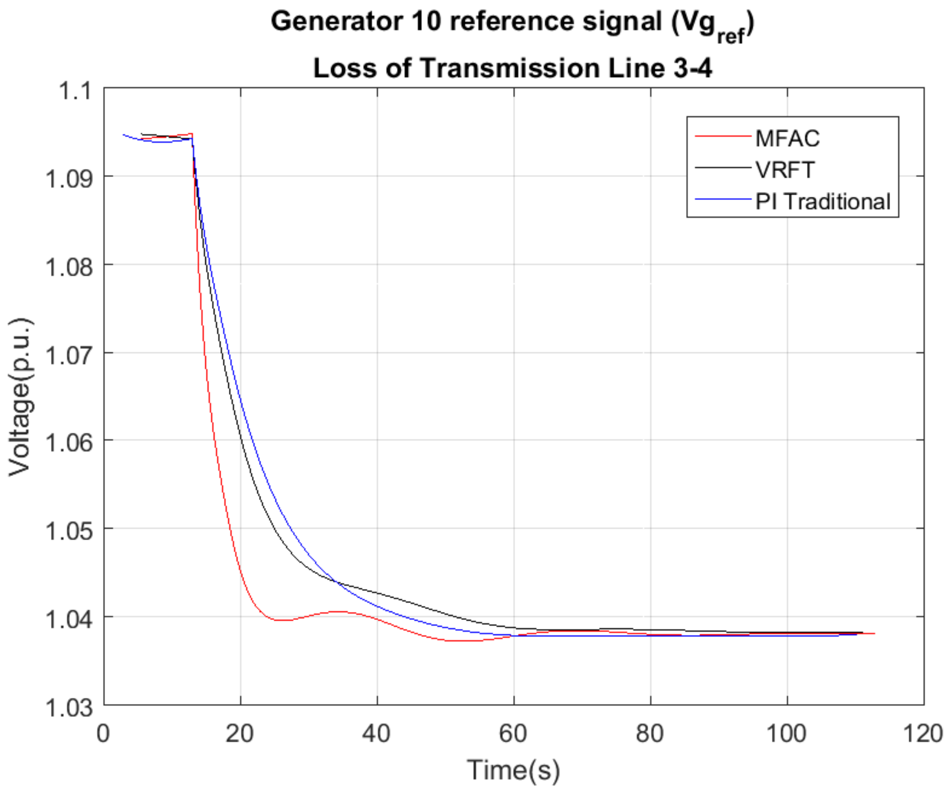

Figure 70 – Reference signal (Vg_{ref}) to generator 10 during Transmission Line 3-4 disturbance.

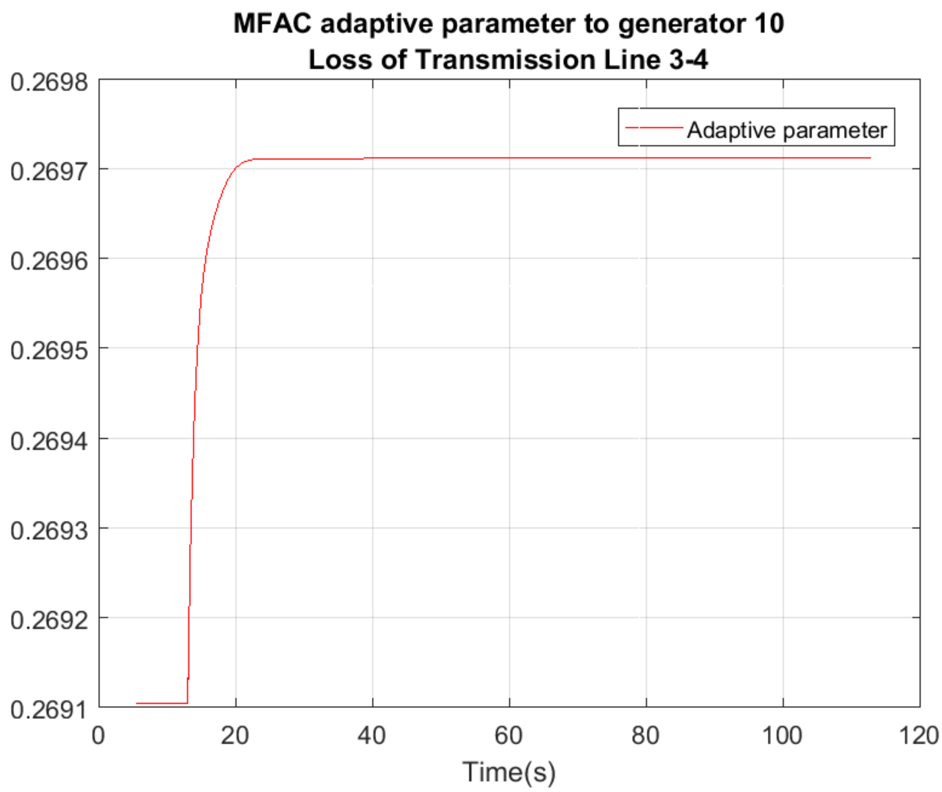

Figure 71 – MFAC adaptive parameter during Transmission Line 3-4 disturbance ($B_{03}G_{10}$).

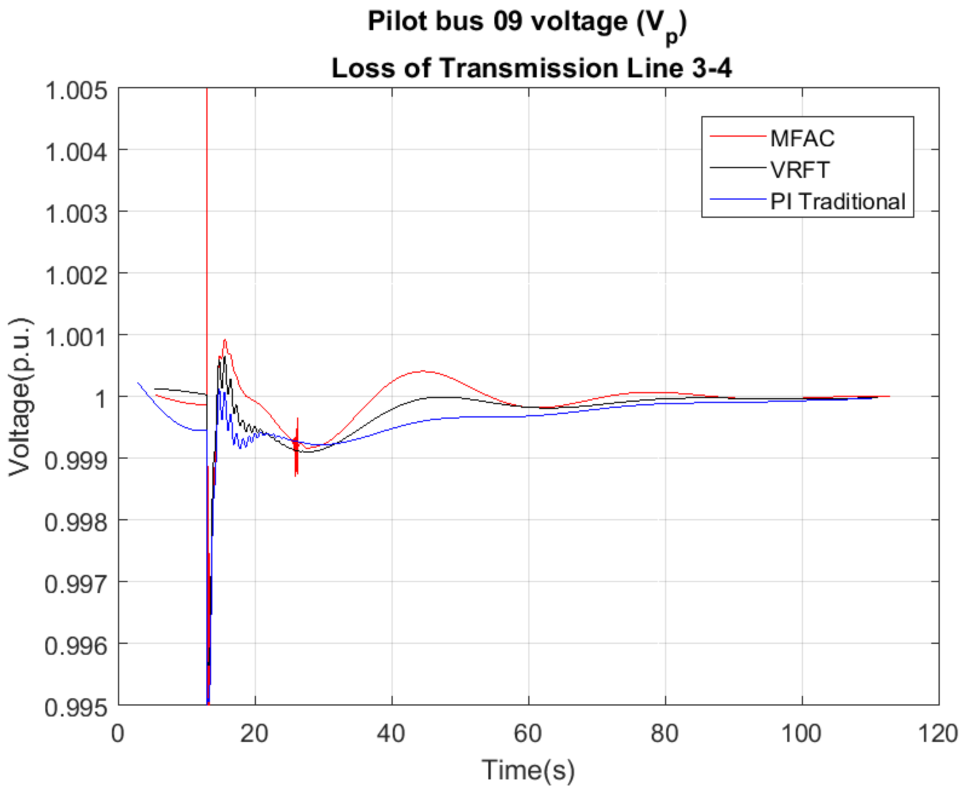

Figure 72 – Pilot bus voltage during Transmission Line 3-4 disturbance (Bus_{09}).

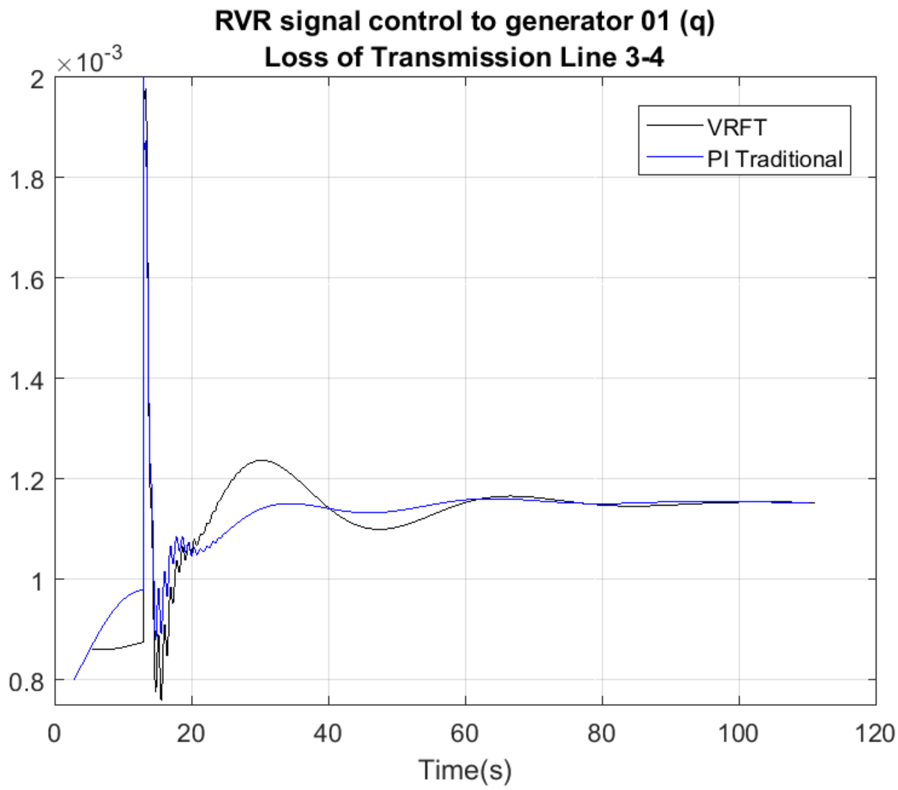

Figure 73 – RVR signal control (q) to generator 01 during Transmission Line 3-4 disturbance.

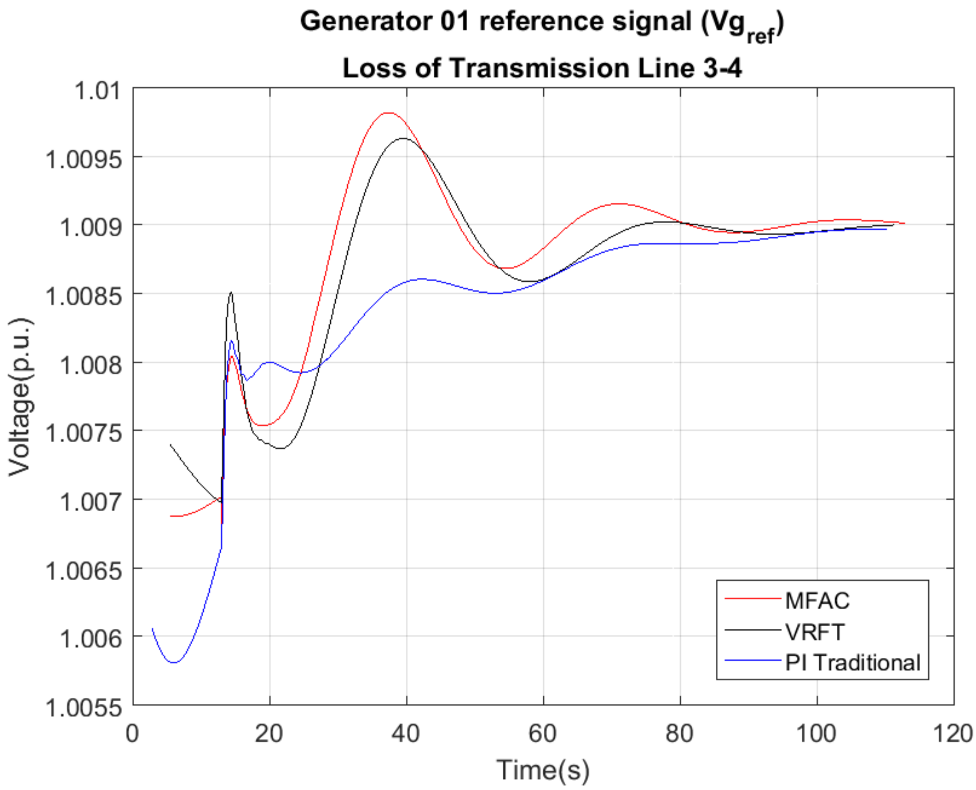

Figure 74 – Reference signal (Vg_{ref}) to generator 01 during Transmission Line 3-4 disturbance.

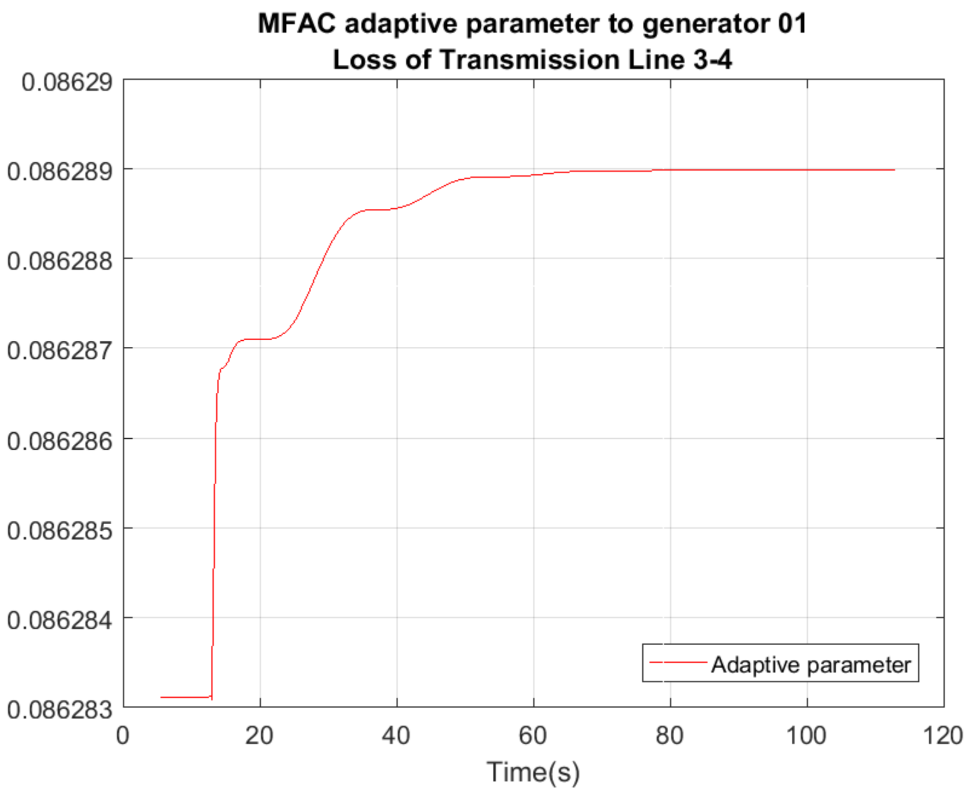

Figure 75 – MFAC adaptive parameter during Transmission Line 3-4 disturbance ($B_{09}G_{09}$).

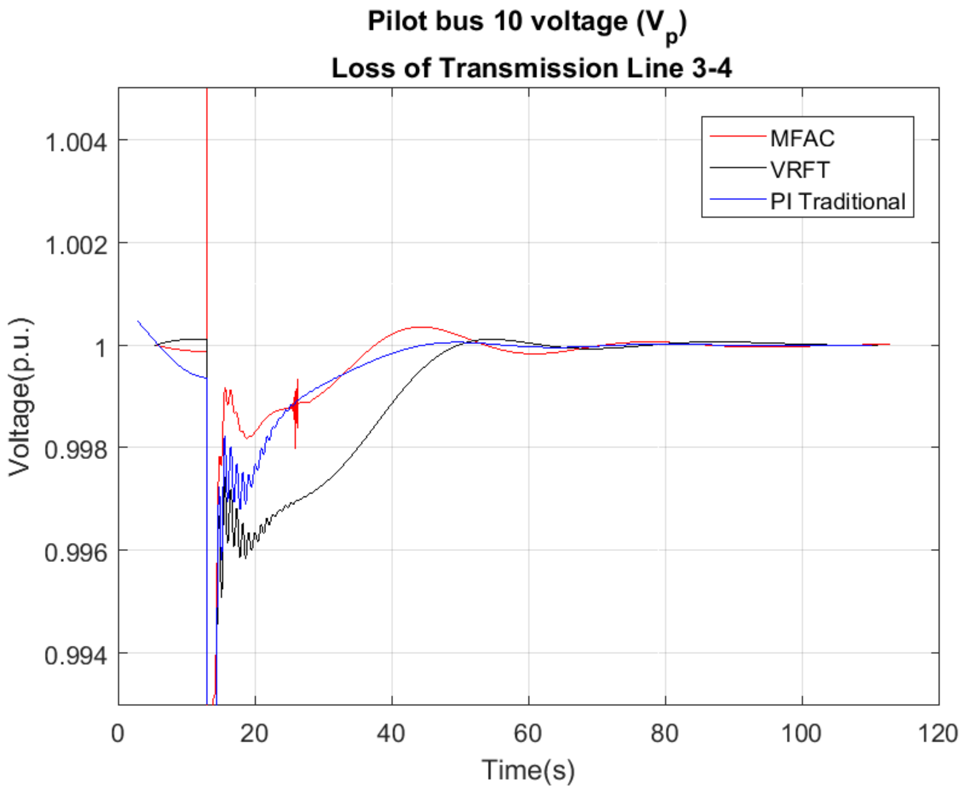

Figure 76 – Pilot bus voltage during Transmission Line 3-4 disturbance (Bus_{10}).

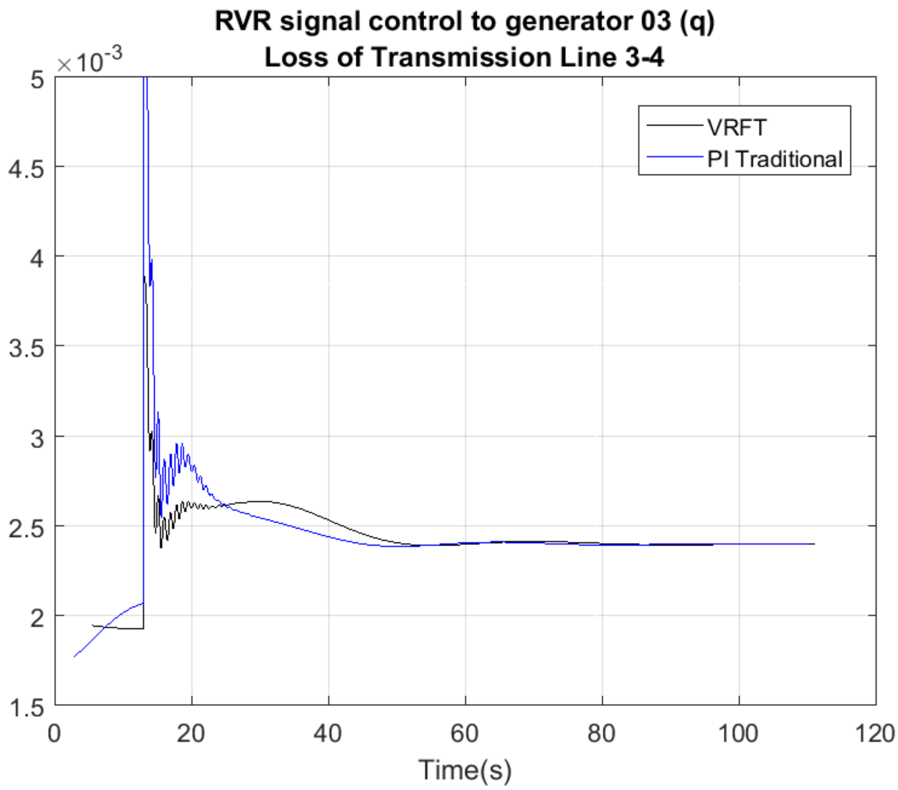

Figure 77 – RVR signal control (q) to generator 03 during Transmission Line 3-4 disturbance.

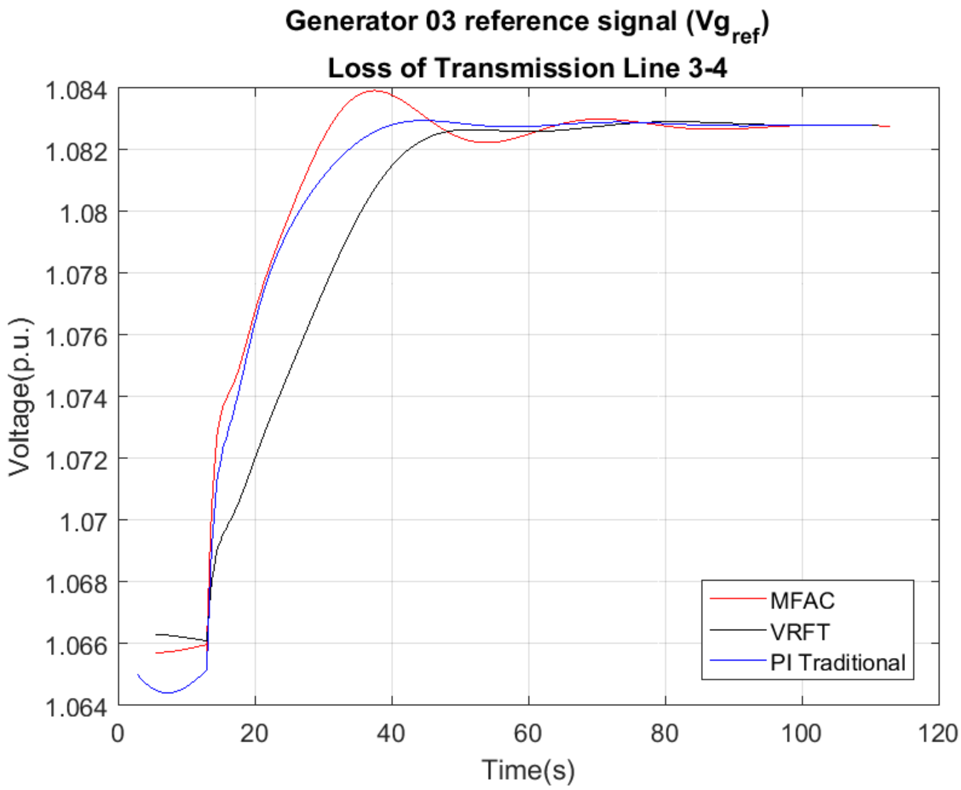

Figure 78 – Reference signal (Vg_{ref}) to generator 03 during Transmission Line 3-4 disturbance.

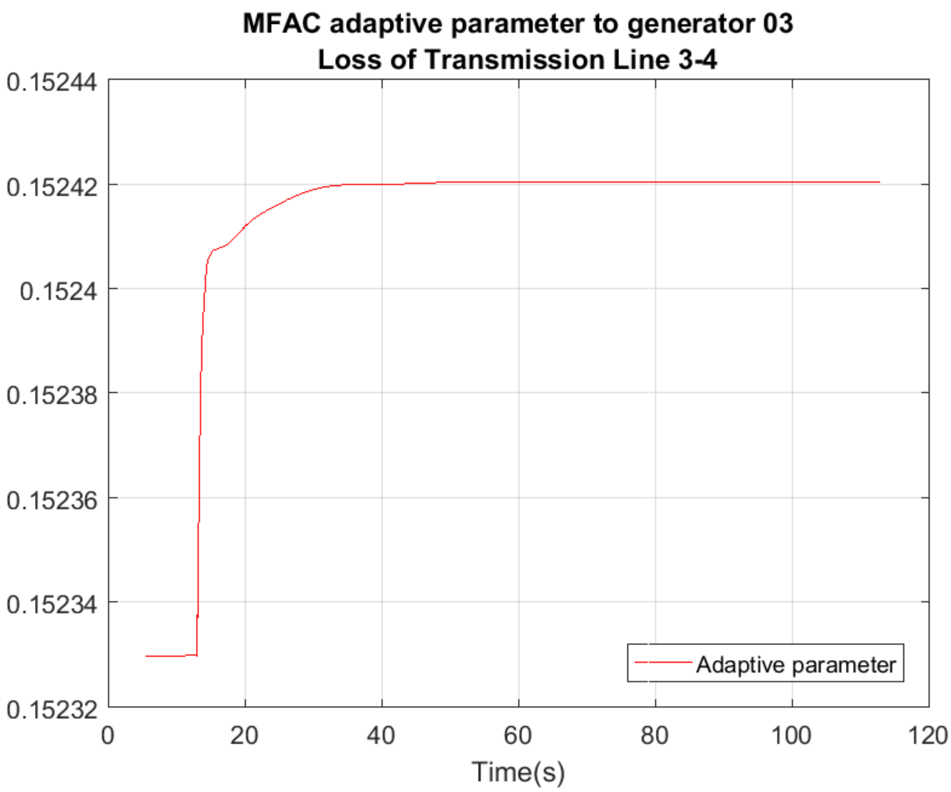

Figure 79 – MFAC adaptive parameter during Transmission Line 3-4 disturbance ($B_{10}G_{03}$).

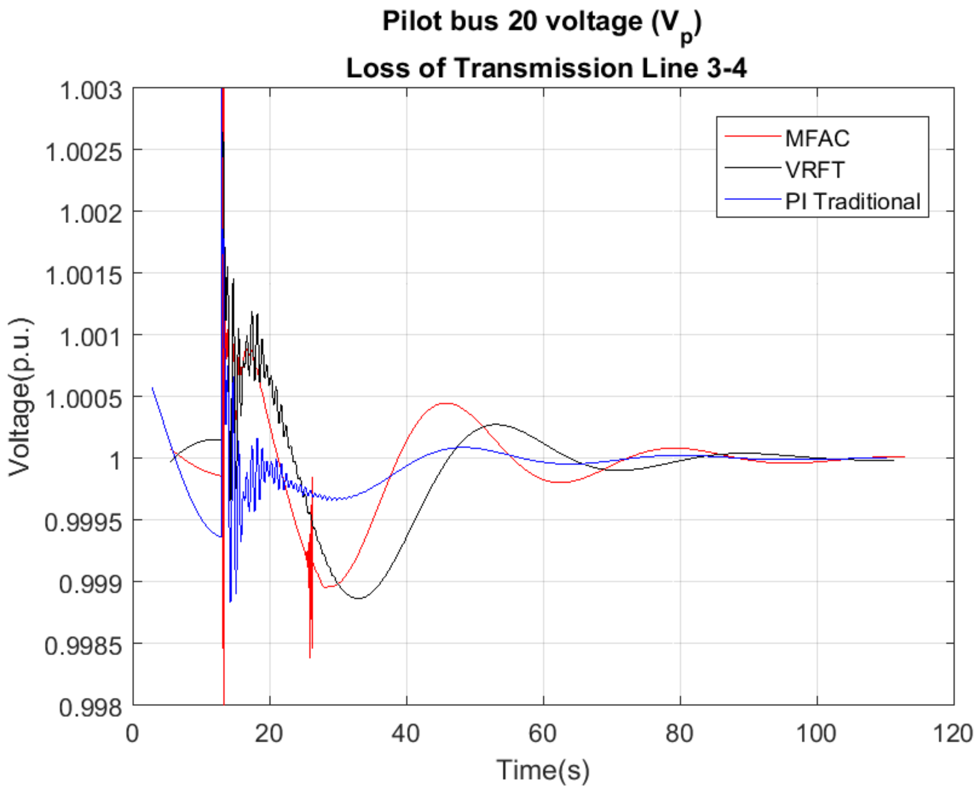

Figure 80 – Pilot bus voltage during Transmission Line 3-4 disturbance (Bus_{20}).

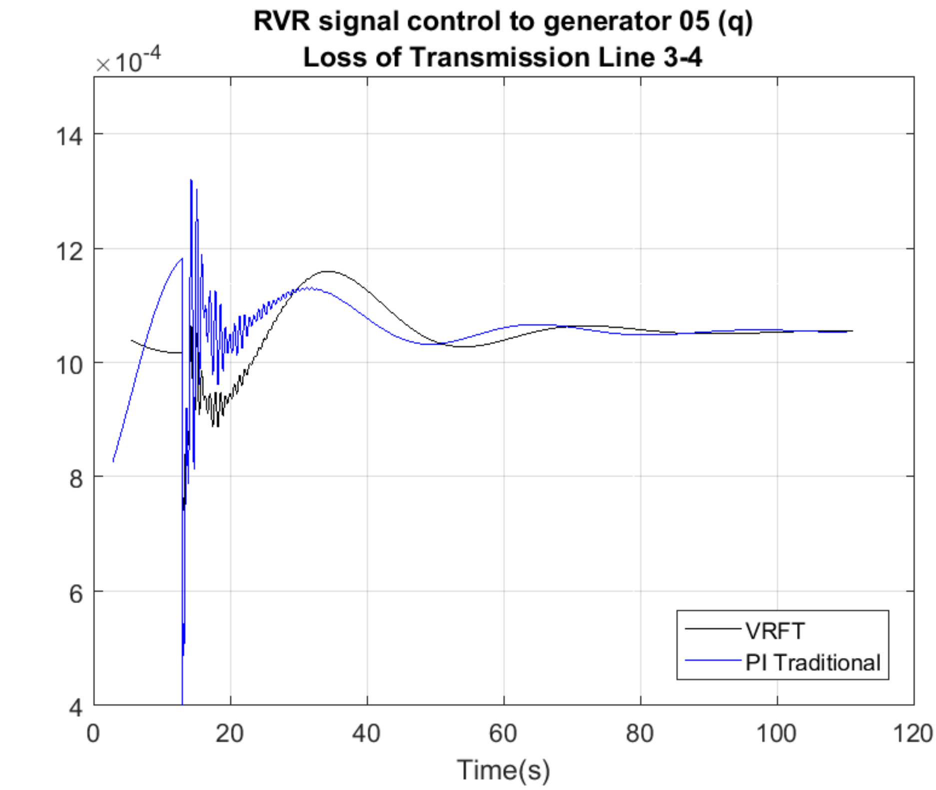

Figure 81 – RVR signal control (q) to generator 05 during Transmission Line 3-4 disturbance.

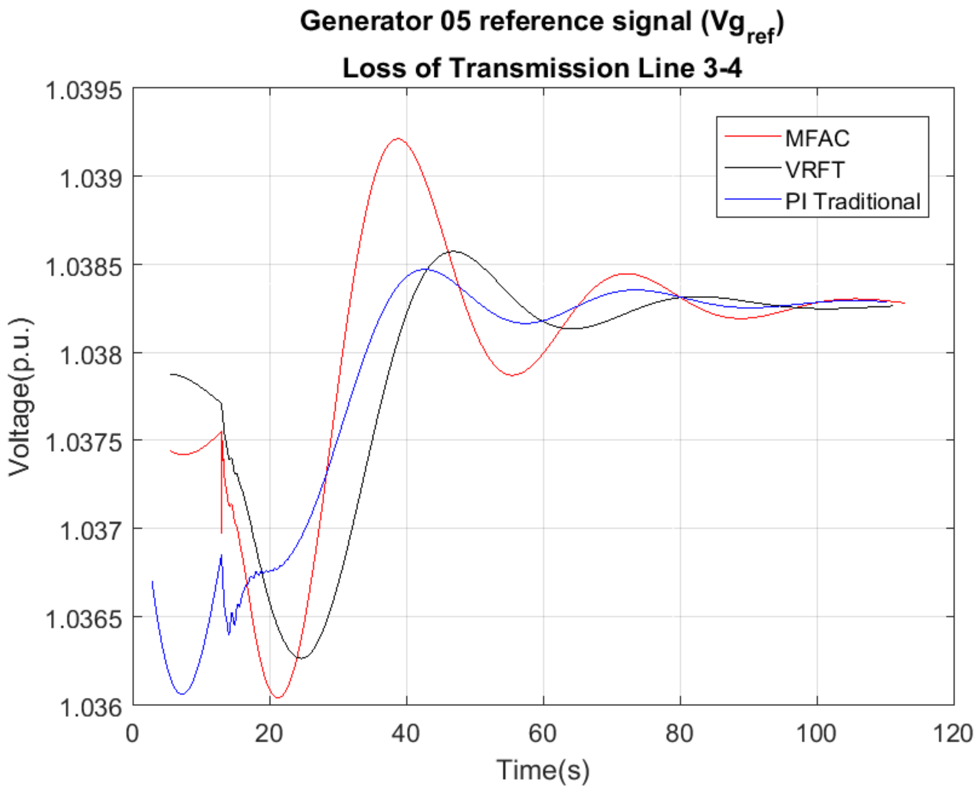

Figure 82 – Reference signal (Vg_{ref}) to generator 05 during Transmission Line 3-4 disturbance.

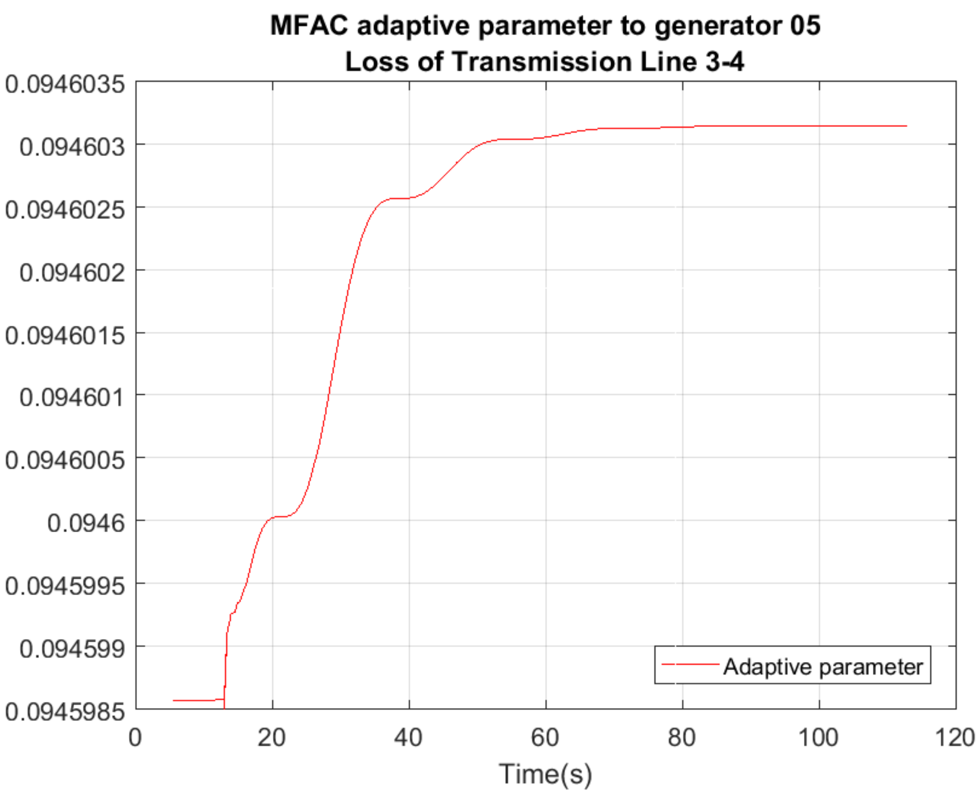

Figure 83 – MFAC adaptive parameter during Transmission Line 3-4 disturbance ($B_{20}G_{05}$).

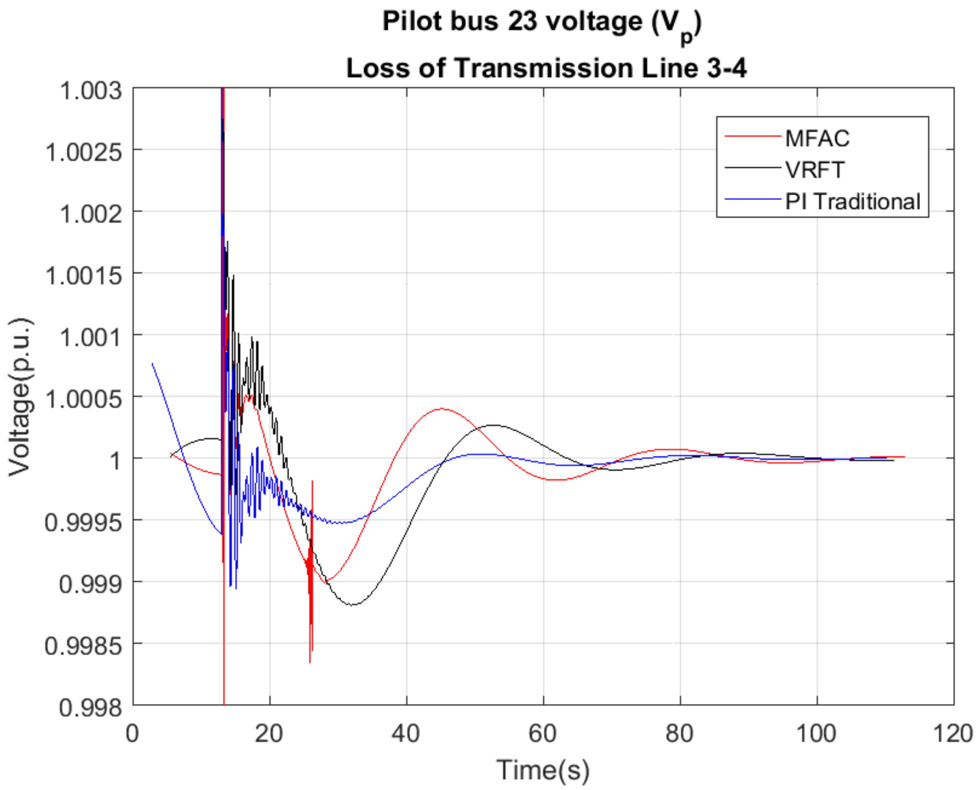

Figure 84 – Pilot bus voltage during Transmission Line 3-4 disturbance (Bus_{23}).

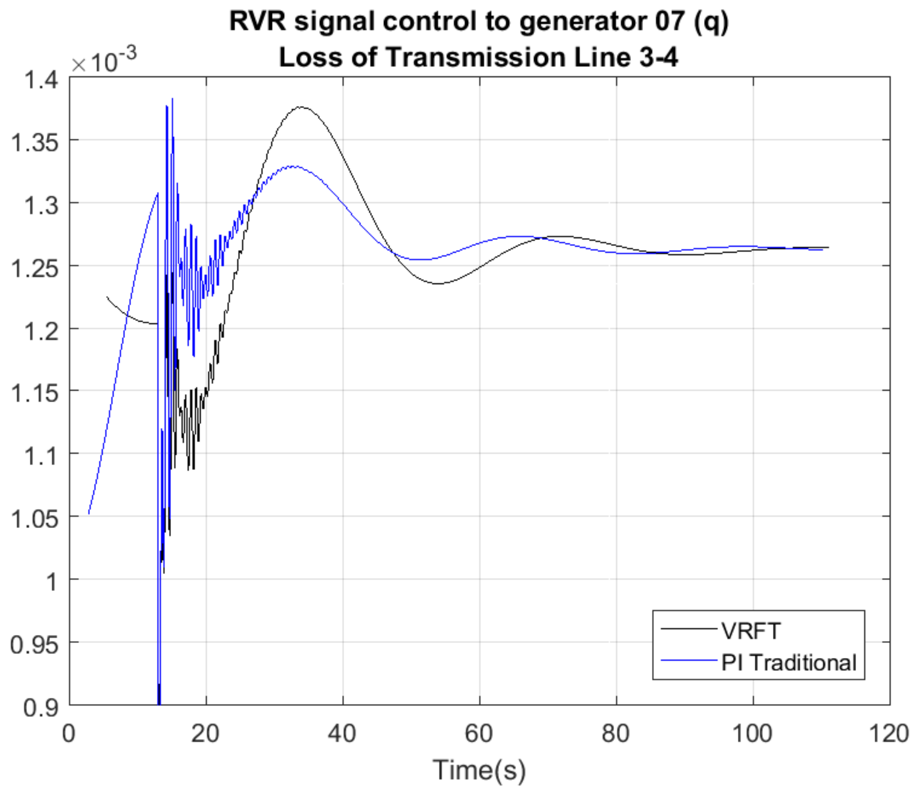

Figure 85 – RVR signal control (q) to generator 07 during Transmission Line 3-4 disturbance.

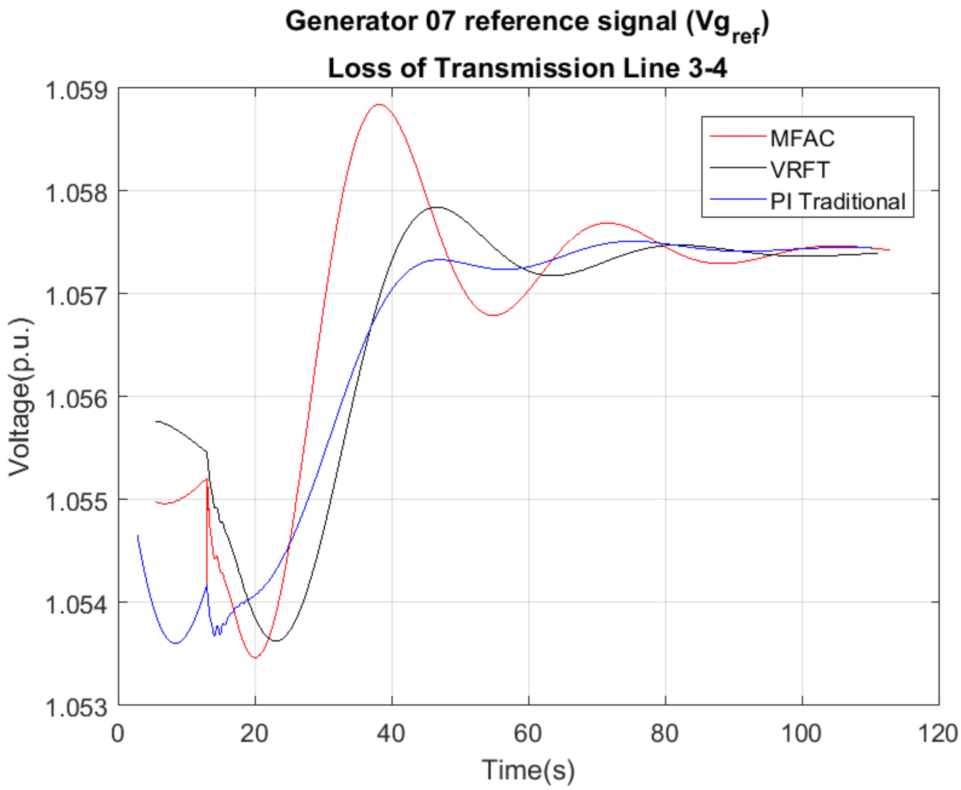

Figure 86 – Reference signal (Vg_{ref}) to generator 07 during Transmission Line 3-4 disturbance.

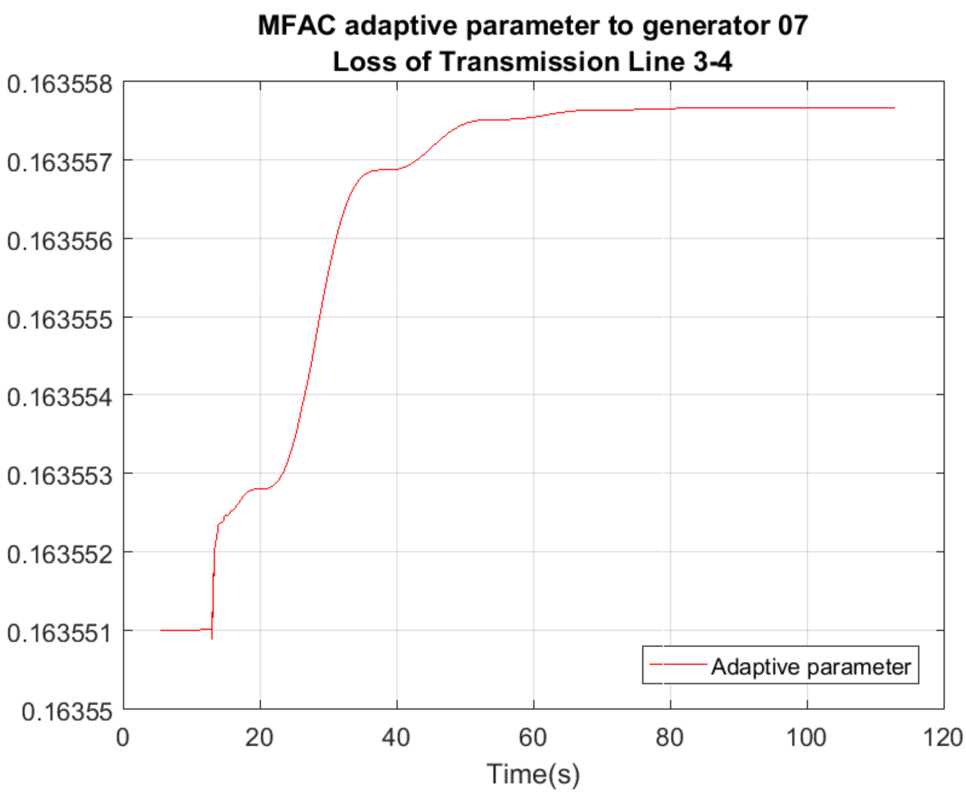

Figure 87 – MFAC adaptive parameter during Transmission Line 3-4 disturbance ($B_{23}G_{07}$).

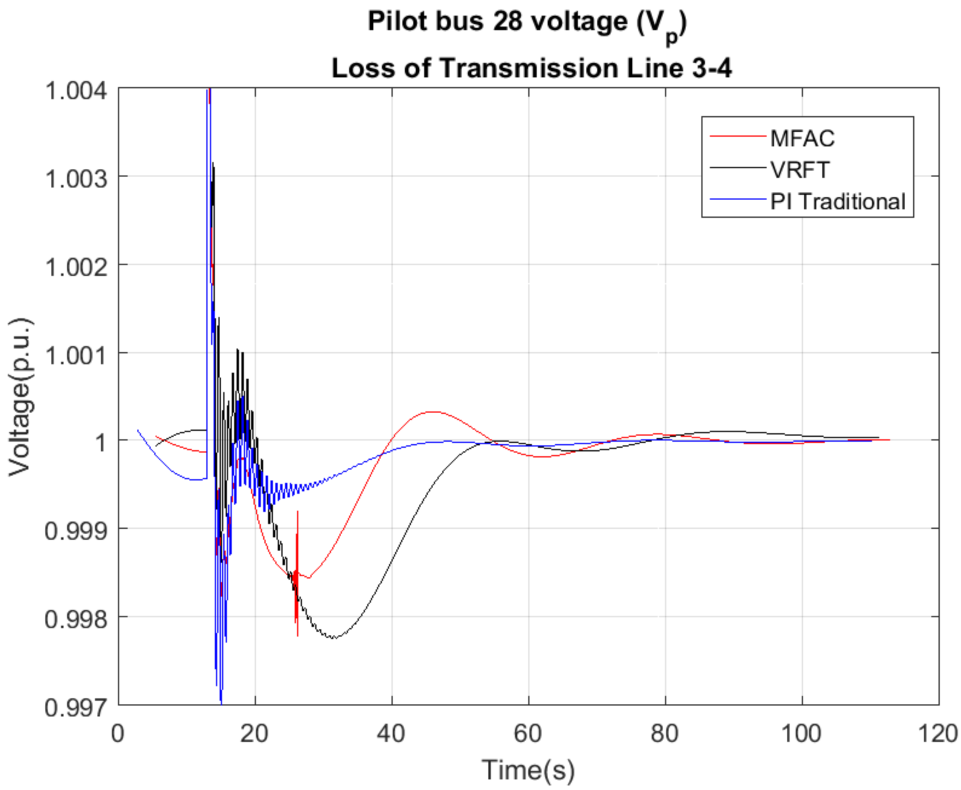

Figure 88 – Pilot bus voltage during Transmission Line 3-4 disturbance (Bus_{28}).

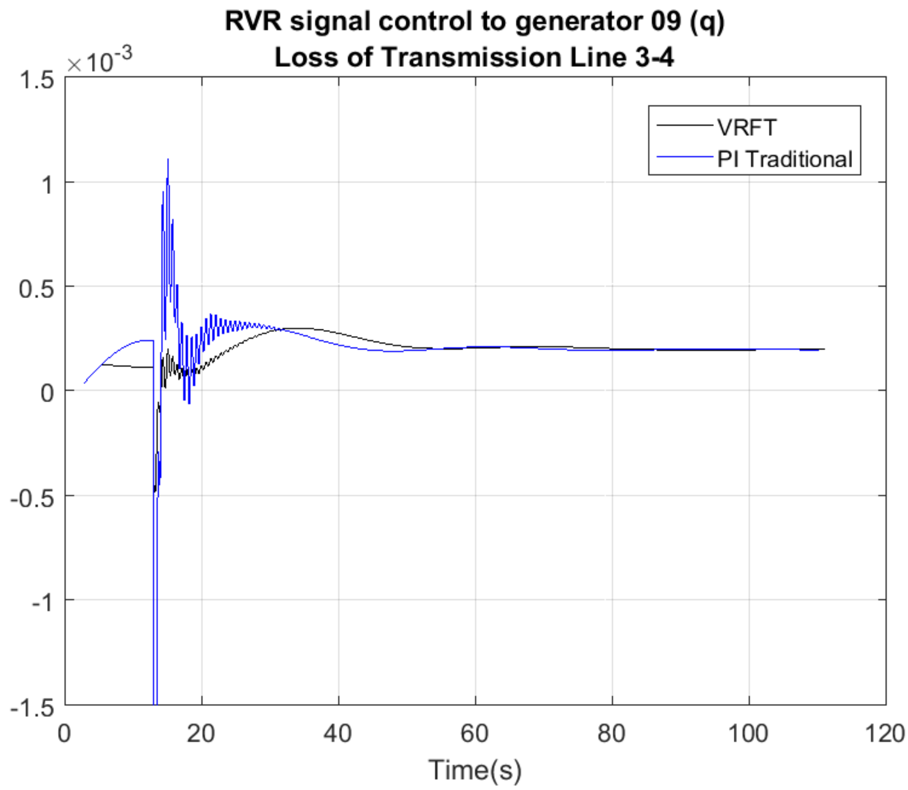

Figure 89 – RVR signal control (q) to generator 09 during Transmission Line 3-4 disturbance.

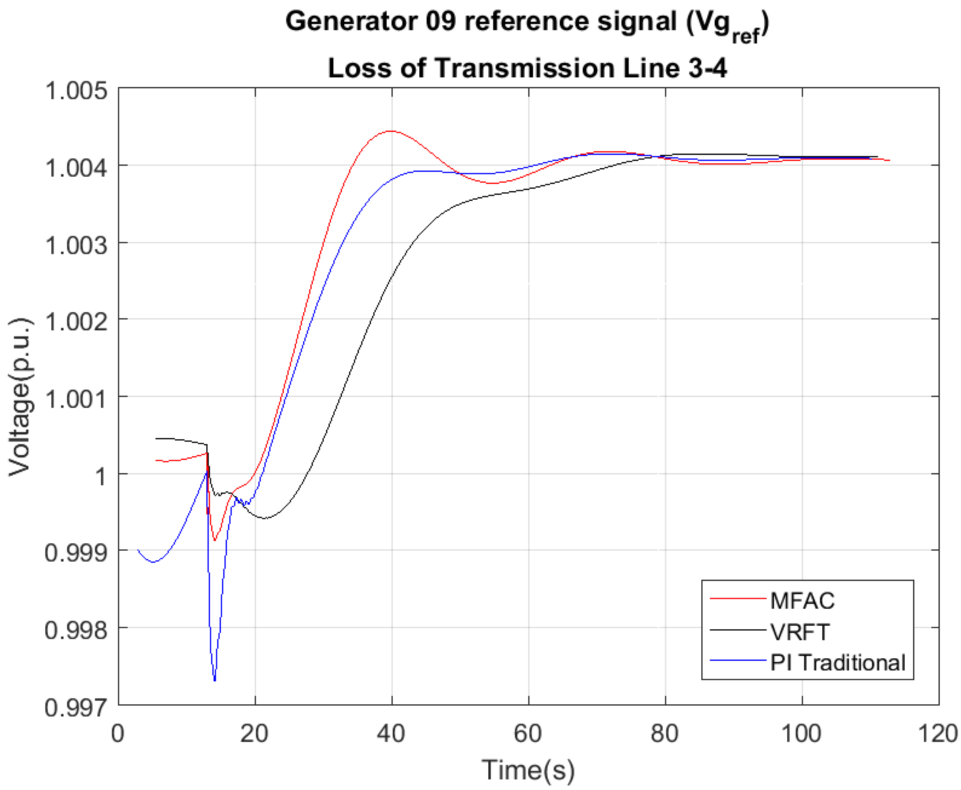

Figure 90 – Reference signal (Vg_{ref}) to generator 09 during Transmission Line 3-4 disturbance.

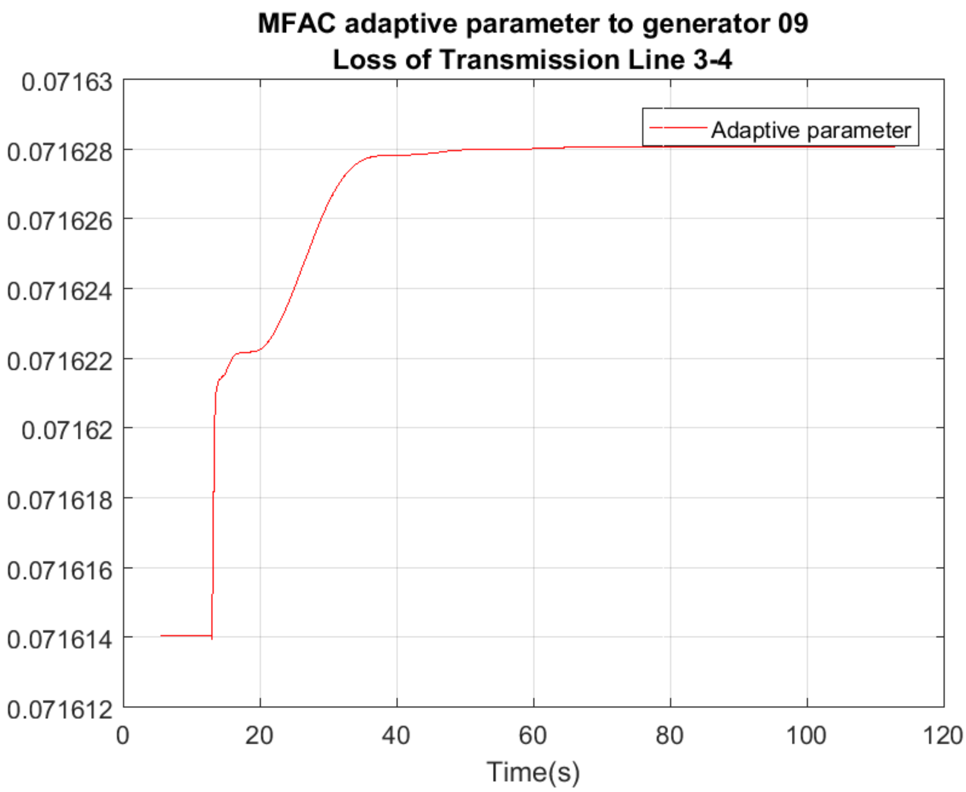

Figure 91 – MFAC adaptive parameter during Transmission Line 3-4 disturbance ($B_{28}G_{09}$).

5.6 Results Discussions

The VRFT and MFAC approaches were applied to the secondary voltage control to keep the voltage stability in the electrical power system. Simulation results in the IEEE 39 bus system have shown that both methods proposed can recover the voltage magnitude of the pilot buses.

The first simulation shows all pilot buses in steady state, but with their values lower than the defined reference 1p.u. Here, no topology changes were imposed. When the controllers are activated, it is possible to notice the behavior of the voltage in these pilot buses and the control signals of each SVC. The gains of PI traditional controllers were obtained through equations that depend on the reactance of the transformer near the generation and the equivalent reactance between the generator and the pilot bus. Thus, it is possible to notice that the pilot buses behave differently the closer they are to their generation of control. The gains of the controllers tuned by the VRFT are obtained through the behavior of a known reference model. This means that the expected behavior does not depend on the electrical distance between the generator and the pilot bar.

The B03G10 pair is electrically distant, so the voltage response in the pilot bus, with controller tuned by traditional methods, is slow and very close to the response obtained by the controller tuned by VRFT, as shown in Figure 14. Note that the VRFT response is very close to the desired response, as shown in the Figure 15. Here, the efforts of the control signals are very close, as shown in the Figure 16. The B20G05 pair is electrically close, so the PI traditional presented an output response faster than the VRFT, as shown in Figure 29, resulting in an even greater control signal effort by the PI Traditional controller, as shown in the Figure 31. The VRFT controller followed a behavior very close to its desired response, as shown in Figure 30.

MFAC controllers provided a faster response than the previous ones. Its characteristic of adapting its parameter to achieve faster response depends on the derivative of the system's output signal. Therefore, when there is a transient, the MFAC parameter will vary to reach the reference more quickly and optimally. As the MFAC control law depends on the system error, therefore the excursion of the output signal to its reference was greater for buses 03 (Figure 14) and 10 (Figure 24). Thus, the controllers of both systems showed greater variations in their parameters, as shown in the Figure 18 and Figure 28.

In the following cases, several contingencies were applied to the systems, including disturbances with changes in the topology to verify the robustness of the controllers presented here. The first disturbance caused an excessive load change at bus 27, significantly altering the power flow of the system. Bus 28 is the closest, and therefore the most affected in the system, as shown in Figure 64. The response obtained by the controller tuned by the

VRFT was slower when compared to the PI traditional, however a great effort of control signal was required from the PI traditional. Note that the reference signal generated for AVR input was higher in the traditional PI, as shown in Figure 66. The MFAC controller showed a higher overshoot among the three controllers, but within acceptable limits. The accommodation time for the three controllers was satisfactory.

The last simulated disturbance is loss of the transmission line. In that case, there is a change in the system's topology, in which the power flows change, and sometimes, the controllers cannot cope, as their design was based on a model that did not foresee this physical change. The first disturbance occurs in the transmission line next to bus 03 (Line 3-4), this is the most affected bus in the system, as shown in the Figure 68. Because of the high voltage variation in this bus, the MFAC controller produces a greater effort on the control signal than the other controllers, as seen in the Figure 70.

5.7 Summary

This chapter presented the simulations carried out to verify the the DDC methods efficiency, face to the traditional Italian method. The IEEE 39 bus system was used to perform the disturbances cases and evaluated the controllers performance.

6 Conclusion and Future Works

6.1 Conclusions

This dissertation presented a review of DDC methods in the literature and their applications in power systems. The importance of these methods is growing as industrial processes become more complex. The power system is an example of these growing processes, as the insertion of renewable sources makes it increasingly complex, making the system increasingly sensitive to voltage instability, for example. To solve this problem, a hierarchical voltage control was proposed based on two DDC methods: VRFT and MFAC. These methods belong to distinct classes of data-based controllers.

VRFT is an offline method that requires a representative set of I/O data from the system to tune a controller of known and linear structure in its parameters. MFAC is an online and adaptive method in its parameters. This method provides a control law in which the controller structure is not defined as in VRFT.

To evaluate the efficiency of these methods, the SVC control of the Italian system, obtained through model-based methods, was used. Therefore, the three forms of control were applied in the IEEE 39 bus system, also known as the New England model.

The present work did not aim to define which method is preferable for the application in SVC, but to study them and look for ways to improve their performance. The methods have unique characteristics that may or may not favor their use. The Italian model used as a benchmark proved to be strongly dependent on the electrical distance between the generator that controls the pilot, which prevents it from achieving the same performance for the different subsystems. With VRFT, this problem did not occur, as the controller is tuned based on a known and desired dynamic response. Thus, it was possible to obtain an answer very close to the desired dynamics for any of the subsystems. The MFAC was shown to be sensitive to abrupt voltage variations, as it depends strongly on the derivative of the output signal. Both methods based on data proved to be robust when applied to contingencies that changed the topology of the system.

An interesting point to stand out in this work is that although both methods proposed have different characteristics and belong to different classes of controllers, they proved to be complementary, because a great difficulty in the MFAC method is to find in the literature a procedure regarding the initialization of its parameters. Here was presented a methodology that used the algorithm VRFT in the initialization of MFAC, and its results were satisfactory.

6.2 Future Work

1. Extend the VRFT and MFAC algorithms for others power systems models, including the Brazilian power systems;
2. Extend the VRFT algorithm for the MIMO, and perform a procedure for applications in SVC problems;
3. Extend the MFAC algorithm for the MIMO, and test other variations of the method such as PFDL and FFDL;
4. Apply DDC methods to problems involving renewable sources in power systems, and test their performance in power systems resilience.

7 References

ARCIDIACONO, V. Automatic voltage and reactive power control in transmission systems. *CIGRE/IFAC, Firenze*, 1983. Cited in page 45.

BAZANELLA, A.; CAMPESTRINI, L.; ECKHARD, D. *Data-Driven Controller Design: The H2 Approach*. [S.l.]: Springer Netherlands, 2011. (Communications and Control Engineering). Cited 5 times in pages 26, 35, 36, 37, and 50.

CAMPI, M.; LECCHINI, A.; SAVARESI, S. Virtual reference feedback tuning: a direct method for the design of feedback controllers. *Automatica*, v. 38, n. 8, p. 1337 – 1346, 2002. Cited 2 times in pages 32 and 37.

CAñIZARES, C. A. et al. Comparing secondary voltage regulation and shunt compensation for improving voltage stability and transfer capability in the italian power system. *Electric Power Systems Research*, v. 73, n. 1, p. 67 – 76, 2005. Cited 5 times in pages 8, 46, 47, 49, and 50.

CHEN, P. et al. Reinforcement-based robust variable pitch control of wind turbines. *IEEE Access*, v. 8, p. 20493–20502, 2020. Cited in page 30.

CHIANDONE, M. et al. Automatic voltage and reactive power regulator for wind farms participating to TSO voltage regulation. In: *2015 IEEE Eindhoven PowerTech*. [S.l.: s.n.], 2015. p. 1–5. Cited in page 22.

CHIANDONE, M. et al. Coordinated voltage control of multi-converter power plants operating in transmission systems. the case of photovoltaics. In: *2015 International Conference on Clean Electrical Power (ICCEP)*. [S.l.: s.n.], 2015. p. 506–510. Cited in page 22.

CHIANDONE, M. et al. Hierarchical voltage regulation of transmission systems with renewable power plants: An overview of the italian case. In: *3rd Renewable Power Generation Conference (RPG 2014)*. [S.l.: s.n.], 2014. p. 1–5. Cited in page 22.

CORLETA, A. et al. Data-driven control design applied to uninterruptible power supplies. In: *2016 IEEE Conference on Control Applications (CCA)*. [S.l.: s.n.], 2016. p. 1312–1317. Cited 2 times in pages 17 and 31.

CORSI, S. *Voltage control and protection in electrical power systems: from system components to wide-area control*. London: Springer, 2015. (Advances in industrial control). Cited 4 times in pages 8, 21, 22, and 24.

CORSI, S. et al. Coordination between the reactive power scheduling function and the hierarchical voltage control of the EHV ENEL system. *IEEE Transactions on Power Systems*, v. 10, n. 2, p. 686–694, May 1995. Cited 2 times in pages 22 and 23.

DISSANAYAKE, A. M.; EKNELIGODA, N. C. Decentralized optimal stabilization of active loads in islanded microgrids. *IEEE Transactions on Smart Grid*, p. 1–1, 2020. Cited in page 30.

DONG, N. et al. Spsa-based data-driven control strategy for load frequency control of power systems. *IET Generation, Transmission Distribution*, v. 12, n. 2, p. 414–422, 2018. Cited in page 30.

DUAN, J.; XU, H.; LIU, W. Q-learning-based damping control of wide-area power systems under cyber uncertainties. *IEEE Transactions on Smart Grid*, v. 9, n. 6, p. 6408–6418, 2018. Cited in page 30.

ELMITWALLY, A.; ELSAID, M.; ELGAMAL, M. Novel multiagent-based scheme for voltage control coordination in smart grids. *Journal of Energy Engineering*, v. 141, n. 3, p. 04014025, 2015. Cited in page 16.

GAO, W. et al. Output-feedback adaptive optimal control of interconnected systems based on robust adaptive dynamic programming. *Automatica*, v. 72, p. 37 – 45, 2016. Cited in page 29.

GUARDABASSI, G. O.; SAVARESI, S. M. Virtual reference direct design method: an off-line approach to data-based control system design. *IEEE Transactions on Automatic Control*, v. 45, n. 5, p. 954–959, May 2000. Cited in page 32.

GUO, W. et al. Online supplementary ADP learning controller design and application to power system frequency control with large-scale wind energy integration. *IEEE Transactions on Neural Networks and Learning Systems*, v. 27, n. 8, p. 1748–1761, 2016. Cited 2 times in pages 17 and 29.

HATZIARGYRIOU, N. et al. Definition and classification of power system stability revisited extended. *IEEE Transactions on Power Systems*, p. 1–1, 2020. Cited in page 17.

HOU, Z.; JIN, S. *Model Free Adaptive Control: Theory and Applications*. [S.l.]: CRC Press, 2013. Cited 8 times in pages 8, 26, 38, 39, 40, 41, 43, and 53.

HOU, Z.-S.; WANG, Z. From model-based control to data-driven control: Survey, classification and perspective. *Information Sciences*, v. 235, p. 3 – 35, 2013. Data-based Control, Decision, Scheduling and Fault Diagnostics. Cited 3 times in pages 17, 26, and 50.

ILIC, M. D. et al. Improved secondary and new tertiary voltage control. *IEEE Transactions on Power Systems*, v. 10, n. 4, p. 1851–1862, Nov 1995. Cited in page 16.

JIANG, Y.; JIANG, Z. Robust adaptive dynamic programming for large-scale systems with an application to multimachine power systems. *IEEE Transactions on Circuits and Systems II: Express Briefs*, v. 59, n. 10, p. 693–697, 2012. Cited in page 29.

JIANG, Y.; JIANG, Z. Robust adaptive dynamic programming with an application to power systems. *IEEE Transactions on Neural Networks and Learning Systems*, v. 24, n. 7, p. 1150–1156, 2013. Cited in page 29.

JIANHUA, F. A. W. et al. Model-free adaptive control for model mismatch power converters. In: *2011 Chinese Control and Decision Conference (CCDC)*. [S.l.: s.n.], 2011. p. 1168–1171. Cited in page 27.

J.V., H. et al. Coordinated voltage control experience in belgium. *CIGRE Session*, Paris, France, 2000. Cited in page 20.

KUNDUR, P. et al. Definition and classification of power system stability IEEE/CIGRE joint task force on stability terms and definitions. *IEEE Transactions on Power Systems*, v. 19, n. 3, p. 1387–1401, 2004. Cited 4 times in pages 8, 17, 18, and 19.

LAGONOTTE, P. et al. Structural analysis of the electrical system: application to secondary voltage control in france. *IEEE Transactions on Power Systems*, v. 4, n. 2, p. 479–486, 1989. Cited in page 49.

LEFEBVRE, H. et al. Secondary coordinated voltage control system: feedback of EDF. In: *2000 Power Engineering Society Summer Meeting (Cat. No.00CH37134)*. [S.l.: s.n.], 2000. v. 1, p. 290–295 vol. 1. Cited in page 16.

LI, J.; WANG, S.; LI, Y. A model-free adaptive controller with tracking error differential for collective pitching of wind turbines. *Renewable Energy*, v. 161, p. 435 – 447, 2020. Cited in page 28.

LIANG, H. et al. Model-free adaptive controller for VSC in AC/DC distribution networks. In: *2018 2nd IEEE Conference on Energy Internet and Energy System Integration (EI2)*. [S.l.: s.n.], 2018. p. 1–9. Cited in page 28.

LU, C.; SI, J.; XIE, X. Direct heuristic dynamic programming for damping oscillations in a large power system. *IEEE Transactions on Systems, Man, and Cybernetics, Part B (Cybernetics)*, v. 38, n. 4, p. 1008–1013, 2008. Cited in page 29.

LU, C. et al. Wide-area power system stabiliser based on model-free adaptive control. *IET Control Theory Applications*, v. 9, n. 13, p. 1996–2007, 2015. Cited 2 times in pages 27 and 54.

MOEINI, A. et al. Open data IEEE test systems implemented in simpowersystems for education and research in power grid dynamics and control. In: *2015 50th International Universities Power Engineering Conference (UPEC)*. [S.l.: s.n.], 2015. p. 1–6. Cited in page 57.

MORADZADEH, M.; BOEL, R.; VANDEVELDE, L. Voltage coordination in multi-area power systems via distributed model predictive control. *IEEE Transactions on Power Systems*, v. 28, n. 1, p. 513–521, Feb 2013. Cited in page 16.

MOSAAD, M. I.; ALENANY, A.; ABU-SIADA, A. Enhancing the performance of wind energy conversion systems using unified power flow controller. *IET Generation, Transmission Distribution*, v. 14, n. 10, p. 1922–1929, 2020. Cited in page 28.

ONS. Operador nacional do sistema eletrico - procedimentos de rede - módulo 2. Submodulo 2.10, 2020. Disponível em: <www.ons.org.br>. Cited in page 22.

PAUL, J. P.; LEOST, J. Y.; TESSERON, J. M. Survey of the secondary voltage control in france: Present realization and investigations. *IEEE Power Engineering Review*, PER-7, n. 5, p. 55–56, May 1987. Cited in page 22.

REMES, C. et al. Virtual reference feedback tuning applied to dc-dc converters. *IEEE Transactions on Industrial Electronics*, p. 1–1, 2020. Cited in page 31.

ROMAN, R.-C. et al. Virtual reference feedback tuning of mimo data-driven model-free adaptive control algorithms. In: *Technological Innovation for Cyber-Physical Systems*. Cham: Springer International Publishing, 2016. p. 253–260. Cited 2 times in pages 8 and 54.

SANCHA, J. L. et al. Secondary voltage control: analysis, solutions and simulation results for the spanish transmission system. *IEEE Transactions on Power Systems*, v. 11, n. 2, p. 630–638, May 1996. Cited in page 45.

SHEN, Y. et al. Adaptive wide-area power oscillation damper design for photovoltaic plant considering delay compensation. *IET Generation, Transmission Distribution*, v. 11, n. 18, p. 4511–4519, 2017. Cited in page 29.

SHEN, Y. et al. Resilient wide-area damping control using GrHDP to tolerate communication failures. *IEEE Transactions on Smart Grid*, v. 10, n. 3, p. 2547–2557, 2019. Cited in page 30.

SHI, X. et al. Data-driven model-free adaptive damping control with unknown control direction for wind farms. *International Journal of Electrical Power & Energy Systems*, v. 123, p. 106213, 2020. Cited in page 28.

SHI, X. et al. Data-driven wide-area model-free adaptive damping control with communication delays for wind farm. *IEEE Transactions on Smart Grid*, p. 1–1, 2020. Cited in page 28.

SHI, Y. et al. Secondary frequency control for islanded MG based on model-free adaptive control. In: *2020 5th Asia Conference on Power and Electrical Engineering (ACPEE)*. [S.l.: s.n.], 2020. p. 612–616. Cited in page 28.

SILVA, G. Gonçalves da; CAMPESTRINI, L.; BAZANELLA, A. Automating the choice of the reference model for data-based control methods applied to PID controllers. *XX Congresso Brasileiro de Automática, SBA*, p. 1088–1095, 2014. Cited 2 times in pages 51 and 52.

SOLINGEN, E. van; MULDERS, S. P.; WINGERDEN, J.-W. van. Iterative feedback tuning of wind turbine controllers. *Wind Energy Science*, v. 2, n. 1, p. 153–173, 2017. Cited 2 times in pages 17 and 30.

SU, Y. et al. Transient overvoltage control for a wind farm based on goal representation adaptive dynamic programming. In: *2014 International Conference on Power System Technology*. [S.l.: s.n.], 2014. p. 705–712. Cited in page 29.

SUN, Q. G. H. et al. Review of challenges and research opportunities for voltage control in smart grids. *IEEE Transactions on Power Systems*, v. 34, n. 4, p. 2790–2801, July 2019. Cited in page 16.

TANG, Y. et al. Reactive power control of grid-connected wind farm based on adaptive dynamic programming. *Neurocomputing*, v. 125, p. 125 – 133, 2014. Advances in Neural Network Research and Applications Advances in Bio-Inspired Computing: Techniques and Applications. Cited in page 29.

TAYLOR, C.; BALU, N.; MARATUKULAM, D. *Power System Voltage Stability*. [S.l.]: McGraw-Hill, 1994. (EPRI power system engineering series). Cited 2 times in pages 19 and 20.

VALDERRAMA, F.; HERNANDEZ, O. Data driven control design applied to single-phase inverters t. In: *2017 IEEE 3rd Colombian Conference on Automatic Control (CCAC)*. [S.l.: s.n.], 2017. p. 1–6. Cited in page 31.

YANG, X.; HE, H.; ZHONG, X. Adaptive dynamic programming for robust regulation and its application to power systems. *IEEE Transactions on Industrial Electronics*, v. 65, n. 7, p. 5722–5732, 2018. Cited in page 29.

YAO, X. J. et al. The research of model-free adaptive control for large scale wind turbine. In: *Advances in Mechatronics and Control Engineering II*. [S.l.]: Trans Tech Publications Ltd, 2013. (Applied Mechanics and Materials, v. 433), p. 1293–1297. Cited in page 27.

ZHANG, H. et al. Data-driven control for interlinked AC/DC microgrids via model-free adaptive control and dual-droop control. *IEEE Transactions on Smart Grid*, v. 8, n. 2, p. 557–571, 2017. Cited in page 28.

ZHANG, P. et al. Adaptive wide-area damping control scheme with stochastic subspace identification and signal time delay compensation. *IET Generation, Transmission Distribution*, v. 6, n. 9, p. 844–852, 2012. Cited in page 31.

ZHAO, Y.; LU, C. An adaptive coordinated secondary voltage control with PMU data. In: *2018 IEEE Power Energy Society General Meeting (PESGM)*. [S.l.: s.n.], 2018. p. 1–5. Cited 4 times in pages 17, 28, 49, and 53.

ZHAO, Y. et al. Improved model-free adaptive wide-area coordination damping controller for multiple-input–multiple-output power systems. *IET Generation, Transmission Distribution*, v. 10, n. 13, p. 3264–3275, 2016. Cited in page 27.

ÅSTRöM, K.; HäGGLUND, T. The future of PID control. *Control Engineering Practice*, v. 9, n. 11, p. 1163 – 1175, 2001. PID Control. Cited in page 27.